HYDROGEOCHEMISTRY AND ISOTOPIC STUDY OF THE ORIGIN OF UNDERGROUND MINE WATER AT GOLDEN STAR BOGOSO/PRESTEA LIMITED (NEW CENTURY MINES)

BY

INNOSAH GIBRILLA

(10396272)

BSc (Cape Coast), 2008

THIS THESIS IS SUBMITTED TO UNIVERSITY OF GHANA, DEPARTMENT OF NUCLEAR SCIENCES AND APPLICATIONS, GRADUATE SCHOOL OF NUCLEAR AND ALLIED SCIENCES IN PARTIAL FULFILLMENT OF THE REQUIREMENT FOR THE AWARD OF MPHIL DEGREE IN NUCLEAR EARTH SCIENCES

JULY, 2014

DECLARATION

This thesis is the result of research work undertaken by Innosah Gibrilla in the Department of Nuclear Sciences and Applications, Graduate School of Nuclear and Allied Sciences, University of Ghana, under the supervision of Dr. T.T. Akiti and Dr. D.K. Adotey.

No part of this research work has been presented in whole or in part to any other University or institution for the award of a degree or diploma.

Works by other people cited in this thesis have all been duly acknowledged under references.

…….	……
INNOSAH GIBRILLA	Dr. T.T. AKITI
(Student)	(Principal Supervisor)
Date……..	Date……..

…….....

Dr. D.K. ADOTEY
(Co- supervisor)

Date…….

DEDICATION

This thesis work is dedicated to my mother, Naye Hamsatu Wadja and my father, Alhaji Gibrilla Alhado Nyamnyam.

ACKNOWLEDGEMENT

"Alhamdulliah Rabbil A'alaamin".

Very special thanks go to my supervisors, Dr. Thomas T. Akiti and Dr. Dennis K. Adotey, for their infinite patience, thorough scientific supervision, encouragement and invaluable guidance.

I would like to register my ultimate gratitude to Prof. Yaw Serfor- Armah, Director of Graduate School of Nuclear and Allied Sciences, Allah shower his blessings on you. Prof. S.B. Dampare, Deputy Director and special appreciation to the entire staff of Department of Nuclear Sciences and Applications. My appreciations also go to Prof. P.M. Nude, HOD, Earth Science, University of Ghana, Legon, and Dr. Boamah of Geological survey Department, for their kind reception during my initial course work.

I thank my family, most especially my brother Bashiru Gibrilla for his ceaseless prayer for me and also Baba Abdulai Ahmed. I also want to show appreciation to Messers Gibrilla Abass, Mike Hayford, David Saka, Nash Bentil, George Cis Crabbe and Ms Bannib Lambon Salamatu of Nuclear Chemistry and Environmental Research Centre of the National Nuclear Research Institute (NNRI), Ghana Atomic Energy Commision.

I would like to thank the management of Golden Star Bogoso Prestea/Limited, most especially, Mr Jerry Agala, the General Manager of New Century Mines (NCM), Mr Samuel Ampiah and Mr Steven Ayidah, the Safety manager of (NCM).

I would like to thank Mr Agyebu Quayson, the Environmental Laboratory Manager, Messrs James German, Stephen Ansah and Ms. Ann for their technical assistance during my sample analysis at the main laboratory situated in Bogoso, the mother company.

I would like to mention those who supported me during this extenuating but fascinating life long trip underground: Messrs Awuku Mensah, Samuel Ntim, Joseph Amihere, Richard Baidoo, Edem Tulasi and Mr. Luckyday Samuel, and the Safety Team.

I am grateful to all my friends at Graduate School of Nuclear and Allied Sciences most especially, Ms. Sandra Yeboah, Ms. Mirian Kretchy, Ms. Kafui Kemetse and Mr. Anthony Amable.

Finally I wish to express my profound gratitude to Ms. Sulemana Amina for her words of encouragement and understanding throughout the period of my course work, I say thank you.

TABLE OF CONTENTS

LIST OF TABLES

LIST OF FIGURES

LIST OF SYMBOLS

µ	Miro
µgmL^{-1}	Micro gram per millilitre
µg g^{-1}	Micro gram per gram
δ	Delta
‰	Permil
α	Alpha
µScm^{-1}	Micro Siemens per centimeter
g	Gram
M	Molarity
mg	Milligram
mgL^{-1}	Milligram per Litre
meq/L	Milliequivalent per Litre
mL	Millilitre
^{o}C	Degree Celcius
A	Average
B	Blank solution
N	Molarity of $AgNO_3$
D_f	Dilution factor
C_{NO3}	Concentration of nitrate
C_{calib}	Calibration concentration

LIST OF ACRONYMS

AMD	Acid Mine Drainage
Al	Aluminum
AOAC	Association of Official Analytical Chemist
As	Arsenic
Ca	Calcium
Cd	Cadmium
Cl	Chlorine
Cu	Cupper
EC	Electrical Conductivity
EDTA	Ethylene Diamine Tetra Acetate
FAAS	Flame Atomic Absorption Spectrometry
Fe	Iron
GAEC	Ghana Atomic Energy Commission
GSBPL	Golden Star Bogoso/Prestea Limited
GMWL	Global Meteoric Water Line
H	Hydrogen
HG-AAS	Hydride Generation Atomic Absorption Spectrometry
IAEA	International Atomic Energy Agency
K	Potassium
LGR	Los Gatos Research Inc.
LMWL	Local Meteoric Water Line
LPG	Liquefied Petroleum Gas
Mn	Manganese

Na	Sodium
NCM	New Century Mines
Ni	Nickel
NIST	National Institute of Standards and Technology
O	Oxygen
OA-ICOS	Off-axis Integrated Cavity Output Spectroscopy
Pb	Lead
pH	Hydrogen ion concentration
PTFE	Polytetraflouroethylene
Q_A	Quality Assurance
Q_C	Quality Control
$R_{(sample)}$	Ratio of sample
$R_{(standard)}$	Ratio of standard
TDS	Total Dissolved Solids
USA	United States of America
UV	Ultra-Violet
VSMOW	Vienna Standard Mean Ocean Water
V_{EDTA}	Volume of EDTA
V_{sam}	Volume of Sample
Zn	Zinc

ABSTRACT

Hydrogeochemical study of the origin of underground mine water at Golden Star Bogoso/ Prestea Limited (New Century Mines) was carried out to determine the geochemical processes controlling surface water, groundwater and underground mine water and to identify the source of recharge to the underground water in the mines; investigate the hydrochemical facies of groundwater in the various aquifers (gallaries), and identify the relationship between surface water and groundwater, and underground mine water using hydrogeochemistry and stable isotope technique. Water from seventeen (17) surface water bodies, ten (10) hand-dug wells, eleven (11) boreholes and twenty-one (21) underground mine water samples were collected within Prestea in the Prestea-Huni Valley district of Western Region of Ghana between October 2013 and March 2014.The objectives of the study was achieved through the determination of pH, temperature, TDS, salinity, alkalinity, electrical conductivity, anions (SO_4^{2-}, HCO_3^-, Cl^-, PO_4^{3-}, NO_3^-), major cations (Ca^{2+}, Mg^{2+}, Na^+, K^+) and trace elements (As, Cd, Cu, Fe, Mn, Pb and Zn). Arsenic,(As), was determined by Hydride Generation Atomic Absorption Spectrometry (HG-AAS). Levels of Cd, Cu, Fe, Mn, Mg, Pb and Zn were determined by Flame Atomic Absorption Spectrometry (FASS). The contents of Na^+ and K^+ were determined by Flame Photometry. Measurement of the levels of SO_4^{2-}, PO_4^{3-} and NO_3^- were achieved by UV-Visible spectrophotometry. Titrimetry was used for the determination of alkalinity, HCO_3^- and Cl^-. Temperature, pH, Conductivity, Salinity and Total Dissolved Solids (TDS) of the surface water, groundwater and underground mine water were all assessed. The stable isotopes (δ^2H and $\delta^{18}O$) compositions of the waters were determined using the Liquid-Water Isotope Analyzer [based on Off-Axis Integrated Cavity Output Spectroscopy (OA-ICOS)

via laser absorption]. The determined Levels of major cations (in ranges, meq/L) for the various waters were as follows: Surface Water: Ca [0.64-33.00], Mg [0.44-18.87], Na [0.12-5.59] and K [0.01-0.24]; Groundwater: Ca [1.01-5.39], Mg [0.76-2.32], Na [0.61-3.57] and K [0.11-3.57]; Underground mine water: Ca [5.91-43.00], Mg [3.61-14.50], Na [0.28-4.14] and K [0.83-0.96];.The determined Levels of major anions (in ranges, meq/L) for the various waters were as follows: Surface Water: SO_4 [3.00-49.30], HCO_3 [0.94-9.02], Cl [0.64-3.28], PO_4 [0.01-3.06] and NO_3 [0.01-0.17]; Groundwater: SO_4 [2.15-5.96], HCO_3 [0.28-2.38], Cl [0.69-3.89], PO_4 [0.01-2.00] and NO_3 [0.01-1.36]; Underground mine water SO_4 [5.48-8.98], HCO_3 [2.22-8.02], Cl [0.16-6.90], PO_4 [0.10-3.23] and NO_3 [0.08-0.43]. Strong correlation between HCO_3^- and SO_4^{2-} demonstrate the formation of H_2SO_4 while groundwater and underground mine water traversing through pyrite bearing shale may dissolve heavy metals into groundwater. The variation of surface water, groundwater and underground mine water hydrogeochemistry revealed the dominance of $Ca^{2+} > Mg^{2+} > Na^+ > K^+$ as relative abundance of cation, and the dominance of relative anions $SO_4^{2-} > HCO_3^- > Cl^- > PO_4^{3-} > NO_3^-$. The Piper trilinear diagram indicated water types from GSBPL (NCM) corresponded to the NaCl or Na - HCO_3 – Cl, Ca – Mg – SO_4 - Cl (water type) and mixed water type Ca – Mg – HCO_3 – Cl. The study approach includes geochemical analysis and conventional graphical plots (Bivariate) of the hydrochemical data to assess the geochemical evaluation of processes. The result suggested different natural hydrogeochemical processes such as simple ion exchange, leaching and dissolution, evaporation and oxidation-reduction are the key factors. The influence on the species of groundwater and underground mine water chemistry is the leaching and dissolution of weathered rock with limited cation ion (reverse ion exchange) at few

locations. Evaporation and oxidation-reduction are not among the major hydrochemical processes controlling the hydrochemistry of groundwater and underground mine water. Gibbs diagram also confirms the dominant process as the leaching and dissolution of minerals. Stable isotope composition measurements (in ranges ‰) for surface water [$\delta^{18}O$ (-2.16 to +0.47); $\delta^{2}H$(-6.66 to +3.02)], hand-dug wells [$\delta^{18}O$ (-2.28 to -0.87); $\delta^{2}H$(-6.48 to +0.58)], boreholes [$\delta^{18}O$ (-2.23 to -0.48); $\delta^{2}H$(-8.88 to -1.68)] and underground mine water [$\delta^{18}O$ (-2.22 to -0.95); $\delta^{2}H$(-8.54 to -1.00)]. This result indicates that stable isotopes ($\delta^{18}O$ and $\delta^{2}H$) in the water samples from the GSBPL (NCM) clustered closely along the Global Meteoric Water Line (GMWL), suggesting an integrative and rapid recharge from meteoric origin (rainfall). Consequently, majority of the water samples are mainly meteoric water with little or no isotopic variations. Finally, recharging relationships were identified for these water samples; groundwater at Himan [borehole (HBH2)] and River Ankobra [ARaW (DS)]; surface water at Prestea [PUWF (DS)] and underground mine water at Prestea Central Shaft [UD-17F]; and surface water at Ankobra [ASP] and Prestea [PUWM(MS)], a borehole at Prestea [PBH6] and underground mine water at Prestea Central Shaft [UD-17B].

CHAPTER ONE

INTRODUCTION

1.1 BACKGROUND TO THE STUDY

Groundwater is water located beneath the earth's surface in soil pore and in the fractures or rock formation (Marios, 2002). Groundwater is also regarded as liquid water flowing through shallow aquifers, [technically includes soil moisture, permafrost (frozen soil), immobile water in very low permeability bedrocks and deep geothermal or oil formation (Wikipedia, 2013). Groundwater is also regarded as a long term" reservoir" of the natural water cycle with residence times from days to millennia (Wikipedia, 2013). Groundwater makes up about twenty percent (20 %) of the world's fresh water supply, which is about 0.61 % of the entire world's water including oceans and permanent ice (Marios, 2002).

Groundwater is naturally replenished (recharged) by precipitation, surface water bodies including streams, rivers etc, when these sources reach the water table. Groundwater and surface water are not isolated components of the hydrologic systems, but instead interact in a variety of physiographic and climatic landscape. Thus, development or contamination of one commonly affects the other. Therefore a thorough understanding of the basic principles of interaction between groundwater and surface water are needed for effective management of water.

Groundwater is present in all underground goldmines. Sometimes the underground goldmines are flooded due the mining process intercepting fractures or faults. The impact of groundwater on underground goldmines includes both inflow to the mine and adverse effects on the groundwater flow systems. These impacts arise not only from the drainage of

water from the surrounding rocks into the goldmine, but also because of changes in the hydraulic properties of the rocks due to strata deformation induced by gold mining. Few studies have directly evaluated the permeability changes due to strata movement. Brown and Parizek et al., (1971) and Hobba (1981), have demonstrated that, goldmine roof collapse and subsidence increase vertical leakage and groundwater velocities, lower groundwater levels and alter the hydrologic characteristics of water shed. Hill and Price (1983) observed that groundwater levels over 550 feet deep long wall panel in Pennsylvania (United States of America) fell dramatically when the subsidence front passed and attributed this drop in groundwater level to leakage to the goldmine and lower aquifer through zones where permeability had been increased by mine-induced fracturing.

Groundwater will drain from shallow aquifers to the mines only if a direct hydraulic connection exists. The most likely locus for such pathways is a narrow zone connecting extensionally stressed periphery of the subsidence trough with the fractured edges of the primary zones above the panel.

As noted above, however, the near surface zone of increased permeability is generally separated from the lower zones by intermediate strata which have subsided without extensive fracturing. In most cases, only the lowest aquifers drain directly into the mines. The upper aquifers respond independently to hydraulic property changes, regardless of drainage to the underground mines.

Sometimes extreme rainfall events on the surface may flow directly into the underground mines. Another source of flooding in the mines is the surface water (rivers, streams, lakes

or ponds) which may be flowing or standing on permeable materials. Also water in the unsaturated zones that move slowly for a long time infiltrates into the underground mines.

In 2004, three days of continuous rainfall in Prestea (a gold mining town in Southwestern Ghana), flooded the underground mines as a result of no electrical power supply to pumping stations, and lately, the activities of the small-scale and artisanal gold miners (popularly called "galamsay" in Ghana) have resulted in the increase of flooding of the underground goldmines.

The pathways of the groundwaters (aquifers) into the underground mine water systems are not well known. The groundwater in the goldmine could be old and deep, meteoric or recent water or recharge from surface water bodies or a mixture of these waters.

It is therefore imperative to study the water-rock interaction and characterization involved in the movement of surface and groundwater through the geologic formations around the underground goldmine (located at Prestea) of the Golden Star Bogoso/Prestea Limited.

The contents of weathering products (major and minor ions, and trace elements), carbonates and silicates provide useful information on the sources of dissolved rocks.

In this study, surface water bodies (rivers, streams, pond and wells) and groundwater from different levels of galleries of the Prestea underground goldmine water would be assessed in order to determine whether the groundwaters have a common or different origin.

Generally, water retains its stable isotopic signature unless mixed or diluted with waters of a different isotopic composition (Fontes, 1980). In the present study, stable water isotope

technique will be used to determine which surface water within the study area infiltrates in the underground mines.

Groundwater recharge and circulation, as one of the issues for groundwater development and management, have been studied extensively in large-scale (Herczeg, 1991). Several studies using hydrochemistry and stable isotopes of water have already been undertaken to characterize recharge processes in similar karst-dominated geologic settings [Cook and Herczeg, (2000); Marifa, et al., (2003); Long and Putnam, (2004); Barbieri et al., (2005); Aravena and Suzuki, (1990) and Harrington et al., (2002)]. In addition, hydrochemistry and stable isotopes have been used to determine the main mechanisms of the water cycle, through study of the dynamic processes of different water bodies, such as their formation, movement, mixture and so in coal mining districts [Duan et al., (1994); Gui et al., (2005); Zhuang, (1997); Pan et al., 2009); Wang and Jiao, (2001); and Hu et al., (2010)].

1.2 STATEMENT OF PROBLEM

Over the past few decades, exploration of gold at the Prestea underground mine of the Golden Star Bogoso/Prestea Limited has gone deeper and deeper in the drilling of deep cast, resulting in frequent and severe water-inrush (flooding) incidents in the gallaries. A typical example is the flooding of the Prestea underground mine due to three days of continuous rainfall. Consrquently, power supply to pumping stations in the mine was adversely affected. In recent times, the activities of small-scale and artisanal goldminers (popularly called “galamsay”) have resulted in the increase of flooding of the underground mines.

In order to understand the cause of flooding and dewatering processes in the gallaries of the Prestea underground mines, it has become imperative to conduct a systematic study into the hydraulic connections between water–inrush (flooding) aquifers and the source of groundwater recharge in the various gallaries of the Prestea underground mines.

1.3 OBJECTIVES OF THE STUDY

The main objectives of this study were to establish the hydrodynamics of the aquifers using environmental isotopes (δ^2H and $\delta^{18}O$) and hydrogeochemistry of the underground mine water and recharge conditions prevailing in the Prestea underground mine of Golden Star Bogoso/Prestea Limited.

1.3.1 Specific Objectives

The specific objectives were;

(a) To identify of source of recharge to the underground mines;

(b) To identify the relationship between surface water, groundwater and unground mine water using hydrochemistry and stable isotope technique;

(c) To identify the dominant water-rock interaction;

(d) To determine the hydrochemical facies of groundwater in the various aquifers (gallaries); and,

(e) To determine pathways of groundwater movements in the underground mines.

1.4 JUSTIFICATION

Different types of data can be used to study groundwater systems in underground mines including hydrogeochemical, piezometric, and isotopic data. Due to the large extent of large area (usually tens of thousands of square kilometers), complex hydrogeological conditions (multiple of aquifers and flow systems) in some of the gallaries in the underground mines and scarce data in scientific literature, the use of traditional methods of groundwater studies such as the piezometric and hydrogeological methods, may be inappropriate to obtain a better understanding of groundwater systems in the underground mines and their relationships with other water bodies (Lu et al, 2011). The isotopic compositions of different water bodies, both surface and groundwater, have been widely used to identify the different components of groundwater systems, as their isotopic compositions differ**,** [Huddart et al., (1999); Subyani, (2004); Aldalla, (2009); and Yao et al., (2009)].

In many cases, conventional hydrogeochemical studies are not sufficient to characterize groundwater hydrodynamics or to delineate recharge areas and source areas of recharge water. Since the isotopic composition of O and H in groundwater does not change at low temperatures due to rock- water interaction, this provides a very vital means to bridge the knowledge gap (Kendall and McDonnell, 1998)**.**

This study will provide extensive understanding of the hydrogeology and hydrodynamics of the underground mine water, groundwater and surface water within the Golden Star Bogoso/Prestea Limited (Prestea Underground Mines).

Little or no attention has been concentrated on the study of deep groundwater, especially in multi aquifer system in the Golden Star Bogoso/Prestea Limited (Prestea Underground Mines). In fact, it is very difficult to obtain groundwater samples in various deep aquifers together from 300 to 1000 meters below surface. However, it is an advantage in the case of Golden Star Bogoso/Prestea Limited (Prestea Underground Mines) that lots of deep underground mine water samples in various aquifers can be obtained.

From this, combine use of hydrochemical and stable isotope data would provide useful information to characterize the groundwater in the mines and baseline data information could be generated for the study area.

Future variations in the underground mine water, groundwater and surface water geochemistry and isotope studies may be comparatively assessed as landscape changes in the Golden Star Bogoso/Prestea Limited. (Prestea Underground Mine).

The useful application of isotope-based methods has become well established for water–resources assessment, development and management in the hydrological sciences, and is now an integral part of many water-quality and environmental studies, (Clark and Fritz, 1997).

CHAPTER TWO

LITERATURE REVIEW

2.1 GROUNDWATER AND RECCHARGE AND DISCHARGE

Groundwater recharge can be defined as infiltrated water through into the unsaturated zone to the saturated zone of an aquifer (Freeze and Cherry, 1979).

Recharge of groundwater may occur from rainfall, rivers, canals and lakes and as man-made induced phenomenon (artificial recharge), in such activities as irrigation and urbanization (Ganyaglo, 2006).

Two principal types of recharge are recognized and categorized as direct and indirect. Direct is defined as water added to the groundwater reservoir in excess of soil moisture deficits and evapotranspiration, by direct vertical percolation of precipitation through the unsaturated zone. Indirect recharge results from percolation to the water table following runoffs, localization in joints as ponding in low-lying area and lakes, or through beds of surface water courses (Freeze and Cherry, 1979).

Recharge and discharge areas can be mapped on the basis of some five field observations, piezometric patterns, topography, hydrochemical trends, environmental isotopes and soil/land surface patterns (Mayboon, 1966). The simplest indicator is topography; discharge areas are topographically low while the recharge areas are topographically high. Piezometric measurements can also give a direct indicator. In this measurement, the nest would show upward flow components in discharge areas and downward flow in recharge areas. The process of recharge is very complicated. Perhaps one of the most important factors is the time delay between the time when meteoric water enters the soil profile, and

the time when it is manifested as an effectively exploitable groundwater source. The actual recharge is controlled by several factors including: (1) the amount and rate of rainfall not lost to surface runoff and evapotranspiration, (2) the initial soil moisture content or saturation ratio of the soil, (3) the elevation of the recharge surface relative to the discharge area, (4) the horizontal hydraulic conductivity of the aquifer being recharged and its hydraulic gradient, which determines the rate at which recharged water will be carried out of the recharge area, (5) the vertical hydraulic conductivity of the soil being recharged, and (6) the presence of man-made alterations to the surface, such as drainage tiles, that carry water away to runoff in surface stream (Leap, 1999).

2.1.1 Groundwater and Underground Mine Water Geochemistry

The impact of underground mining on the flow regime is not only confined at or near the mine workings, but also influence large areas around the mines. Blasting may expose fresh rock surfaces to the groundwater and creates a new hydrogeochemical environment, causing changes in groundwater quality. The present study area may be treated as an example, exhibiting the following characteristics as an impact of underground mining.

An underground mine resembles a pumping well creating a head difference towards the mine. The area of influence depends primarily upon aquifer type, permeability (horizontal and vertical), and depth of mine. Blasting, an essential part of mining operations readily, increases porosity and permeability of rocks at depth, thereby inducting larger areas under cone of depression. The observed area of influence in many underground coal mines is limited to few hundred meters only (Nielsen et al., 1998). In the mining areas of South-

Eastern Coalfield Limited of India, the impact zone has been often restricted within 100 m to 300 m from the mine edge (Subba rao et al., 2007).

The geochemistry of groundwater and underground mine water is governed by mineral reaction present in rocks and water. The minerals in the Earth's crust are mainly composed of silicon, aluminum, and oxygen, with varying amount of alkalis (e.g. potassium, sodium) and alkaline earth elements (e.g. calcium and magnesium) (McSween et al., 2003). These minerals are collectively referred to as aluminosilicates. The most common aluminosilicate minerals found in the earth's crust are the feldspars ($KAlSi_3O_8$, $NaAlSi_3O_8$, and $CaAl_2Si_2O_8$) common in granites.

Groundwater and underground mine water reservoirs have other types of minerals, commonly found carbonate: calcite ($CaCO_3$) and dolomite [$CaMg(CO_3)_2$]. When rainwater percolates into the earth's crust, it interacts with the minerals forming the groundwater reservoirs. The composition of the water, thus, reflects the composition of the rocks (White, 1995).

Granite groundwaters and underground mine waters are mostly dominated by positively charged (cations) Na^+ and Ca^{2+}. Ca^{2+} is the major cation in calcium carbonate bedrocks. The pH of granitic waters is generally low (pH 5-6). Carbonate waters have intermediate pH value of 7.5 (Ragnarsdottir et al., 2010).

Carbonates have the usual property of having a solubility, which decreases with increasing temperature. On the other hand, silicates, which resemble common salt are sugar, have

high solubility as temperature rises. Dissolved constituents of waters from granite and basaltic rocks therefore increase with temperature (Ragnarsdottir et al., 2010).

The concentrations of inorganic constituents in aqueous solutions are thus, controlled by chemical equilibria, which can be described in terms of the solubilities of given minerals. The reactions between minerals and water involve the transfer of protons (H^+) referred to as hydrolysis reactions (Elango, 2010).

2.1.2 Hydrogeology and Groundwater Recharge

The rock basement underlying about 90% of the basin have very little intergranular pore-space and are thus, characterized by little or negligible primary porosity and permeability. This means the rocks are cemented to a degree that the hydrogeological meaning of the original porosity in the rock has lessened and the major part of the groundwater flows occurs in secondary formed structures, mostly fractures, joining, shearings and deep weathering in the rocks (Banoeng Yakubu, 1989). The secondary porosity and flow guiding structures were mainly created by tectonic processes such as folding, mineral orientation (foliation), fracturing and faults (displacement along fractures), shrinking during cooling of rock mass and weathering [Davies and Tauk, (1964); and Banoeng Yakubu, (2000)]. The development of the secondary porosity gives rise to the two distinct types of aquifers in the basin, that is the fractured zone aquifer and the weathered zone aquifer.

The fractured zone aquifer developed in the bedrock at depth of 20 m or more below surface tend to be localized in nature and groundwater occurrences are controlled by

degree of fracturing and the nature of groundwater recharge. Boreholes yields within the fractured zone are determined by the extent of degree of fracturing (Buckley, 1986). Transmissivity varies between 1 and 72 m^3/day. Aquifers in this zone occur below the transition zone and are characterized by high transimissivity but low storage (Kusimi, 2007).

In the Tarkwa-Prestea area, groundwater occurrence is associated with secondary porosity through weathering. Weathering depth is greatest in the Birimian system, where depths of 90- 120 m have been reached. Also in garnites, porhyrites, felsites and other intrusive rock, the weathering depth is great (Kusimi, 2007).

Groundwater circulation in the Tarkwa-Prestea area is localized due to a number of hills that act as groundwater divides. Flows are restricted to quartz veins and fissures-faults-brecciated zones (Kusimi, 2007).

The weathered zone varies greatly depending on the climatic conditions of the rocks and ranges between 4 to 20 m as a unit (Prackla Seismors, 1984).

In most communities, the most weathered zone aquifer is developed for water supply by hand-dug wells, but most of these wells dry during dry seasons. The thick weathered zone aquifer occurs in the forest area in the basins. A formation, which combines the thick weathered zone with well fractured bedrock, provides the most productive aquifers (Acheampong et al., 1985).

The weathered aquifers occur mainly above the transition zone between fresh and weathered rock. Due to the soil content of clay and silt, these aquifers have high porosity and storage but low permeability (Kusimi, 2007).

The Birimian formations are generally well folded and deeply weathered, hence groundwater occurrences in this formation is very high. The granites in this basin are less fractured and weathered; hence groundwater occurrences are moderately low. The granitic aquifers, thus, formed are usually phreatic to semi-confined in character, structurally dependent and often discontinuous in occurrences (Prickla and Seismos, 1984).

Therefore for a thorough understanding of surface–water bodies (River Ankobra and Assesre), groundwater and underground mine water, all three factors should be taken into account.

2.1.3 Hydrochemistry

Groundwater chemistry evolves by interacting with aquifer minerals or internal mixing among different groundwater along flow paths in the subsurface. However increase in the solute concentrations in the groundwater are normally caused by spatially variable recharge, governed by microtopographic controls. (Domenico, (1972); Wallick and Toth, (1976); Toth, (1984); Schuh et al., (1997)]

Groundwater often contains seven major elements (K^+, Na^+, Ca^{2+}, Mg^{2+}, HCO_3^- Cl^-, SO_4^{2-}, NO_3^- and PO_4^{3-}) (Sadashivaiah et al., 2008).

Hydrochemical studies are based on the measurement of the major ions and series of parameters that control the interactions of the major ions.

During the course of its migration and salinitization, the chemical composition of groundwater is the product of geological history, and is also the results of ions' migration and transformation under the action of physical and chemical equilibrium. Common ions (such as K^+, Na^+, Ca^{2+}, Mg^{2+}, HCO_3^-, Cl^-, SO_4^{2-}, NO_3^- and PO_4^{3-}) in groundwater play an important part in the equilibrium. TDS is a comprehensive reflection of common ions' accumulation in groundwater, and is also important index for groundwater's salinitization. Usually, the TDS of groundwater increases in the direction of runoff. Therefore, based on the theory of hydrogen and oxygen stable isotope, the relationship between TDS and hydrogen or oxygen stable istope is of great practical importance to the analysis of the distribution of groundwater flow field (Lu-wang et al., 2010).

2.2 GEOCHEMICAL PROCESSES GOVERNING CHEMICAL EVOLUTION OF GROUNDWATER

Geochemical and hydrochemical studies play a vital role in understanding the chemical evolution of aquifers. The chemical compositions of groundwater and underground mine water change as they move through the groundwater and underground water reservoir. These changes are brought about by weathering, dissolution, ion-exchange reaction, and oxidation and reduction. These chemical processes depend to large extent on the mineralogical composition of the various rock types encountered in the GSBPL terrain.

2.2.1 Dissolution and Leaching

Dissolution is one of the most generally effective processes in groundwater chemistry and could be considered as the first in the chemical evolution of the groundwater (Toth, 1999). It affects both gases and solids. Typically, regions of gas dissolution by groundwater are the soil zone, unsaturated zone and gas accumulation. Gases, which commonly interact with groundwater include N_2, CO_2, NH_3, O_2, to mention a few (Freeze and Cherry, 1979).

Dissolution of gases such as CO_2 render the water weakly acidic. Thus, the water becomes chemically aggressive. The degree of dissolution depends on the solubility of the available minerals, the antecedent concentration of the water and the presence and the temperature of the locality. The dissolution of the oxides iron and manganese from decomposition processes will in turn enrich the soil solution with the release of other metals, which were adsorbed or co-precipitated with iron and manganese under oxidizing conditions.

Also, groundwater has dissolved oxygen-bearing minerals and aggravates the groundwater' salinitation during the process of flowing (Li et al., 2006). On the other hand, with the dissolution of oxygen-bearing minerals in groundwater, the lighter oxygen ions (^{16}O) are easy to produce isotope exchange reaction with groundwater containing a lot of the heavier oxygen ions (^{18}O) after experiencing evaporation effect. So, the isotope exchange equilibrium equations move leftward and $\delta^{18}O$ decreased in accordance with the increase of TDS value, that is, $\delta^{18}O$ decreases in the runoff direction as shown in equations 2.1, 2.2, 2.3 and 2.4.

$$CaCO_2{}^{18}O_{(calcite,dolomite\ and\ limestone)} + H_2O \rightarrow H_2{}^{18}O_{(l)} + CaCO_2 \quad \textbf{2.1}$$

$$SiO^{18}O_{(quartz\ and\ \ calcededony)} + H_2O \rightarrow H_2{}^{18}O + SiO_2 \quad \textbf{2.2}$$

$$CaAl_2Si_2O_7{}^{18}O_{(feldspares)} + H_2O \leftrightarrow H_2{}^{18}O + CaAl_2Si_2O_8 \quad \textbf{2.3}$$

$$14(Mg,Fe)_5\ Al_2Si_3O_{10}(OH)_7(^{18}OH)_{(chlorite)} + H_2{}^{18}O \leftrightarrow 14(Mg,Fe)_5\ Al_2Si_3O_{10}(OH)_8 + H_2{}^{18}O \quad \textbf{2.4}$$

On the one hand, much hydrogen bearing-minerals (such as H_2S, CH_4, and the organic materials that is easy to dissolve) in aquifer is dissolved into the groundwater during the course of flowing and the groundwater' salinitization aggravates (Li et al., 2006).

On the other hand, with the hydrogen-bearing mineral's dissolution into the groundwater, the lighter hydrogen ions (H) are easy to be absorbed into the clay mineral. The heavier hydrogen ion (^2H) is easy to produce isotope exchange reaction with groundwater containing less the lighter hydrogen ions (H). So the isotope exchange equilibrium equation moves rightward and δ^2H decreased in accordance with the increase of TDS value, that is, δ^2H increase in the runoff direction as illustrated in equation 2.5.

$$H_2O + {}^2H_{(hydrocarbonic\ material)} \leftrightarrow H{}^2HO + H \quad \textbf{2.5}$$

2.2.2 Weathering

Weathering processes include a combination of physical and chemical processes causing alteration and dissolution of existing minerals and precipitation of new mineral forms (Koch et al., 1992; Velbel, 1993; Hodson, 2002). During these processes, alkaline cations (K, Na and Ca) are released to the soil solution. Depending on their solubility, the elements

are retained in the soil or leached out of the soil by percolating water under surplus precipitation conditions. Consequently, strong weathered rocks/soil are enriched with elements such as Al, Fe and Ti that form heavily soluble oxides and depleted with elements like Na, K and Mg, which form easily soluble compounds.

The weathering of silicate solution products are more difficult to quantify due to the degradation of silicates being incongruent, generating a variety of solid products, such as clays (Davies and Dewiest, 1966).

A general reaction for weathering of silicate rocks with H_2CO_3 is written in equation 2.6.

$$\left(Na^+, K^+, Mg^{2+}, Ca^{2+}\right)Silicates + H_2CO_3 \leftrightarrow H_2SiO_4 + HCO_3^- + \left(Na^+, K^+, Mg^{2+}, Ca^{2+}\right) + Clay \quad \textbf{2.6}$$

The chemistry of groundwater in the Southern Voltain Sedimentary Basin of Ghana is controlled by weathering of the albitic plagioclase felspares and which accounted for the high concentration of Na and bicarbonates (Acheampong and Hess, 1998).

In the Prestea-Huni valley area, groundwater occurrence is associated with secondary porosity through fissuring and weathering. Weathering depth of between 90 and 120 m has been reached. Also, in garnites, porhyrites, felsites and other intrusive rocks, the weathering depth is great (Kusimi, 2007).

The weathered aquifers occur mainly above the transition zone between fresh weathered rocks, because of low content of clay and silt; these aquifers have high porosity and storage but low permeability. The aquifer in the fractured zone occurs below the transition zone and is characterized by high transimissivity but low storage.

Recharge occurs mainly by direct seepage or infiltration. In some places, groundwater is in hydraulic contact with surface water bodies (rivers, streams, etc) and recharge from them can also take place. Groundwater in the Prestea-Huni valley circulation is localized due to a number of hills that act as groundwater divides. Flows are restricted to quartz veins and fissure faults-brecciated zones (Kusimi, 2007).

2.2.3 Ion- exchange reaction

Most heavy metals (with certain exceptions, including the metalloids As, Sb and Se and the metals Mo and Y) exist mainly as cations in the soil solution and their adsorption therefore depends on the density of negative charges on the surface of the soil colloids. In order to maintain electroneutrality, the surface negative charges are balanced by an equal quantity of cations. Ion exchange refers to the exchange between the counter-ions balancing the surface charge on the colloids and the ions in the soil solution (Brown, 1954).

Ion-exchange has the following characteristics: it is reversible, diffusion controlled, stoichiometric and, in most cases, there is some selectivity or preference for one ion over another by the adsorbent (Gast, 1979). This selectivity gives rise to a replacing order amongst the cations, determined by their valency degree of hydration. The higher the valency of an ion, the greater its replacing power; H^+ ions behave like polyvalent ions and the greater the degree of hydration, the lower its replacing power, other things being equal.

Adsorption by cation exchange can also be described as the formation of outer sphere complexes with the surface functional groups to which they are electrostatically bonded (Sposito, 1985).

The most important substance capable of ion exchanges is clay minerals, mainly kaolinite, montmorillonite, illite cholorite, vermiculite and zeolite, as a result of formation of colloids with large surface area. The occurrence of $NaHCO_3$ water, is an indication of cation Base Exchange in which, sodium on montmorillonite clay is replaced with calcium resulting in sodium rich water, consequently, softening the water. The ions of different elements have different tendencies to be adsorbed or desorbed. The tendency for adsorption amongst the major cations in natural waters is showm in equation 2.7.

$$(Strongly\ \ adsorbed)\ \ Ca^{2+} \succ Mg^{2+} \succ K^{+} \succ Na^{+}\ \ (Weakly\ \ adsorbed) \qquad \textbf{2.7}$$

2.2.4 Oxidation and Reduction reaction

Oxidation as a process of modifying water quality, is the most important in the vadose zone, where there is copious supply of O_2 from air and from CO_2. Below the water table, in the unsaturated zone, water is rapidly depleted in O_2. Consequently, the significance of oxidation decreases with depth. The probable oxidation process in the GSBPL is the oxidation of pyrite (FeS_2) producing iron (III) oxides and SO_4^{2-} in solution (Rowell, 1981).

In gold mining areas, sulphide oxidation leads to production of low pH in groundwater that encourages the dissolution of trace elements in the groundwater in very high concentrations (Kortatsi, 2004).

2.3 HYDROCHEMICAL FACIES

Hydrochemical facies are used to describe the bodies of groundwater in as aquifers differ in the chemical compositions. The facies are function of lithology, solution kinetics and flow patterns of aquifer (Back, 1960; 1961).

Hydrochemical facies can be classified on the basis of dominant ions in the facies by Piper Trilinear Diagram. The major ionic species in most natural waters are Na^+, K^+, Ca^{2+}, Mg^{2+}, Cl^-, CO_3^{2-}, HCO_3^- and SO_4^{2-}.

A Piper Trilinear Diagram can show the percentage composition of these ions, by grouping Na^+ and K^+; the major cations can be displayed on one diagram. Likewise, if CO_3^{2-} and HCO_3^- are grouped, also, there are three groups of major anions. The major types of water are Ca-Mg-HCO_3^- (Alkali Earth dominated water), Na-Ca-Mg- HCO_3^- (water mixed type), Na-Cl or Na-HCO_3-Cl, Ca-Mg-HCO_3^- and Na-HCO_3^-.

Groundwater of Niva river in India, studied show that Na-HCO_3, Na-Cl, Na-Mg-HCO_3^-, Ca-Mg-Na- HCO_3^- types of water were found in geological terrain of weathered and fractured granites, gneiss and contact zone of crushed dykes.

2.4 STABLE ISOTOPE HYDROLOGY

Oxygen and hydrogen ratios are the ultimate tracers of the physical processes affecting water because of the water molecule itself. Stable isotope data are conventionally expressed in ‰ (permil) with respect to Vienna Standard Mean Ocean Water (VSMOW) on the delta scale (Craig, (1961); and Gonfiantini, (1986)]. The stable isotope ratios of

deuterium (^{2}H) to hydrogen (^{1}H) and oxygen-18 (^{18}O) to oxygen-16 (^{16}O) of water have been used as natural tracers in many studies in order to explore hydrological processes (Mazor, 2004). The differences in the ratio of the same element in species or phases A (R_A) and B (R_B) can be described by the fractionation factor **α** in equation 2.8.

$$\alpha = \frac{R_A}{R_B} \qquad \textbf{2.8}$$

Since the changes in isotopic values are generally very small, values are typically given as part per thousand (permil ‰) deviations from a standard; as shown in equation 2.9:

$$\delta = \frac{\left(^{18}O/^{16}O\right)_{(Sample)} - \left(^{18}O/^{16}O\right)_{(Standard)}}{\left(^{18}O/^{16}O\right)_{(Standard)}} \bullet 10^{3} \qquad \textbf{2.9}$$

When the isotopic compositionS of two phases in equilibrium are measured, their differences can be related to the fractionation factor as shown in equation 2.10.

$$\delta^{18}O_A - \delta^{18}O_B \approx \left(\alpha_{[A-B]} - 1\right) \bullet 10^{3} \qquad \textbf{2.10}$$

The fractionation factors between two phases are obtained by measuring the difference in isotopic composition between two phases in equilibrium. Heavy isotopes will favour species in which the element has the stiffest bonds. Often equilibrium is not maintained

between chemical spicies or phases and the source reservoir. In this, the isotopic composition of the source evolves according to Rayleigh distillation, in which small increment of the species is formed in equilibrium with the source, but immediately removed from further interaction, and does not remain in equilibrium with the changing source (Kendal and McDonnell, 1998).

Criag (1961) proposed that the relationship between ^{18}O and ^{2}H isotopes in rainfall over most of the earth's surface could be approximated by the equation 2.11

$$\delta^{2}H = 8^{18}O + 10 \qquad \textbf{2.11}$$

The commonly-observed slope of ~ 8, particularly for temperate zone stations, is less than that predicted by the action of an equilibrium fractionating process during evaporation from the ocean. This indicates that, non-equilibrium (kinetic) fractionation and mixing are important factors in the development of the isotopic content of atmosphere water vapour. This is not expected, given the amount of atmospheric activity occurring during the creation of vapour masses (Mook et al., 2000).

The intercept value of 10 is an average figure and is related to the humidity conditions above the ocean-atmosphere boundary layer in the moisture source area (Gonfiantini, 1986). By contrast, the condensation of atmospheric vapour is much more of an equilibrium process. Condensation occurs when the temperature of a particular air mass

falls below its dew point, where humidity reaches 100%, as result of adiabatic expansion and or heat radiation. At this point raindrops form, will be enriched in the heavier isotopes of ^{18}O and ^{2}H while the remaining vapour will be depleted by the amount dictated by the mass balance of the rainfall–vapour system. In reality, this tends to be a continuous process of the Rayleigh distillation type (Clark and fritz, 1997).

The consequence is that any process resulting in temperature loss in a moist air mass leads to progressively more isotopically – depleted rainfall. This can take the form of the 'continental effect' (movement of the air mass over land), the 'altitude effect' (passage of the air mass over upland barriers) and the amount effect (Rozanski et al., 1993). For most part, $\delta^{18}O$ and $\delta^{2}H$ are highly correlated in rainfall and some variations can also occur as a result of atmospheric conditions. A useful index of this d, the deuterium excess or d – value defined by Dansgaard, 1964, defined as in equation 2.12:

$$d = \delta^{2}H - 8\delta^{18}O \qquad \textbf{2.12}$$

The d-value is considered to be largely controlled by conditions of atmospheric humidity during the vapour forming process. For Global Meteoric Water Line (GMWL) in equation **(2.12),** d has a value around this value, though high, it sometimes fluctuates seasonally mainly due to changes in humidity in the moisture source area (Merlivat and Jouzel, 1979).

Stable isotope ratios of rainfall are strongly correlated with air temperature, a distinct seasonal pattern of rainfall more enriched in heavy isotopes during summer and more

depleted in winter is found in humid climates. In the absence of kinetic fractionation, this variability determines the atmospheric boundary condition for hydrological stable isotope studies at the scale (Mazor, 2004).

The propagation and attenuation of seasonal isotope signal with increasing soil depth also allows the investigation of vertical water movement in the unsaturated zone. The water isotopes in the subsurface may occur in the uppermost part of soil colum due to evaporation (Windhorst et al., 2012).

Rainwater

Rainfall is a component of the hydrologic cycle in which water condenses and produces rains that reach the land surface. Isotopic compositions of the parent cloud and the temperature at which condensation occurs determine the isotopic compositions of each parent cloud that generates rainfall will vary depending directly on; temperature, the distance the air mass has travelled from its sources area, the change in altitude over topographic features, differences in latitudes and seasonal variations (Clark and Fritz, 1997). Mostly, due to Rayleigh's processes which occur while condensation takes place from the vapour source, heavier isotopes ^{2}H and ^{18}O are enriched in the liquid or solid phase and the lighter isotopes remain in the vapour phase because of mass difference which will allow heavier isotope forms to precipitate first (Araguas-Araguas et al., 2000).

As moisture is transported from higher altitudes, more evaporation and re-evaporation processes take place, causing more enrichment in ^{2}H and ^{18}O compositions in the lowlands

and more depleted compositions in the mountains (Bowen, 1986). Isotopic compositions vary with distance inland as the heavier isotope forms precipitate first, leaving the vapour enriched in the lighter isotope forms with increasing distance from the origin of vapour source (Mazor, 2004). Evaporation also occurs with seasonal changes, as rainfall is more susceptible to fractionation processes with the increase in temperature during summer than winter (Barnes and Turner, 1998). These isotope composition variations give an input signal characterized by Local Meteoric Water Lines (LMWL) particularly to each region, thus permitting the tracing of recharge sources (Mook, 2002).

CHAPTER THREE

MATERIALS AND METHODS

This chapter consists of six sections (Sections 3.1 to 3.6). Section 3.1 describes the study area (location, climate, relief, drainage, vegetation, and geology). Section 3.2 is a description of data collection (desk study and field reconnaissance survey), and protocols used for sample collection and sample preparation. In Section 3.3, the analytical methods used for the determination of water quality parameters (pH, conductivity, turbidity, HCO_3^-, salinity, alkalinity, temperature) are described. The analytical methods and protocols: UV-Visible Spectrophotometry (for the determination of PO_4^{3-}, NO_3^-, SO_4^{2-}), atomic absorption spectrometry (for determination of As, Cd, Cu, Fe, Mg, Mn, Pb and Zn), and flame photometry (for determination of K and Na) are described in Section 3.4. Section 3.5 describes the determination of the stable isotopic (δ^2H and $\delta^{18}O$) composition of the water samples using the Liquid-Water stable Isotope Analyzer [based on Off-axis Integrated Cavity Output Spectroscopy (OA-ICOS) via Laser Absorption]. In the last section of this chapter, i.e. Section 3.6, Quality Control (QC) and Quality Assurance (QA) techniques employed during the course of the study are described.

3.1 STUDY AREA

3.1.1 Geographical Location of Study Area

The study was conducted at the Golden Star Bogoso/Prestea Limited (New Century Mine). The mine is located in Prestea [(latitudes: 05^o 26' 00" and 05^o 26' 28") and (Longitude: 02^o 06' 17" and 02^o 09' 00")], in the Prestea-Huni Valley district of the Western Region of

Ghana. The Prestea-Huni Valley district was carved out of the former Wassa West District in 2004, in pursuance of the Government of Ghana decentralization and local government reform policy (MLGRD, 2006). The district has Bogosu as its administrative capital, and covers an area of 1514.7 km^2 with a population density of 105.2 inhabitants/km^2 (GSS, 2010).

The Prestea-Huni Valley district shares boundaries with Mpohor –Wassa East district to the east, Wassa-Amenfi West district to the west, Tarkwa-Nsuaem and Nzema East municipalities to the south, and Wassa-Amenfi East district to the north (MLGRD, 2006).

3.1.2 Climate and Relief

Prestea is under the influence of the wet semi-equatorial climate and characterized by a double rainfall maxima. The two rainfall seasons are interspersed by a dry season.

The main rainy season is from March to June and the minor season from September to November. Dry season occurs from December to February with little rain in January. The mean annual rainfall is between 1250 mm and 2000 mm. Temperature and Relative Humidity are usually uniformly high throughout the year with mean values not less than 26.6 ^oC and 70 % respectively (Dickson and Benneh, 1998).

3.1.3 Drainage and Vegetation

The vegetation of Prestea is classified under the moist deciduous forest, which is located within the wet semi-equatorial climate. The vegetation belt is classified into three strata,

the upper, middle and lower layers and contain most of the country's valuable timber such as *Triochinton scleroxylon* "Wawa", *Antiaris africana* "Kyenkyen", Chlorophora excels "Odum", and other tropical plants. Trees of the upper and middle layers of the moist deciduous forest exhibit deciduous characteristics during November to March when the harmattan conditions prevail. The middle and lower layers form a continuous canopy, which hinders undergrowth as much light does not reach the floor of the forest. Trees of the upper layer are however, scattered called emergent. Due to the all year round high temperatures and rainfall within the south western equatorial climate, plant growth is throughout the year giving rise to luxuriant and evergreen covering within the rain forest. The rapid growth characterized by shedding of leaves, flowering and fruiting produces much litter to the floor of the forest, (Dickson and Benneh, 1998).

The Prestea town is drained by River Ankobra and its tributary, River Assesre.

3.1.4 Geology of the area.

Ghana is geologically divided into four distinct major lithostratigraphic complexes composing of Paleoprotozoic supercrustal and intrusive rocks (Birimian supergroup, Tarkwaian Group, 'Tamnean' Plutonic Suite, Eburnean Plutonic Suite); Neoprotozioc to Early Cambrian Rocks (Voltaian Supergroup); the Panafrican Dahomayide Orogenic Belt Rocks (Buem Structural Units, Togo Structural Units and Dahomeyan Supergroup) and Isolated and Spatially restricted Coastal Sedimentary Basins of Odavician to Crataceous age (Sekondian Group, Accraian Group, Amisian Group and Appollonian group) (GSD, 2009).

Folded and metamorphosed rocks of early Protozoic age that were intruded by granitoids during the Eburnean Orogeny, largely make up the man shield (Hirdes et al., 1992). The Man shield is relatively stable around 1.7 Ga ago and comprises western domain mainly of Archean rocks of Liberian age (3.0 – 2.5 Ga) and an eastern domain of early Protozoic Birimian Supergroup [Hirdes et al., (1992); and Tailor et al., (1992)].

Significant part of Ghana's geology is the Birimian Supergroup (Fig. 3.1). The Birimian Supergroup, which hosts most of the mineral deposits, occupies most of the southern, western and northernmost parts that forming one-sixth potion of the country,

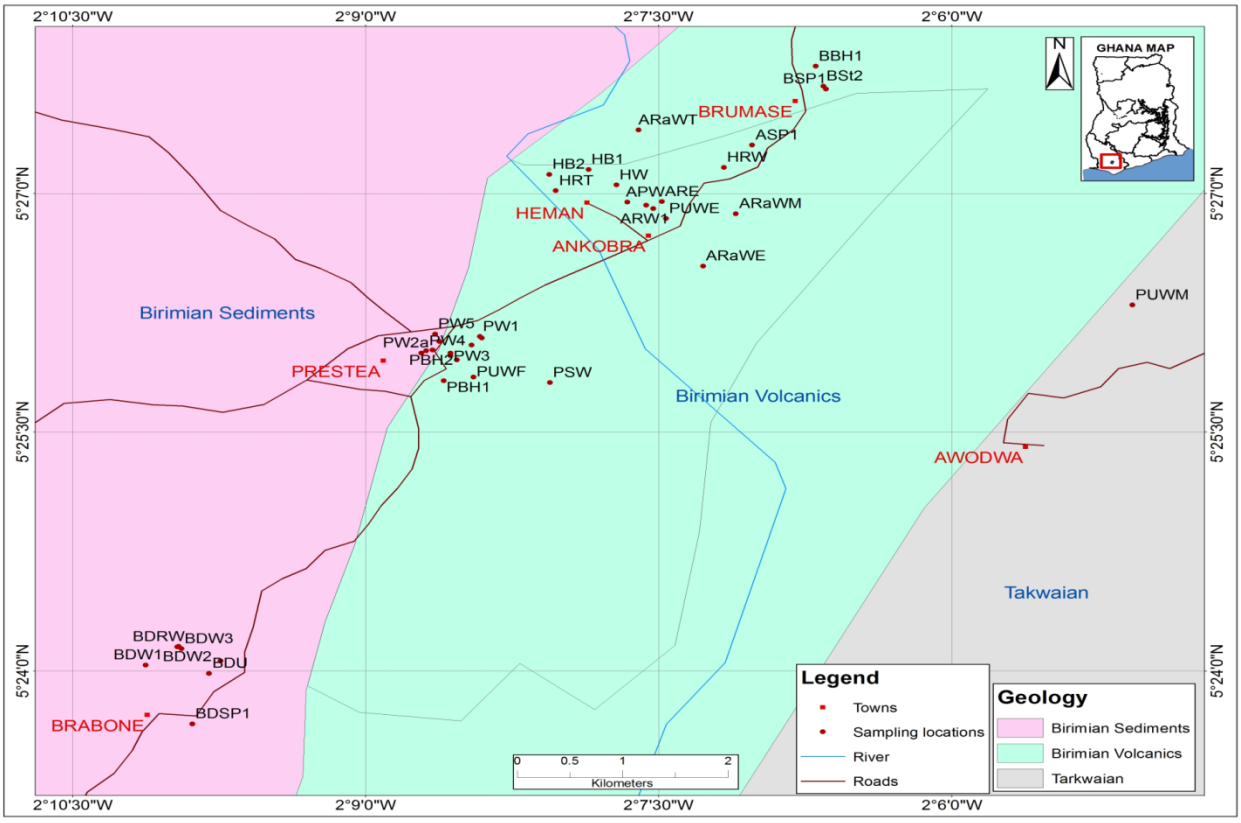

Fig. 3.1: Geological map of Ghana showing the Birimian Supergroup

Volcano-Plutonic and Sedimentary-Volcanic-Sedimentary groups are the two-fold lithostratigraphic systems, with overlying younger arenaceous and clastic Tarkwa Group are intruded by granitoids [Leube et al., 1990); Hirdes et al., (1992); Taylor et al., (1992); GSD, (2009)].

The Volcano-Plutonic group is separated from Sedimentary-Volcano-Sedimentary group although they represent contemporaneous lateral facies with sedimentation probably from the bulk of belt volcanic, volcanoclastics and associated synvolcanic belts formed in the time span between 2195 and 2150 Ma (GSD, 2009).

Chemical facies occur between belt volcanic and basin sediments in the transition zone. Cherts, manganiferous and carbon-rich sediments, Fe-Ca-Mg carbonate and sulphide mineral dissermination define these zones.

In the course of the Eburnean tectono-thermal event, the Birimian lavas and sediments were folded, intruded by various types of granotoids, uplifted and eroded. The sediments that were deposited as erosion product is the Tarkwaian Group, which is a long narrow intramontane garbens, formed due to rifting preferentially in the central portions of the Birimian Volcanic belts. Gravity tectonics deformed Tarkwaian Sediments (Leube et al., 1990).

Sandstones minor agillites, polymictic and quartz –pebble conglomerates, siltstones and tuffs make up the Tarkwaian Group (GSD, 2009). The studies on the Birimian rocks, geochronogically suggested by Abouchani et al., (1992) showed that, they were formed during the interval – 2.3 to 2.0 Ga.

3.1.4.2 The Birimian Volcano-Plutonic Group

In Ghana, most of the mineral resources are hosted by the Birimian Volcano-Plutonic Group (Birimian metavolcanic rocks), consisting of six belts; the Wa-Lawra, Bole-Nangodi, Bui-Banda, Sefwi, Ahanti and Winneba-Kibi belts.

The Five belts trend along the regional strike (NE-SW) and are several hundred-kilometers long, evenly spaced and parallel while the remaining Wa-Lawra belt trends in the N-S direction (Leube et al., 1990).

Comagmatic, synvolcanic trondhjemite-tondite-grandiorite (TTG) granitoides plutons, mainly tonalities and grandiorites are intruded in the volcanic belts (GSD, 2009).

The synvolcanic intrusives in the Birimian supergroup are the belt-type granitiods, basin-type granitiods, Bongo granitiods, Tongo granitiods, and the Winneba granitiods. Other post-Birimian intrusive rocks include granite, apalite, porphyry and pegmatite (Asiedu et al., 2004).

Lithologically and genetically, rocks of the volcano-plutonic are diverse. It is a low grade metamorphic theoleitic basalts with intercalated volcaniclastics, minor andesitic and felsic flow rocks and chemical sediments composed of manganese-stones and cherts dominate this group [Attoh et al., (2006); GSD, (2009)].

The Birimian greenstone belts formed in oceanic island arc environment was as a result of lithologic association, together with geochemical characteristic of the volcanic rocks [Attoh et al., (2006); Dampare et al., (2008)].

3.1.4.1.3 The Birimian Sedimentary-Volcano-Sedimentary Group

The Birimian Sedimentary-Volcano-Sedimentary group rocks, formally called Birimian metasedimentary basin show similar pattern to that of the Birimian Volcano-Plutonic group [Taylor et al., (1992); GSD, (2009)]. They consists of banded manganese and tightly isoclinically folded sediments comprising volcanoclastics, turbidite-related wackes, argilitic rocks and volcanogenic sediments [Attoh et al., (2006); GSD, (2009)].

The volcaniclastics consist of the sand-to-silt-sized partly reworked pyroclastics and volcanogenic epiclastic rocks of varying proportion. The turbidite-related wackes consist of cherts (syn- or epigenic), graphic schists and quartz. The agilitic rocks consist of phyllites and carbonaceous schists which are frequently interbedded with fragmental sediments. The sediments that formed the Birimian Sedimentary-Volcano-Sedimentary group rocks were probably largely derived from the adjacent volcano-plutonic belts either as detritus or as proximal distal ejacta from belt volcanism (GSD, 2009).

3.2 DATA COLLECTION, SAMPLING AND SAMPLE PREPARATION PROTOCOL

3.2.1 Data collection

3.2.1.1 Desk Study

In order to achieve the objectives of the study, a desk-study was carried out to assess the general hydrological and hydrochemical facies prevailing in the surface and groundwaters in and around Golden Star Bogoso/Prestea Limited (GSBPL) [New Century Mine (NCM)]. This task involved literature review, collection of topographical maps, and collection of

data from Ghana Meteorological Agency. Availability of equipment at Ghana Atomic Energy Commission (GAEC), GSBPL (Environmental laboratory) and Geological Survey Department was assessed.

3.2.1.2 Reconnaissane Field Work

This task was carried out prior to actual sampling, in order to identify the type of kits that were required for the sampling task, to identify the types of surface water (rivers, stream) and groundwater(hand-dug wells and boreholes) to be collected and also to locate the sampling points.

For the underground mine, a trip was organized during the one-week training for familiarization (activities taking place) and to locate the, sumps, streams and reservoirs sampling points.

3.2.2 Sampling

Sampling of surface water, spring water, underground mine water, and ground water was carried out between October 2013 and March 2014.

3.2.2.1 Sampling containers

All polyethylene containers (bottles) with the exception of stable isotopes containers were immersed for at least 48 hours in a 10% (v/v) HNO_3 solution and thoroughly rinsed with

double-distilled water before use [Mahpatatra et al., (2001); Morren et al., (2006); Bohrer et al., (2007)].

3.2.2.2 Field work

Three different types of water samples (surface water, groundwater and underground mine water) were collected using the sampling scheme in (Fig 3.1).

3.2.2.2.1 Collection of water samples

Collection of Groundwater and Surface water

The groundwater samples were collected in pre-conditioned high density polyethylene bottles (HDPB) of volume 500 mL at the sampling sites, prior to the collection of the surface water samples. The sampling bottles were rinsed three (3) times with the water to be sampled, followed by filling the bottle with water to the brim [Donkor et al., (2006); Serfo-Armah et al., (2004)].

At each sampling point, three (3) water samples were taken; for the determination of trace metals, major ions and stable isotopes. Trace metals and major cations samples were acidified with two (2) drops of concentrated 65 % HNO_3 just after the collection of the water samples; this was to prevent the adsorption of the metals to the walls of the container as well as water hydrolysis.

The Global Positioning System (Germin eTrex 20, U.S.A.) reading for the sampling points was taken and recorded together with the date of sampling in the field after collection of the samples (Fig. 3.2 and Fig. 3.3).

The water samples were stored in thermo-insulated container with ice packs. However, samples for stable isotopes were also stored in thermo-insulated container without ice packs to prevent condensation of the lighter isotopes. One half of the samples collected were transported to the laboratories of Ghana Atomic Energy Commission (GAEC), Kwabenya in Accra. The other half were sent to the Golden Star Bogoso/Prestea Limited (GSBPL) Environmental laboratory situated at Bogoso for analysis of trace, major and minor elements.

Table 3.1: Description of sampling towns, sampling codes and type of samples

Surface water			Groundwater			Underground mine water		
Sampling Town	Sampling Code	Description of Sample	Sampling Town	Sampling Code	Description of Sample	Sampling Town	Sampling Code	Description of Sample
Ankobra	ASP	Spring from the foot of a hill	Ankobra	ABH	Borehole	Bondaye	UD-3A	Main Sump (Sources: 1, 2 & 3)
Brumase	BSP	Spring from a rock	Brumase	BBH	Borehole	Bondaye	UD-3B	Overflow Pipe (Level 1 & 2)
Brumae	BSt2	Surface water from BSP	Himan	HBH1	Borehole	Bondaye	UD-9A	Central Sump (Sources: 8L & 9L)
Bondaye	BDSt	Spring from the foot of a hill	Himan	HBH2	Borehole	Bondaye	UD-9B	Level 9 drive to Central Sump
Bondaye	BDSt2	Spring from the foot of a hill	Himan	HW	Well	Bondaye	UD-9C	Central Sump (Sources: 4,5,6,7 & 8)
Prestea	PSW	Spring from a rock	Bondaye	BDW1	Well	Prestea	UD-6B	Spring water from tunnel 1
Ankobra	ARaW (US)	River Ankobra	Bondaye	BDW2	Well	Prestea	UD-6C	Spring water from tunnel 2
Ankobra	ARaW (MS)	River Ankobra	Bondaye	BDW3	Well	Prestea	UD-6E	Flow from Level 7 pipe
Ankobra	ARaW (DS)	River Ankobra	Bondaye	BDW4	Well	Prestea	UD-6F	Drainwater before Central Sump
Himan	HRMT (US)	River Assesre	Prestea	PW1	Well	Prestea	UD-6G	Central Sump
Himan	HRMM (MS)	River Assesre	Prestea	PW2	Well	Prestea	UD-6H	D/S Cross Cut 23
Ankobra	ARWE (DS)	River Assesre	Prestea	PW3	Well	Prestea	UD-17A	Settling Dam A (North Shaft Water)
Prestea	PUWF (US)	Pumped Underground water	Prestea	PW4	Well	Prestea	UD-17B	Settling Dam B (North Shaft Water)
Prestea	PUWM (MS)	Pumped Underground water	Prestea	PW5	Well	Prestea	UD-17C	Ankobra Shaft Water and 17L
Prestea	PUWE (DS)	Pumped Underground water	Prestea	PBH1	Borehole	Prestea	UD-17D	24L water to 17L Central Sump
Bondaye	BDU (MS)	Pumped Underground water	Prestea	PBH2	Borehole	Prestea	UD-17E	Central Sump (Sources:14,15,16,&17)

Table 3.1: Description of sampling towns, sampling codes and type of samples

Surface water			**Groundwater**			**Underground mine water**		
Sampling Town	Sampling Code	Description of Sample	Sampling Town	Sampling Code	Description of Sample	Sampling Town	Sampling Code	Description of Sample
Bondaye	BDUWF (MS)	Pumped Underground water	Prestea	PBH3	Borehole	Prestea	UD-17F	Drilling Discahrge line (Sources:10-24L)
			Prestea	PBH4	Borehole	Prestea	UD-24A	Central Sump
			Prestea	PBH5	Borehole	Prestea	UD-24B	North End No 2 Shaft Sump
			Prestea	PBH6	Borehole	Prestea	UD-24C	Ore Pass (Source: above 24L)
			Prestea	PBH7	Borehoe	Prestea	UD-24E	Bondaye water (Gutter water)

US (Upper Stream) **MS** (Mid-Stream) **DS** (Down Stream) **L** (Level) **A** (Settling Dam) **B** (After Settling Dam)

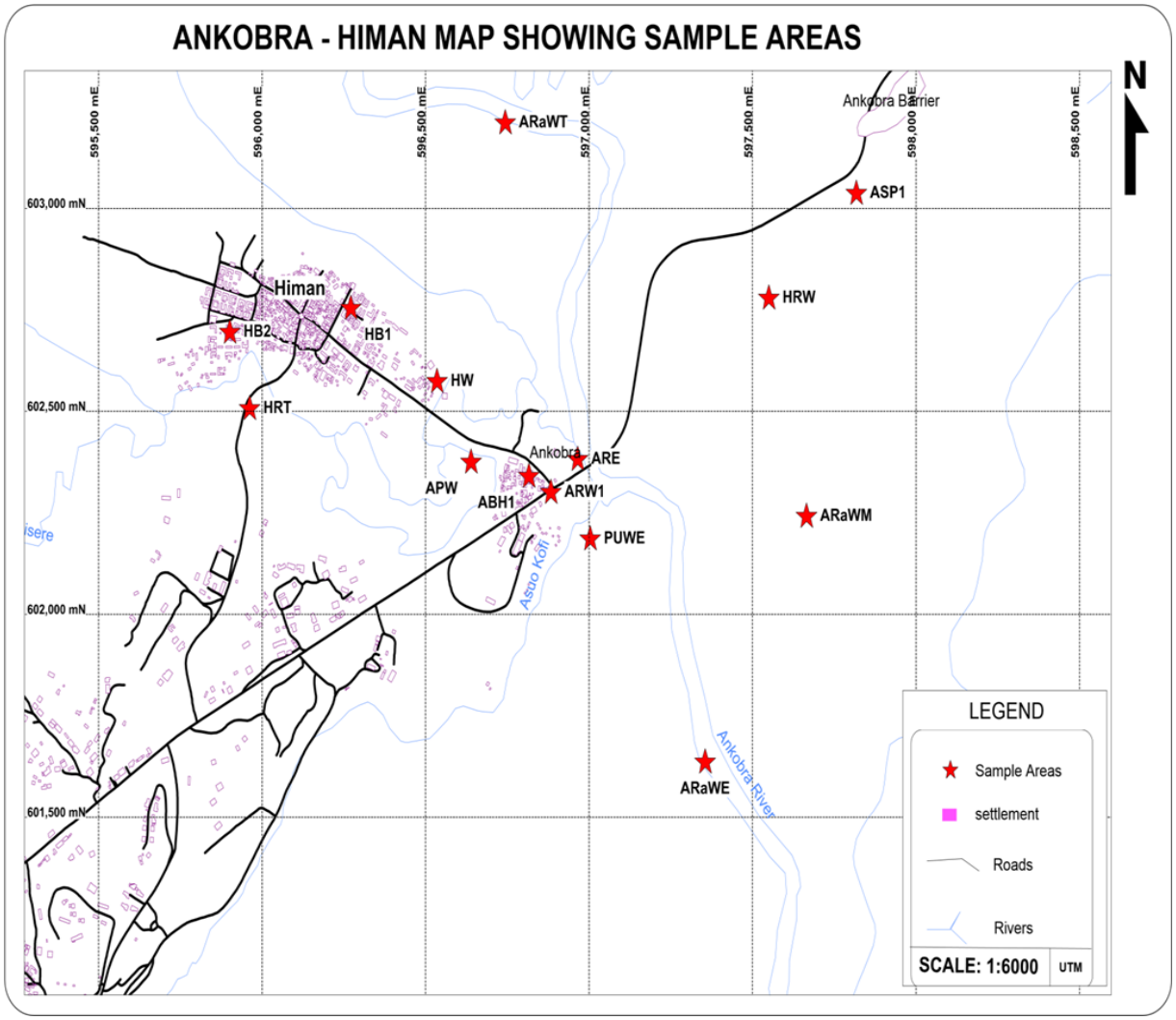

Fig.3.2: Sampling map showing Ankobra-Himan areas

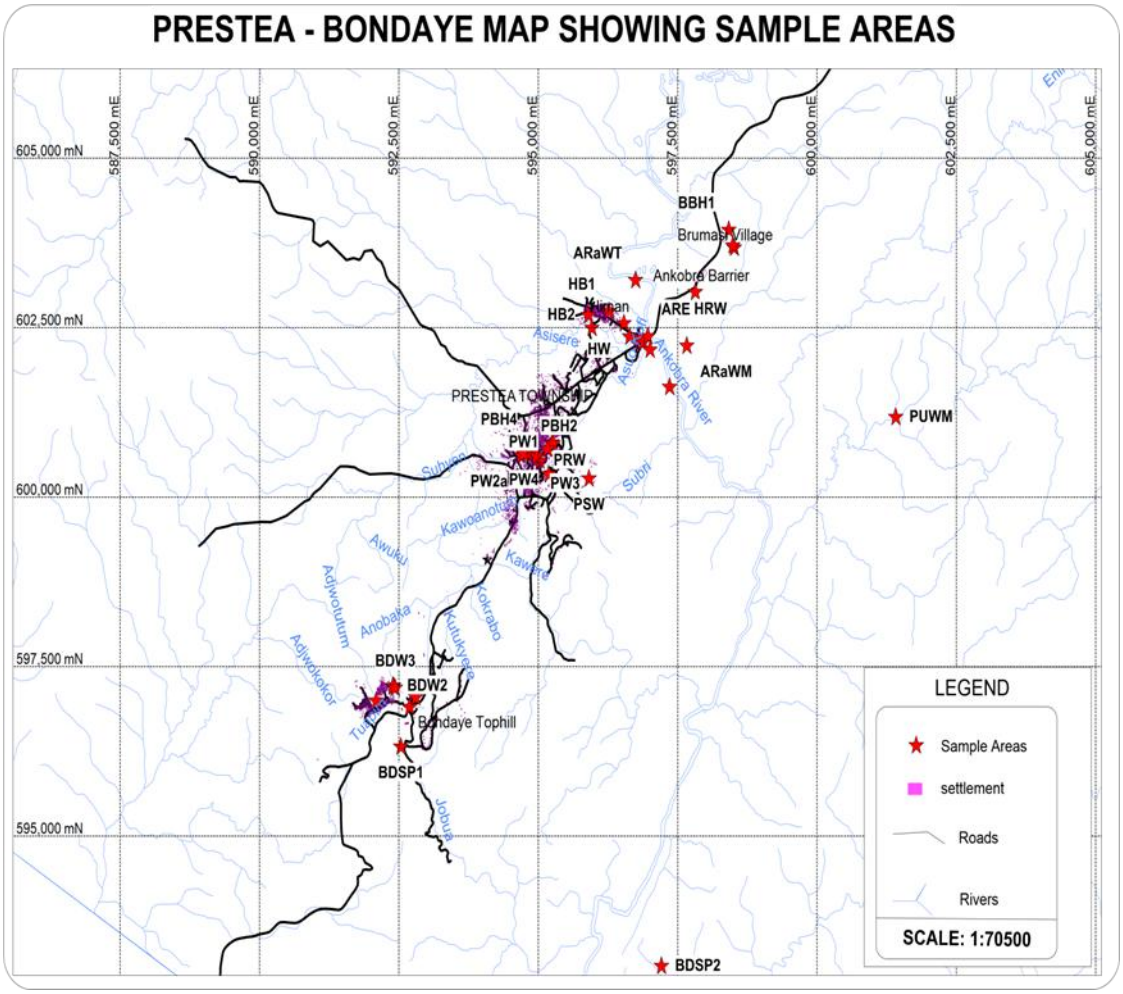

Fig. 3.3: Map of sampling area for the study area

3.2.2.2.2 Collection of water samples from New Century Mines (NCM) underground mine water

A one-week intensive in-service training course preceded the sampling of underground mine water at the GSBPL (NCM). The course was organized by the Safety Department of GSBPL (NCM). All the resource persons were professionals with several years of experience in the gold mining industry.

3.2.2.2.2.1 In-service Training Course Prior to Sampling

A one-week training course was organized by the Safety Department of the GSBPL (NCM). The syllabus for the training comprises the following:

(a) Safety in the mines, safety procedures and job description readiness (This was done with the aid of a hand-out produced by GSBPL and captioned 'Take 5- Stay Alive.")

(b) Procedures for proper handling of equipment and gadgets (example: the use of the device for breathing during rescue missions in underground operation called "proto mak five").

(c) Appropriate out-fits to wear during underground operations [These included: headlamp, headgear, eye goggles, overall jacket, safety belt, hard-boots and oxy-box (an emergency breathing aid used for 30-60 minutes when foul gases are encountered underground)].

(e) Emergency preparedness, as well as escape routes in the underground mine during emergencies.

(f) History of the GSBPL (NCM)

3.2.2.2.2.2 Collection of underground mine water

Underground mine water was collected at two (2) major sampling points within the mine; these are the Central shaft (located at Central Prestea) and the Bondaye shaft (located at the southern part of Prestea). Cages (a means of transport in underground mines) were used at both the Central Shaft and Bondaye Shaft.

Before departure to the underground mine, 500 mL pre-conditioned high density polyethylene (HDPB) sampling bottles were labelled and put in rubber sacks for easy transportation and handling following the scheme presented in (Table 3.2). With the assistance of the underground mine inspection team, and the direction given on the underground sampling map (Fig 3.4), the underground sampling points (Table 3.1) were located. However, most of the water samples were collected from the sumps, reservoirs, settlers and springs as well as streams along the drive ways and cross cuts (Fig 3.5).

Prior to the collection of underground mine water sample, the sampling bottles were rinsed three (3) times with the water to be sampled, followed by filling the bottle with water to the brim [Donkor et al., (2006); Serfo-Armah et al., (2004)]. At each sampling point, three (3) water samples were taken for determination of trace metals, determination of major ions and stable isotopes composition respectively.

All the water samples collected were transported to about 5 m from the Gangway (main entrance into the main drive after disembarking from the cage) and the following activities carried out:

(a) Trace metals and major cations samples were acidified with two (2) drops of concentrated 65% HNO_3 just after the collection of the water samples; this was to prevent the adsorption of the metals to the walls of the container as well as water hydrolysis [Mahapatra et al., (2001); Morren et al., (2006); Bohrer et al., (2007)]

(b) The depths of underground sampling points were taken and recorded together with the date of sampling at the Survey Department of GSBPL (NCM) after collection of the water samples.

The water samples were brought unto the surface via the same cages at both Central and Bondaye shafts. The water samples were stored in thermo-insulated containers with ice packs. However, samples for stable isotope analysis were stored in separate thermo-insulated containers without ice. The samples were transported to the laboratories of the Ghana Atomic Energy Commission (GAEC) located at Kwabenya, Accra, and Golden Star Bogoso/Prestea Limited (GSBPL) Environmental Laboratory situated at Bogoso. Aliquots of the water samples were used for all analysis at both laboratories.

Table 3.2: Scheme for sampling of water samples in GSBPL (NCM) underground mine

Prestea (Central Shaft)			Bondaye Shaft (Southern Part)		
Code/Level	Depth (m)	Number of samples	Code-Level	Depth (m)	Number of samples
UD-6	175.8	18	UDB-3	71.8	6
UD-17	597.3	18	UDB-9	323.8	9
UD-24	888.8	12			

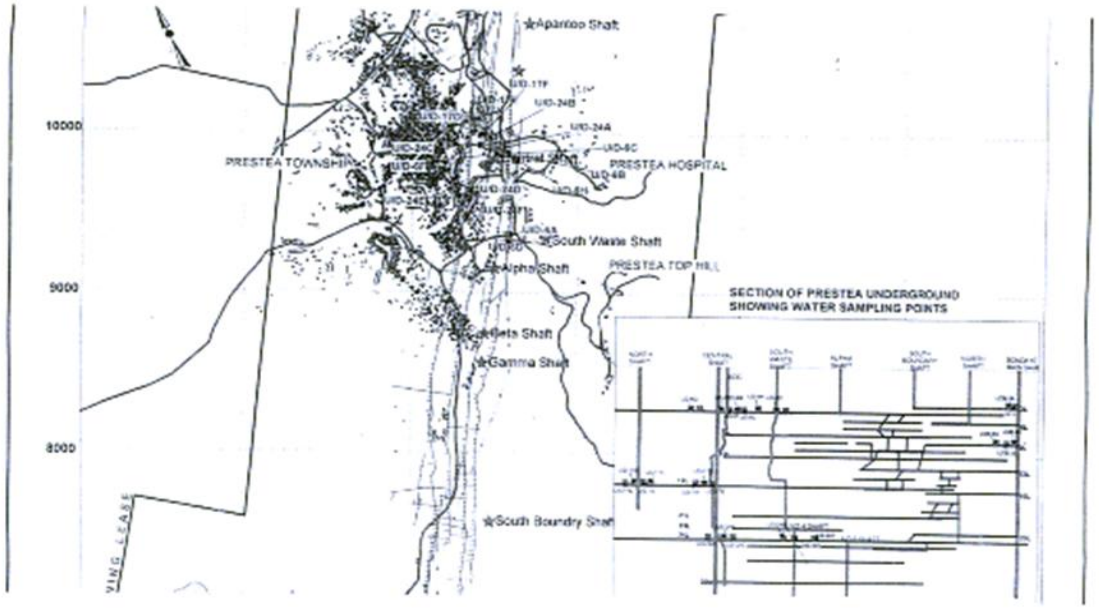

Fig. 3.4: Map of Prestea underground mine water sampling points (Adopted from N.C.M.)

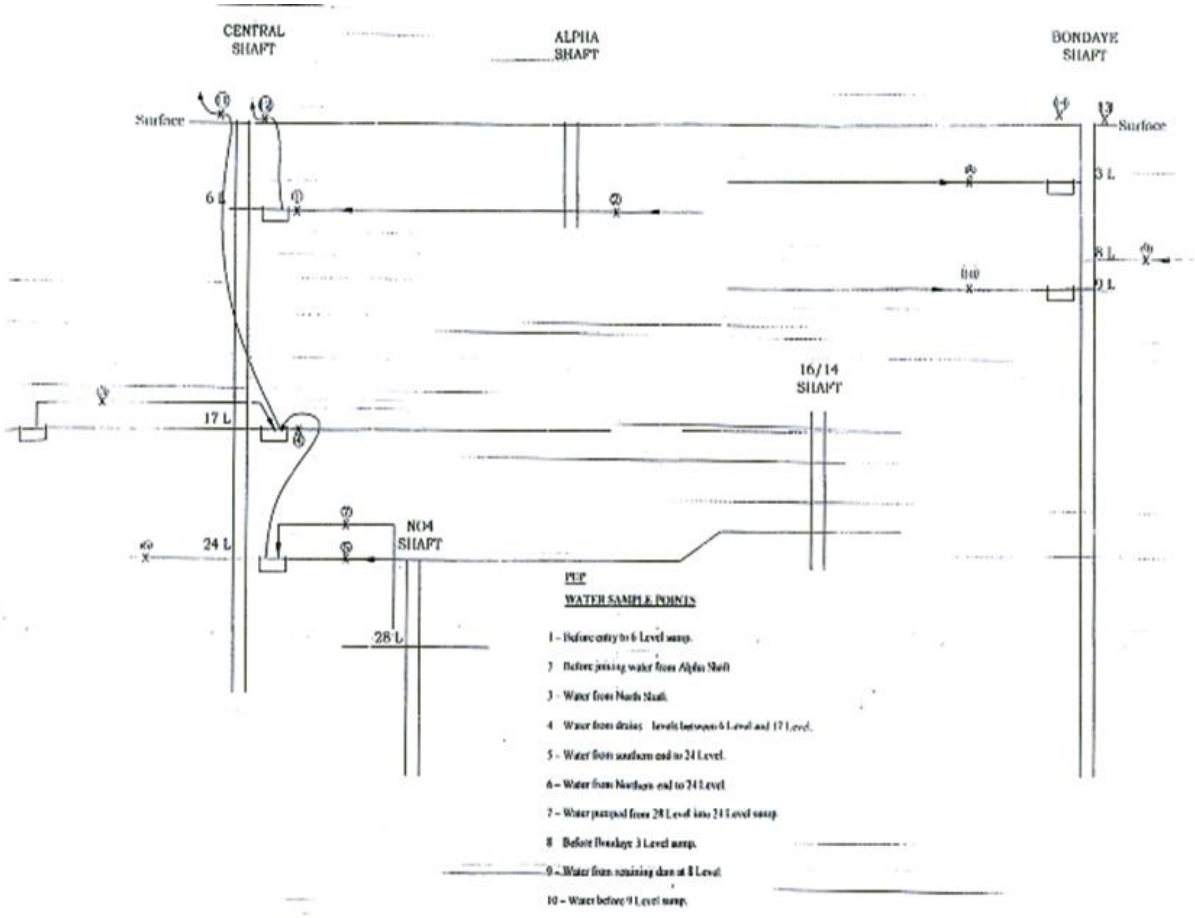

Fig. 3.5: A cross section of Prestea/Bondaye underground water sampling points (Adopted from NCM)

3.3 DETERMINATION OF WATER PARAMETERS

3.3.1 Measurement of field parameters

The following parameters were measured on the field. Theses were: pH, Temperature, Conductivity, Total Dissolved Solids (TDS), Bicarbonate, Alkalinity and Salinity.

pH, Temperature, Conductivity, Total Dissolved Solids (TDS) and Salinity were measured ***in-situ*** using the Hanna HI 991301 multi-functional pH/EC/TDS meter (Hanna Instruments, Canada). Alkalinity and bicarbonate were determined by titrimetry.

3.3.1.1 Conductivity, Salinity and Total Dissolved Solids (TDS)

Measurement of conductivity, TDS and salinity were done using the Hanna HI 991301 multi-functional pH/EC/TDS meter (Hanna Instruments, Canada). The meter was first calibrated (for conductivity) using the following standard solutions; 0.01 M KCl (Condictivity: 1413 µS/cm) and 0.1 M KCl (Conductivity: 12880 µS/cm). This was followed by the simultaneous determination of conductivity, TDS, and salinity.

3.3.1.2 pH and Temperature

3.3.1.2.1 Calibration of meter and determination

The pH of the water samples was determined on the field just after sampling, using the Hanna HI 991301 multi-functional pH/EC/TDS meter (Hanna, Canada). Prior to the determination, the pH meter was calibrated using two standard buffer solutions of pH 4.01 and 7.01, respectively.

The procedure for the pH determination is described below:

Sufficient volume of water samples were placed into separately labelled 100 mL beakers. The samples were stirred with a magnetic stirrer, and the sensing electrode of the pH meter

placed into the water sample. The pH and temperature of the samples were simultaneously read and recorded.

The calibration of the meter was verified after measurement of every four water samples. After each reading, the electrode was rinsed with double-distilled water and a small portion of the next sample water to be determined.

3.3.1.3 Determination of Alkalinity and Bicarbonate

Alkalinity and bicarbonate contents of the water samples (surface water, groundwater and underground water) were determined by titrimetry using HCl as titrant and methyl orange indicator.

Principle

The alkalinity of water is attributed to the presence of: caustic alkalinity (due to OH^- and CO_3^{2-}) and temporary hardness (due to HCO_3^-). Alkalinity of water means the total content of the substances (OH^-, CO_3^{2-} and HCO_3) in it which causes an increase in the OH^- ion concentration due to dissociation or hydrolysis. Alkalinity is therefore a measure of ability of water to neutralize acids.

In the determination of total alkalinity, the contents of OH^-, CO_3^{2-} and HCO_3^- are estimated together by titration against a standard acid (HCl) using methyl orange as indicator.The determination is based on the following reactions as shown in equations 3.1, 3.2 and 3.3.

$$OH^-_{(aq)} + H^+_{(aq)} \rightarrow H_2O_{(l)} \qquad \textbf{3.1}$$

$$CO_3^{2-}{}_{(aq)} + H^+{}_{(aq)} \rightarrow HCO_3^-{}_{(aq)} \quad \textbf{3.2}$$

$$HCO_3^-{}_{(aq)} + H^+{}_{(aq)} \rightarrow H_2O_{(l)} + CO_{2(aq)} \quad \textbf{3.3}$$

Apparatus

50 mL Burette; 25 mL pipette; 250 mL conical flask

Experimental procedure

About 5 mL aliquot of the water sample was transferred into a 250 mL conical flask. This was followed by the addition of two drops (~ 1 mL) of methyl orange indicator. The contents of the conical flask were mixed thoroughly by swirling (a deep yellow colour was developed). The water sample was then titrated against 0.02M HCl solution, till the deep yellow colour changed to pale yellow (signifying the end point of the titration). The titration was stopped and the volume of titrant (HCl) used was recorded. Two replicate titrations were carried out.

Alkalinity was calculated using equation 3.4.

$$Alkalinity(mg/L\ CaCO_3) = \frac{A \cdot M \cdot 5000}{V_{sam}} \quad \textbf{3.4}$$

where: **A** is the average titre value in mL; **M** is the molarity of acid (HCl solution); and, $\mathbf{V_{sam}}$ is the volume in mL of the water sample.

The bicarbonate concentration was calculated using equation 3.5.

$$\left[HCO_3^-\right] = (1.2191817) \cdot (Alkalinity) \qquad \textbf{3.5}$$

3.3.1.4 Determination of Chloride by Titrimetry (Argentometric Method)

The chloride content was determined by titrimetry using the Argentometric method (APHA 1992, 4500-Cl-B).

Principle

The method is based on the titration of the water sample with silver nitrate ($AgNO_3$) using potassium chromate ($K_2Cr_2O_4$) as indicator. As the silver nitrate solution is slowly added, a precipitate of silver chloride forms as illustrated in equation 3.6.

$$Ag^+_{(aq)} + Cl^-_{(aq)} \rightarrow AgCl_{(s)} \qquad \textbf{3.6}$$

The end point of the titration occurs when all the chloride ions are precipitated. Then additional silver ions react with the chromate ions of the indicator, potassium chromate, to form a red-brown precipitate of silver chromate as in equation 3.7.

$$2Ag^+_{(aq)} + CrO_4^{2-}{}_{(aq)} \rightarrow Ag_2CrO_{4(s)} \qquad \textbf{3.7}$$

Apparatus

50 mL Burette; 25 mL pipette; 250 mL conical flask

Standards solutions and Reagents

Potassium Chromate Indicator Solution

A 50 mL potassium chromate indicator was prepared by dissolving 2.5 g $K_2Cr_2O_4$ in 250 mL volumetric flask with double-distilled water and allowed to stand for 12 hours. The supernatant was filtered and diluted to 50 mL mark with double-distilled water.

Silver Nitrate Titrant Solution (0.0141 M)

A 0.0141 M silver nitrate ($AgNO_3$) solution was prepared by dissolving 2.395 g of $AgNO_3$ in double-distilled water and diluted to the mark in a 1000 mL volumetric flask. The solution was standardized against NaCl solution and stored in amber coloured bottle in a cool place away from light.

Experimental procedure

The procedure for the determination of chloride in the water samples (surface, groundwater and underground mine water) was as follows:

About 25 mL aliquot of the water sample was placed in a 250 mL conical flask, followed by the addition of two drops (~ 1.0 mL) of potassium chromate ($K_2Cr_2O_4$) indicator. The contents of the conical flask were thoroughly mixed by swirling. The contents of the conical flask turned yellow. The water was then titrated against the standardized 0.0141 M

$AgNO_3$, till the colour of the water changed to pinkish red (signifying the end point of the titration). The volume of titrant used was computed and recorded. For each water sample, two replicate titrations were performed.

The amount of chloride in the unknown water samples was determined using equation 3.8.

$$Cl^- \ (mg/L) = \frac{(A - B) \cdot N \cdot 35.45 \cdot 100}{V_{sam}} \qquad \textbf{3.8}$$

where: A is the average titre, B is the titre value for the blank solution; N is the molarity of $AgNO_3$ (0.0141 M), and 35.45 is Relative atomic mass of chlorine.

3.3.1.5 Determination of Calcium (Ca^{2+}) content in water samples

Complexometric titration was used for the determination of Ca^{2+}. The titration is based on the titration of water samples with ethylene diamine tetra-acetic acid (EDTA) using ammonium purpurate (murexide) powder as indicator. Murexide at pH 11 is purple in colour, however, in the presence of Ca^{2+} ions, it forms a pink complex.

Apparatus

50 mL Burette; 25 mL pipette; 250 mL conical flask

Standard solutions and Reagents

Murexide indicator

200 mg of the murexide was mixed with 100g of solid NaCl, the mixture were grinded to 40-50 meshes and was used as the indicator.

Standard EDTA solution (0.01 M) [Titrant]

A 0.01M EDTA solution was prepared by dissolving 1.179 g of disodium salt of ethylene diamine tetra-acetic acid dehydrate (analytical reagent grade) and 780 mg magnesium sulphate ($MgSO_4.7H_2O$) in 50 mL double-distilled water. The solution was added to 16.9 g NH_4Cl and 142 mL of concentrated NH_4OH by mixing and diluted to 250 mL volumetric flask with double-distilled water.

Experimental procedure

The procedure for the determination of chloride in the water samples (surface, groundwater and underground mine water) was as follows:

About 50 mL of distilled water (blank) and a 50 mL aliquot of the water sample were transferred into two different 250 mL conical flasks. This was followed by the addition of 5 mL of 1 M NaOH solution and approximately 50 mg of the powdered murexide indicator to each conical flask. The contents of the conical flask were thoroughly mixed by swirling resulting in the formation of a pink colour. The content of each conical flask was then titrated against 0.01 M EDTA, till the pinkish colour of the water changed to purple (signifying the end point of the titration).

In the final stage of the titration, ETDA was added drop-wise as the colour change was not instantaneous and the end point colour of the sample was compared to the end point colour of the blank solution. The volume of titrant used was computed and recorded. For each water sample, two replicate titrations were performed.

Reaction taking place during the titration is shown in equation 3.9:

$$Ca^{2+} + EDTA \xrightarrow{Murexide} [Ca^{2+} - EDTA\ complex] \qquad \textbf{3.9}$$

Calculation

The amount of calcium in each the water sample was calculated using equation 3.10.

Molarity of EDTA solution is 0.01 M mL of 0.01 M EDTA = 1 mg of $CaCO_3$

EDTA molarity x EDTA volume (L) = Ca^{+2} molarity x Ca^{+2} volume (L) using volumes

$$CaCO_3\ (mg/L) = \frac{V_{EDTA}\ (mL) \cdot 1\ mg\ CaCO_3}{V_{Sam}\ (L) \cdot 1\ mL\ EDTA} \qquad \textbf{3.10}$$

3.4 DETERMINATION OF MAJOR ANIONS AND ELEMENTAL COMPOSITIONS

3.4.1 Determination of Phosphate (PO_4^{3-}), Sulphate (SO_4^{2-}) and Nitrate (NO_3^-)

The phosphate, sulphate and nitrate concentrations in the water samples were determined according to the official methods in the Association of Official Analytical Chemists

(AOAC International, 2007). Phosphate was determined by Official method 4500-P E (Ascorbic acid method). Official method 4500-SO_4^{2-} E (Turbidimetric method) was used for the determination of sulphate. Nitrate was determined using AOAC Official method 973.50.

3.4.1.1 Determination of Phosphate (PO_4^{3-})

Principle

Ammonium molybdate and potassium antimonyl tartrate react in acid medium with orthophosphate to form an antimonyl-phosphomolybdate complex, which is reduced to intensely coloured molybdenum blue by ascorbic acid. The absorbance of the molyddenum blue is measured at a wavelength of 880 nm on a UV-visible spectrophotometer.

Instrumentation

A Shimadzu UV-1201 UV-visible Spectrophotometer (Japan) with 1 cm matching quartz cells was used for absorbance measurements.

Chemicals and Reagents

Ammonium heptamolybdate, $[(NH4)_6Mo_7O_{24}{\cdot}4H_2O]$, Potassium antimonyl tartrate $[K(SbO)C_4H_4O_6.5H_2O]$, Sulphuric acid (96% H_2SO_4), Ascorbic acid.

Potassium Antimony Tartrate [$K(SbO)C_4H_4O_6$ ½H_2O]

500 mL potassium antimony tartrate solution was prepared by dissolving 1.375 g $K(SbO)C_4H_4O_6$ ½H_2O in about 400 mL double-distilled water and diluting to 500 mL. The solution was stored in a glass-stoppered bottle.

Ammonium Molybdate [$(NH_4)_6Mo_7O_{24}\cdot 4H_2O$] Solution

A 500 mL ammonium molybdate [$(NH_4)_6Mo_7O_{24}\cdot 4H_2O$] solution was prepared by dissolving 20 g ammonium molybdate with double-distilled water and diluting to the 500 mL mark.

Ascorbic Acid

A 0.1 M ascorbic acid solution was prepared by dissolving 1.76 g ascorbic acid in double-distilled water and diluting to the 100 mL mark. Since ascorbic acid solutions are not stable for long periods of time at room temperature, they were always prepared fresh.

Combined Reagent

The combined reagent is an acidic (H_2SO_4) solution of potassium antimony tartrate, ammonium molybdate and ascorbic acid.

About 100 mL combined reagent was prepared by adding 50 mL of 5 M H_2SO_4 to a mixture of 5 mL potassium antimony tartrate, 15 mL ammonium molybdate and 30 mL ascorbic acid. After the addition of the reagents, it was allowed to attain room temperature, followed by thorough mixing. The combined reagent was stored in a plastic bottle. The reagent is always prepared fresh because it is stable for only four hours.

Phosphate Standard

A stock standard phosphate solution (50 $mg \cdot L^{-1}$) was prepared by dissolving 219.5 g of oven-dried potassium dihydrogen phosphate, KH_2PO_4, in double distilled water to make 1000 mL of solution. Working solutions of concentrations 0.2, 0.4, 0.6, 0.8, and 1.0 mg L^{-1} were prepared daily by appropriate dilution of the stock.

Calibration of UV-Visible spectrophotometer

In order to construct a calibration curve, 10 mL aliquot of the calibrant solutions were transferred into separate 20 mL test tubes. To each test tube, 2 mL of the combined reagent was added to each test tube, and left for about 5 minutes. During this period, the blue colour of antimonyl-phosphomolybdate complex was developed in each test tube. Appropriate aliquot of each blue-coloured calibrant solution was transferred into a 1 mL cuvette; the cuvette was inserted into the spectrophotometer and the absorbance measured at a wavelength of 880 nm against a reagent blank.

A calibration graph of absorbance against concentration of PO_4^{3-} in each calibrant solution was plotted. The concentration of PO_4^{3-} in the water samples were deduced from the calibration graph.

Determination of phosphate in water samples

About 10 mL aliquot of the water sample was transferred into a 20 mL test tube and the same procedure as used for the establishment of the calibration graph was followed to

obtain the absorbance of each water sample at a wavelength of 880 nm on the UV-visible spectrophotometer. The concentration of PO_4^{3-} in each water sample was obtained from the calibration graph.

3.4.1.2 Determination of sulphate (SO_4^{2-})

Principle

The method is based on the reaction of sulphate ion (SO_4^{2-}) with barium chloride ($BaCl_2$) under acidic conditions to precipitate barium sulphate ($BaSO_4$). The absorbance of the white $BaSO_4$ suspension is measured at a wavelength of 420 nm on a UV-visible spectrophotometer.

Instrumentation

A Shimadzu UV-1201 UV-visible Spectrophotometer (Japan) with 1 cm matching quartz cells was used for absorbance measurements.

Chemicals

Barium chloride ($BaCl_2$, 99.999 %), Sodium chloride (NaCl), Hydrochloric acid (HCl), Sodium sulphate (Na_2SO_4), glycerol

Reagents and Standards

Acid Salt Solution

60 g NaCl was dissolved in 5 mL of 37 % HCl and diluted to volume with double-distilled water in a 250 mL volumetric flask.

Sulphate Standards

A stock standard sulphate solution (100 mgL^{-1}) was prepared by dissolving 0.1479 g of anhydrous Na_2SO_4 in double distilled water to make 1000 mL of solution. Working solutions of concentrations 15, 20, 25, 30 and 35 mgL^{-1} were prepared daily by appropriate dilution of the stock.

Calibration

About 10 mL of the standard SO_4^{2-} calibrant solutions were quantitatively transferred into separate test tubes. To each test tube, 1 mL of the acid salt solution, 0.5 mL of glycerol solution (conc.) and 0.5 g $BaCl_2$ were added. The resulting cloudy solution was shaken for 60 sec and left for 5 min. appropriate aliquot of the cloudy solution was transferred into 1 cm cell and the absorbance of the coloured solution measured at a wavelength of 420 nm on the UV-visible spectrophotometer. The absorbance of each calibrant solution was plotted against the concentration of the calibrants. A straight line graph was obtained. The concentration of the water samples were deduced from the graph after measurement of the absorbance of each water sample at a wavelength of 420 nm on the UV-visible spectrophotometer.

Determination of Sulphate in water samples

About 10 mL aliquot of the water sample was transferred into a 20 mL test tube and the same procedure as used for the establishment of the calibration graph was followed to obtain the absorbance of each water sample at a wavelength of 420 nm on the UV-visible

spectrophotometer. The concentration of SO_4^{2-} in each water sample was obtained from the calibration graph.

3.4.1.3 Determination of Nitrate (NO_3^-)

Principle

The method is based on the reaction of the nitrate ion with brucine sulfate in a H_2SO_4 solution at a temperature of 100 °C. The yellow colour of the resulting complex is measured at a wavelength of 410 nm.

Standards

A stock standard nitrate solution of concentration 100 mg/L was prepared by dissolving 0.7218 g of KNO_3 (pre-oven dried at 105 ºC for 24 hours) in double distilled water to make 1000 mL of solution. The stock solution was preserved with 2 mL $CHCl_3$ .Working calibrant solutions of concentrations 0.2, 0.4, 0.6, 0.8, and 1.0 mg L^{-1} were prepared daily by appropriate dilution of the stock.

Reagents

Brucine-Sulfanilic Acid Reagent

About 1 g of brucine sulfate $[(C_{23}H_{26}N_2O_4)_2\ H_2SO_4\ 7H_2O]$ and 0.1 g sulfanilic acid $(NH_2C_6H_4SO_3H\ H_2O)$ were dissolved in 70 mL hot double-distilled water. 3 mL conc. HCl

was added; the resulting solution was cooled and diluted to the 100 mL mark with double-distilled water. The reagent was stored in a dark bottle at 5 °C.

Calibration

5 mL of each calibrant solution was pipetted into separate 20 mL test tube. To each test tube, 1 mL of 30% NaCl was added, followed by the addition of 5 mL of 6.5 M H_2SO_4. The test tubes were swirled to ensure thorough mixing of the reagents. 0.5 mL of the brucine-sulfanilic acid reagent was added to the content of each tube (except blank). The test tubes were then placed on a rack and lowered into a water bath at 95 ºC for 25 minutes. At the end of the 25 minutes, the rack of test tubes was removed from the bath and immersed in ice. An appropriate aliquot of the yellow coloured calibrant solutions was transferred into a 1 cm cell. The cell was placed into the spectrophotometer and the absorbance of the solution measured at a wavelength of 410 nm.

A standard graph of absorbance of standards against concentration of standards was plotted.

Determination of nitrate in samples

About 5 mL aliquot of the water samples were transferred into separate 20 mL test tube and the same procedure as used for the establishment of the calibration curve was followed to obtain the absorbance of each water sample at a wavelength of 410 nm on the UV-visible spectrophotometer. The concentration of NO_3^- in each water sample was deduced

from the calibration graph. The concentration was calculated from the relation in equation 3.11.

$$C_{NO_3^-} = C_{Calib.} \cdot D_f \qquad \textbf{3.11}$$

Where: $C_{NO_3^-}$ is the nitrate concentration, $C_{Calib.}$ is the concentration from the calibration curve and D_f is the dilution factor.

3.4.2 Determination of Sodium (Na) and Potassium (K) Contents

The levels of sodium (Na) and potassium (K) in the water samples were determined by the flame emission absorption photometric method, using the Sherwood 420 Flame Photometer (Sherwood, UK).

Reagents

Suppressor solution- A 100 mg/L lithium (Li) solution was prepared by dissolving 6.941g $Li_2SO_4.H_2O$ in double-distilled water and diluted to 1000 mL volumetric flask.

The suppressor solution is important because Na, K and Li are in group one of the periodic table. The addition of Li is to suppress the other group one elements (Rb, Cs and Fr) present in the water samples with the exception of Na and K.

Standards

Mixed Na/K calibration standard-A 100 mgL^{-1} mixed Na and K calibration standard was prepared by pipetting 1 mL of each commercially-available stocks Na and K standards into a 10 mL volumetric flask and diluted to the mark.

Calibration

2 mL of the suppressor solution was added to 5 mL of the mixed Na and K standards thoroughly mixed by swirling. The combined solution was aspirated into the liquefied petroleum gas LPG-fed flame of the Shewood 420 Flame Photometer. The concentrations of Na and K were read at their respective wavelengths (Na: 589 nm and K: 766.5 nm). This was preceded by the analysis of blank solution and subsequently the water samples.

Analysis of water samples

A blank solution made of thoroughly mixed double-distilled water-suppressor solution (5:2) was aspirated into the LPG-fed flame of the Sherwood 420 Flame Photometer. After blank analysis, the Na and K contents of the sample water (surface water, groundwater and underground mine water) was as follows:

About 5 mL of the water sample was measured and transferred to a10 mL test tube followed by the addition of 2 mL of the suppressor solution. The mixture was homogenized for a minute, and then aspirated into the flame of the photometer. The contents of Na and K were read and recorded.

3.4.3 Determination of Elemental Concentration in water samples

Determination of the trace metals contents in the water samples was achieved by atomic absorption spectrometry (AAS). Hydride generation atomic absorption spectrometry (HG-AAS) was used for the determination of As; and flame atomic absorption spectrometry (FAAS) was used for the determination of Cd, Fe, Mn, Pb, Zn, and Cu.

3.4.3.1 Determination of As by HG-AAS

Hollow cathode lamps

The radiation sources were the hollow cathode lamp of As (wavelength 193.7 nm; spectral slit width 0.5 nm; lamp current 10 mA).

Reagents

For As determination, hydride generation was performed with a 0.6 % (w/v) $NaBH_4$ in 0.5 % (w/v) NaOH as the reductive solution with 6 M HCl as the carrier solution

The water used throughout the study was double distilled water (Aquatron A4000D) obtained by passing the distilled water through Nanopure Diamond Gamma irradiated Hallow Fibre 0.2µm filter column (Banstead D3750 from Fischer Scientific Company).

Reagents

For As determination hydride generation was performed with a 0.6 % (w/v) $NaBH_4$ in 0.5 % (w/v) NaOH as the reductive solution with 6 M HCl as the carrier solution.

Standards

Calibration standards for As (0.2, 0.4, 0.6 mg/L) was prepared daily by appropriate dilution of the commercial stock standard solution for As.

Reduction of As^V to As^{III}

To reduce all As^V to As^{III}, 4 mL of freshly prepared 5 M KI was added to the digest solution as shown in equation 3.12.

$$As^{5+} + 2I^- \rightarrow As^{3+} + I_2 \qquad \textbf{3.12}$$

This was followed by hydride generation and subsequently by atomic absorption measurement.

Calibration

The HG-AAS system was calibrated with As standard calibrants (0.2, 0.4, 0.6 mg As L^{-1}) and the absorbance obtained were used for linear regression analysis (plot of absorbance against the concentration of the calibrants). The concentration of As was deduced from the equation of the regression line.

Hydride generation and atomic absorption measurement

The continuous flow approach of an HG-AAS system was used to merge sample solution and reagents. The sample solution (flow rate: 5 mL/45 sec) was mixed in a PEEK (polyetheretherketone) cross connector with both HCl (flow rate: 5 mL/45 sec) and $NaBH_4$ (flow rate: 5 mL/45 sec) solutions (both solutions pumped and added with the peristaltic pump) and pumped into the reaction coil. During the mixing, the tetrahydroborate ion, BH_4^- converts As(III) into the hydride (AsH_3). Furthermore, the tetraborohydrate is hydrolyzed in the presence of HCl producing considerable hydrogen as illustrated in equations 3.13 and 3.14.

$$3BH_4^- + 3H^+ + 4H_3AsO_3 \rightarrow 3H_3BO_3 + 4AsH_3 + 3H_2O \qquad \textbf{3.13}$$

$$BH_4^- + H^+ + 3H_2O \rightarrow H_3BO_3 + 4H_2 \qquad \textbf{3.14}$$

The gaseous hydride formed together with the hydrogen gas generated were separated from the liquid in the A-shaped gas-liquid separator component of the vapour generator, and transferred with a flow of argon gas into the Perma-pure dryer and dried by a stream of nitrogen gas. The liquid goes to waste and the gaseous hydride and excess hydrogen formed were swept out of the vapour generation vessel by the argon gas (flow rate: 13.5 mL min^{-1}) into the AAS detection system. In the detection system, AsH_3 was atomized in the air-acetylene flame (also fed by the excess hydrogen generated) aligned in the light path of a As lamp in an atomic absorption spectrometer. Absorbance measurements were recorded and the concentration deduced from the regression line.

Calculation of concentration

The concentration of As in each water sample was obtained from the equation of the regression line. The concentration of As in the sample (mg L^{-1}) was done using the equation 3.15.

$$C_{Sample}\ (\mu g\ g^{-1}) = \frac{C_{AAS} \cdot D_f \cdot V_N}{m_{Sample}} \qquad \textbf{3.15}$$

Where: C_{AAS} = Concentration of analyte obtained from calibration regression line (mg L^{-1}), D_f = Dilution factor, V_N = Nominal volume or sample volume (mL), C_{sam} = Actual concentration of analyte in sample (µg g^{-1}) and m_{sam} = Mass of homogenized sample measured for digestion (g).

Where: D_f is dilution factor, and $Conc_{calib}$ is the concentration from calibration curve

3.4.3.2 Determination of Cd, Cu, Fe, Mn, Pb and Zn

Instrumentation

A Fast Sequential Atomic Absorption Spectrometer (VARIAN, AA 250 FS, Australia) equipped with a deuterium background corrector was used for determination of trace elements at Inorganic Chemistry Laboratory of GAEC, Kwabenya, Accra.

An AGILANT 280 FS AA Atomic Absorption Spectrometer (USA) equipped with a deuterium background corrector was used for trace element determination at the Environmental laboratory of Golden Star Bogosu/Prestea Limited situated at Bogoso.

Chemicals

The under-listed commercially available stock standard solutions of Cd, Cu, Fe and Pb were used: 1000 ± 4 mg Cd/L in 2 % (w/w) HNO_3, 1000 ± 4 mg Cr/L in 2 % (w/w) HNO_3, 1000 ± 4 mg Cu/L in 2 % (w/w) HNO_3, 1000 ± 4 mg Fe/L in 2 % (w/w) HNO_3 and 1000 ± 4 mg Pb/L in 2 % (w/w) HNO_3 (Trace CERT®, Fluka, Chemie, Switzerland).

Digestion of water samples

Digestion of water samples was done according to the procedure described by Hoeing et al., (1998). The procedure was as follows:

About 6 mL of concentrated nitric acid (65 % HNO_3), 3 mL of concentrated hydrochloric acid, (37 % HCl) and 0.25 mL of hydrogen peroxide (30 % H_2O_2) was added to 5mL of water sample into labeled 100 mL polytetraflouroethylene, (PTFF),Teflon digestion tubes mixed together in a fume chamber. The samples were then loaded on a microwave carousel. The vessel cap, using a screw, was secured tightly. The complete assembly was microwave irradiated for 21 minutes in a Milestone microwave Lab station (Ethos 900), using the following operation parameters described in (Table 3.3).

Table 3.3: Microwave digestion programme used for digestion of water samples

Digestion Step	Digestion Time (min)	Microwave			
		Power (W)	Pressure (bar)	Temperature1 (^{o}C)	Temperature 2 (^{o}C)
1	5	250	100	400	500
2	1	0	100	400	500
3	10	250	100	100	500
4	5	450	100	400	500

Temperature **1** and Temperature **2** represents the initial and final digestion temperatures

After digestion, the Teflon bombs mounted on the microwave carousel were cooled in a water bath to reduce the internal pressure and to allow volatilized materials to re-solubilize. The digestate was made up to 20 mL with double distilled water and assayed for the presence of Fe, Cd, Mn, As, Cu, Pb and Zn using VARIAN AA240FS and AGILANT 280FS AA- Fast Sequential Atomic Absorption Spectrometer in an acetylene-air flame.

After each round of digestion, the Teflon bombs were washed in dilute detergent, rinsed in copious volumes of double distilled water and soaked in 10 % HNO_3 for 30 min. the acid was decanted and 5 mL of fresh 10 % HNO_3 reintroduced into each Teflon bomb and digested to wash as described earlier. The Teflon bombs were rinsed in copious volume of double distilled water and oven dried.

Atomic absorption measurement

The VARIAN AA 250 FS, Australia and AGILANT 280FS AA, USA, working conditions used for the FAAS of Fe, Cd, Mn, As, Cu, Pb and Zn were as follows: The air-acetylene

flame atomizer was made up of air oxidant (flow rate: 13.50 L/min) and acetylene as fuel (flow rate: 2.00 L/min).

The lamp current and wavelength of hollow cathode lamps and the spectral slit width used for Fe, Cr, Mn, As, Cu, Pb and Zn determinations are shown in Table 3.4.

Table 3.4: FAAS conditions used for the determination of Cd, Cu, Fe, Mn, Pb and Zn

Elements	Hollow cathode lamp		
	Current (mA)	Wavelength (nm)	Slit width (nm)
Cd	5.0	213.9	1.0
Cu	4.0	324.8	0.5
Fe	5.0	248.3	0.2
Mn	5.0	279.5	0.2
Pb	10.0	217.0	1.0
Zn	5.0	213.9	1.0

Calibration of atomic absorption spectrometer

The AAS was calibrated with the calibration standards for the element being determined. The absorbances obtained were used to plot calibration graphs for each element and these graphs are shown in (Appendix X) for the various elements analyzed. Three standard solutions (of the same element) of increasing concentrations were used to establish the reliability of readings since the equipment is already fixed to a computer programmer that reads out concentration and absorbance directly. The calibration function was established by plotting absorbance (% absorption) for a set of calibration solutions against the analyte

concentration. Linearity of the calibration curves were checked before samples were aspirated. “Resloping” was carried out with standards during readings to account for instrumental drift.

After calibration, each of the elements was determined by measurement of the absorbances of the water samples aspirated into the absorption cell.

Calculation of Concentration

The concentration of each analyte in the water sample was calculated from the calibration curve for the analyte. In cases of dilution of a sample, the concentration deduced from the calibration curve was multiplied by the dilution factor to give the actual concentration of the analyte in the sample, using equation 3.14 (page 66).

3.4.3.3 Magnesium determination in the water samples

The magnesium (Mg^{2+}) concentration in the water samples (surface water, groundwater and underground water) was determined using FAAS. (VARIAN AA240FS)

Suppressant Reagent

11.730 g of La_2O_3 was dissolved in minimum volume of 10% HNO_3 in the ratio 1:1 and then diluted with distilled water to 1000 mL volumetric flask to the mark to give 10000 µg/mL La.

About 1 mL of water sample (surface water, groundwater and underground mine water) was pipetted into different test tubes and 9 mL of Lanthanium solution of concentration 10000 mg/L was added to each sample to serve as ion suppressants in order to bring out the precipitates in the solution, which were used for the determination of Mg.

Atomic absorption

The VARIAN AA 250 FS, Australia, working conditions used for the FAAS of Mg was as follows:

The air-acetylene flame atomizer was made up of air oxidant (flow rate 13.50 L/min) and acetylene as fuel (flow rate 2.00 L/min) with following specification (wavelength: 285.2 nm, Slit width: 0.1 nm, and Lamp current: 4 mA).

The calibration function was established by plotting absorbance (% absorption) for a set of calibration solutions against the analyte concentration. Linearity of the calibration curves were checked before samples were aspirated. “Resloping” was carried out with standards during readings to account for instrumental drift.

After calibration, Mg was determined by measurement of the absorbances of the water samples aspirated into the absorption cell. The concentration of Mg in the water sample was calculated from the calibration curve, in cases of dilution of a sample, the concentration deduced from the calibration curve was multiplied by the dilution factor to give the actual concentration of the analyte in the sample using equation 3.15 (page 66).

3.5 DETERMINATION OF STABLE ISOTOPES OF WATER (δ^2H AND $\delta^{18}O$) USING LASER SPECTROSCOPY

Stable isotope ratios of hydrogen and oxygen in natural waters (δ^2H and $\delta^{18}O$) are effective tracers of the terrestrial water cycle (Aggarwal et al., 2005), and provide unique insights into hydrological, climatic, and ecological processes at local, regional and continental scales-such as the role of groundwater in rivers and lakes, groundwater recharge, sources of moisture in precipitation, recycling and transport of atmospheric moisture, and water uptake by plants (IAEA, 2009).

A spectroscopic instrument, LGR DT-100 liquid water stable isotope analyzer, (Los Gatos Research Inc., USA), uses off-axis integrated cavity output spectroscopy (OA- ICOS) to measure absolute abundances of ^2HHO, $HH^{18}O$, and HHO via laser absorption (IAEA, 2009).

The LGR instrument measures absorption around a wavelength of 1390 nm to calculate molecular concentrations of ^2HHO, $HH^{18}O$, and HHO. Molecular concentrations are converted into atomic ratios, $^2H/^1H$ and $^{18}O/^{16}O$ and a post-processing procedure is used to calculate delta-scale (δ) values with respect to Vienna Standard Mean Ocean Water [VSMOW] (Coplen, 1996) usiung equation 3.16.

$$\delta = \frac{\left(R_{(SAMPLE)} - R_{(VSMOW)}\right)}{R_{VSMOW}} \qquad \textbf{3.16}$$

Where: R is $^2H/^1H$ or $^{18}O/^{16}O$

Instrumentation

Determination of the composition of the stable isotopes (δ^2H and $\delta^{18}O$) in the water samples was accomplished using the Los Gatos DLT-100 Liquid-water Stable Isotope Analyzer [off-axis integrated cavity output spectroscopy (OA-ICOS) via laser absorption] (Los Gatos Research, Mountain View, CA, USA). The equipment is made up of a laser analysis system, an internal computer, a CTC LC-PAL liquid autosampler (Sigma-Aldrich, USA), a small membrane vacuum pump, and a room air intake line that passes air through a Drierite column for moisture removal. The autosampler and the DLT-100 are connected by a ~1 m long polytetrafluoroethylene (PTFE) transfer line. A 1.2 µL microliter syringe (Model 7701.2N, Hamilton) is used to inject 0.75 µL of sample through a PTFE septum in the autosampler.

Reference Material

The validity of the isotopic composition analysis (δ^2H and $\delta^{18}O$) using the liquid-water stable isotope analyzer was checked by analysis of International Atomic Energy Agency (IAEA) reference material, GISP [(Water) (δ^2H_{VSMOW} and $\delta^{18}O_{VSMOW}$)]. This reference material is also known as NIST RM 8536, and was developed by the IAEA in cooperation with the US National Institute of Standards and Technology (NIST).

Standard

Three secondary standards were used for the analysis: two calibration standards [prepared from IAEA reference material, LSI [(Water) ($\delta\ ^{18}O_{V\text{-}SMOW}$ and $\delta\ ^{2}H_{V\text{-}SMOW}$)], and a control standard ("in-house" prepared). These were:

Calibration standard 1:STD_1 (LSI) – enriched: $\delta^{18}O = 0.24 \pm 0.03$ and $\delta^{2}H = 2.10 \pm 0.3Hg$

Calibration standard 2:STD_2 (KWK3) – depleted: $\delta^{18}O = -11.13 \pm 0.1$ and $\delta^{2}H = -76.50 \pm 1.0$

Calibration standard 1: STD_1 (ER) – control: $\delta^{18}O = -4.78 \pm 0.8$ and $\delta^{2}H = -24.34 \pm 0.6$

Experimental procedure

The experimental procedure was according to the methods prescribed in the IAEA Training Course Series 35 [IAEA, 2009]. The procedure is as follows:

1 mL of aliquot of each standard (in-house, working and control) and 1ml of aliquot of the water sample were quantitatively transferred into 1.5 ml auto-sampler glass using the 1000 µL Eppendorf disposable tip pipette. The 1.5 ml auto-sampler glass vial was then capped with PTFE septum caps. This was followed by the arrangement of the samples on the CTC LC PAL auto-sampler. The arrangement of the samples and the standards is also according to the procedure described below (IAEA, 2009):

A dummy sample (de-ionized water) was placed in the first portion to prime the flow line. The dummy vial was followed by three secondary standards (two calibration standards and

a control standard); five water samples, followed by another set of three standards. This array of standards and water samples were repeated up to a maximum of six times (30 water samples) for a single run. Each standard and water sample was individually measured by injections lasting for 25 minutes. Measurement for each batch of 30 samples lasted for 20 hours. The measurement results for the last four of the six injections from each vial were averaged. The measured and the known δ (delta) values of calibration standards before and after each batch of five water samples were used for a linear regression to convert absolute isotope ratios to δ (delta) values.

The instrument is prone to give erratic results during the start of a run, the dummy sample used, allowed the system to stabilize before the first standards were run on the Liquid-Water Analyzer. The arrangement of the vials in the CTC LC PAL auto-sampler was designed to overcome the effect of instrumental drift, which can be significant during a daily run (IAEA, 2009). The first two injections were disregarded due to often less stable and the injections with the most potential for carrying a memory effect of the previous sample (IAEA, 2009).

3.6 QUALITY ASSURANCE/QUALITY CONTROL (QA/QC) MEASURES EMPLOYED

Quality Assurance consists of quality control and quality assessment. Quality control refers to the set of procedures undertaken by the laboratory for continuous monitoring of operations and results in order to ensure the results are good enough to be released (Ibe and Kullenberg, 1995).

Quality Assurance is defined as the total sum of activities employed by the laboratory to ensure that the data it produces meet the quality desired for decision making (Ibe and Kullenberg, 1995).

The following QA/QC guidelines were undertaken during sampling and analysis to produce acceptable results.

- All glassware and sampling containers were soaked in nitric acid (10 % HNO_3) for three (3) days and rinsed with deionized water before use. This was to ensure that the sample bottles were free from contamination, which could affect the concentrations of various ions in the water samples.
- In sampling from the land, boreholes were purged for ten minutes to flush the stagnant water retained in pipes. In the case of hand-dug wells, it was properly checked and confirmed that the dug well was constantly used. This was to ensure that stale and stagnant water was not sampled.

- The water samples collected, were provided with an identification label on which the following information were legibly and indelibly written,

  - Sample identification number
  - Date and time of sampling
  - Record of any stability treatment
  - Prevailing weather conditions at the time of sampling

- Samples that require preservation and special treatment for transportation to prevent their deterioration were treated promptly.

- Reagents used during analysis were of all analytical grades.
- Every instrument used was calibrated with standard chemical solutions prepared from commercially available chemicals and validated with Standard Reference Materials (SRM) and Certified Reference Materials (CRM). The SRM were analyzed repeatedly at predetermined intervals to confirm that the method remained in a state of statistical control.

CHAPTER FOUR

RESULTS AND DISCUSSION

In this chapter, the results obtained in the study are presented in the form of tables, figures and diagrams. This is followed by detailed discussions of the results. The chapter is divided into six (6) Sections. Section 4.1 deals with discussions on the Physico-chemical parameters. The major anions (SO_4^{2-}, HCO_3^-, Cl^-, PO_4^{3-} and NO_3^-) and major cations (Ca^{2+}, Mg^{2+}, Na^+ and K^+) are discussed in Section 4.2 under the caption, Major Ions. Also discussed in Section 4.2 is Charged Balance Error (Ionic Balance). The Geochemical Processes governing the compositional relationship (Bivariate Plots) of groundwater and underground mine water are discussed in Section 4.3. Trace Elements (As, Cd, Cu, Fe, Mn, Pb and Zn**)** contents and Stable Isotope Compositions (δ^2H and $\delta^{18}O$) are discussed in sections 4.4 and 4.5, respectively.

4.1 PHYSICO-CHEMICAL PARAMETERS

The detailed results for the physico-chemical parameters determined in water samples (surface water, groundwater and underground mine water) from the study area are presented (Table 4.1).

Table 4.1: Physico-chemical paramters for Surface water

Surface water

Sampling ID	Elevation (m)	pH	Temp (°C)	EC (µS/cm)	TDS (mg/L)	Sal ‰	Sampling ID	Elevation (m)	pH	Temp (°C)	EC (µS/cm)	TDS (mg/L)	Sal ‰
PSW	62.00	6.10	24.45	126.72	68.36	0.10	PUWF(US)	68.00	7.62	25.85	3770.00	2075.00	0.10
BDSt	86.00	6.54	25.25	19.89	23.45	0.10	PUWM(MS)	63.00	7.45	24.60	4460.00	2460.00	0.21
BDSt2	73.00	6.80	26.90	116.60	58.26	0.10	PUWE(DS)	35.00	7.54	24.50	2840.00	1570.00	0.13
ASP	60.00	6.77	24.90	190.00	100.00	0.02	BDU(US)	78.00	7.96	27.35	780.00	410.00	0.73
BSP	52.00	6.94	25.65	113.95	59.49	0.11	BDUWF(MS)	73.00	7.43	24.10	770.00	420.00	0.16
BST2	48.00	7.15	25.05	37.49	36.99	0.10	ARaWT(US)	34.00	6.95	24.60	140.00	80.00	0.10
ARWT(US)	35.00	6.45	24.45	158.72	84.36	0.13	ARaWM(MS)	33.00	6.99	25.00	680.00	380.00	0.10
HRWM(MS)	27.00	7.02	27.00	224.00	119.51	0.20	ARaWE(DS)	30.00	6.83	24.80	570.00	310.00	0.10
ARWE(DS)	29.00	7.17	25.65	297.75	158.26	0.16							
Range		**pH (6-8)**		**EC (20-4460)**			**Temp(24.1-27.4)**		**TDS (24.5- 2460.0)**		**Sal (0.02-0.73)**		

Temp (Temperature) **EC** (Electrical Conductivity) **TDS** (Total Dissolved Solids) **Sal** (Salinity)

Table 4.1: Physico-chemical paramters for Groundwater and Underground mine water (Continuation)

Groundwater							Underground mine water						
Sampling ID	Depth (m)	pH	Temp (^oC)	EC (µS/c)	TDS (mg/L)	Sal ‰	Sampling ID	Depth (m)	pH	Temp (^oC)	EC (µS/cm)	TDS (mg/L)	Sal ‰
PW1	49.00	6.43	24.80	5290.50	150.00	0.11	UD-3A	71.50	7.76	25.06	84500	465.00	0.10
PW2	54.00	5.83	27.00	424.05	224.55	0.46	UD-3B		7.84	25.35	720.00	400.00	0.05
PW3	58.00	3.63	26.00	863.35	454.30	0.85	UD-6B	175.80	5.37	25.70	995.05	450.00	0.10
PW4	59.00	5.71	26.00	404.35	212.15	0.38	UD-6C		5.42	27.75	1035.00	615.00	0.09
PW5	63.00	6.24	25.70	395.65	210.35	0.38	UD-6E		7.13	25.85	1050.00	580.00	0.10
HW	27.00	6.16	25.80	552.80	143.20	0.06	UD-6F		6.66	26.05	825.00	455.00	0.07
BDW1	93.00	5.48	26.05	173.50	91.59	0.19	UD-6G		6.63	25.95	840.00	460.00	0.06
BDW2	85.00	6.31	26.00	273.00	146.85	0.25	UD-6H		6.80	25.90	795.00	440.00	0.05
BDW3	80.00	5.97	27.35	373.80	196.95	0.20	UD-9A	323.30	7.94	25.85	865.00	475.00	0.06
BDW4	78.00	4.80	24.50	280.00	75.50	0.02	UD-9B		7.85	25.00	850.00	465.00	0.07
BBH	39.00	5.78	26.00	86.37	48.19	0.08	UD-9C		7.88	22.00	855.00	475.00	0.06
ABH	36.00	6.22	25.60	214.20	114.61	0.28	UD-17A	597.30	7.54	25.65	1695.00	935.00	0.06
HBH1	41.00	6.09	27.45	329.75	177.40	0.31	UD-17B		7.62	25.00	1775.00	975.00	0.04
HBH2	41.00	6.00	26.95	319.20	166.95	0.31	UD-17C		7.24	25.60	1305.00	645.00	0.07
PBHI	58.00	4.14	26.00	405.15	117.60	0.43	UD-17D		7.10	25.60	4140.00	2280.00	0.10
PBH2	59.00	6.44	25.95	378.05	199.05	0.41	UD-17E		7.82	25.40	2755.00	1515.00	0.70

Table 4.1: Physico-chemical paramters for Groundwater and Underground mine water (Continuation)

Groundwater							Underground mine water						
Sampling ID	Depth (m)	pH	Temp (^{o}C)	EC (µS/c)	TDS (mg/L)	Sal ‰	Sampling ID	Depth (m)	pH	Temp (^{o}C)	EC (µS/cm)	TDS (mg/L)	Sal ‰
PBH3	54.00	6.03	27.05	453.25	199.50	0.37	UD-17F	597.30	7.46	23.10	1660.00	910.00	0.70
PBH4	60.00	6.59	25.95	230.25	122.64	0.20	UD-24A	888.80	7.57	25.95	3065.00	1690.00	0.10
PBH5	48.00	6.00	26.00	191.80	103.41	0.19	UD-24B		7.83	25.30	2900.00	1600.00	0.10
PBH6	45.00	6.30	24.30	220.00	65.00	0.04	UD-24C		7.57	25.70	5650.00	3110.00	0.06
PBH7	69.00	5.07	24.08	320.00	90.00	0.05	UD-24E		7.68	25.30	4615.00	2520.00	0.04
Range		**3.6-6.6**	**24.3-27.5**	**86.4-863.3**	**66.4-454.3**	**0.04-0.19**	**Range**		**5.4-7.9**	**22-26.1**	**720-5650**	**400-3110**	**0.04-0.70**

Temp (Temperature) **EC** (Electrical Conductivity) **TDS** (Total Dissolved Solids) **Sal** (Salinity)

4.1.1 pH

Surface Water

Generally, the pH of surface water from the study area was acidic to slightly alkaline ranging from 6.10 to 7.96 (Table 4.1). The pH of surface water from the study area is influenced by agrochemicals used by farmers, droppings of farm animals, waste from mining companies as well as waste from the communities within the catchment area. The use of nitric acid (HNO_3), (commonly called "salt petre") during the gold recovery processes by the small scale and artisanal gold miners also influences the pH of surface water in the study area. This is because the miners discharge all the tailings directly into the water bodies within the catchment area.

Groundwater and Underground mine water

The pH of groundwater and underground mine water; ranges from 3.36-6.59 and 5.37-7.94 (Table 4.1), respectively. The pH of groundwater and underground mine water can be described as acidic to mildly alkaline. The lowest pH was recorded at PW3 (Prestea), while the highest pH was at BDU (Bondaye). Groundwater pH is affected by the geology of the study area, Birimian formation, which is composed of phyllites, schist and grey-wacke, volcanoclastics and metavolcanic rocks (including lavas, pyroclastics and some fine-grained metasedimentary rocks), and chemical facies occuring between volcanic and basin sedimentary in the transition-zone. Cherts magnifrerous and carbon-rich sediments, Fe-Ca-Mg carbonates minerals dissermination produce acidic waters. While in the granite and due to the dissolution of silicate and carbonates, slightly alkaline waters are produced. (Pelig-Ba, 1987). The pH of groundwater may be affected by the decay of vegetation or hydrolysis of

iron or aluminum (Davies and Dewiest, 1996). The acidity of ground water is affected by the concentration of Al and Fe, which can undergo hydrolysis to produce excess hydroxonium ions. The hydrolysis of Al and Fe are represented by equations 4.1, 4.2 and 4.3.

$$Al + 6H_2O_{(l)} \rightarrow Al(H_2O)_6 \quad \textbf{4.1}$$

$$Al(H_2O)_6 + H_2O_{(l)} \rightarrow \left[Al(H_2O)_5(OH)\right]^{-} + H_3O^{+} \quad \textbf{4.2}$$

$$Fe^{3+} + H_2O \leftrightarrow Fe(OH)_2 + 2H^{+} \quad \textbf{4.3}$$

In gold mining areas, sulphide oxidation leads to low pH in groundwater that encourages the dissolution of trace metals in the groundwater in very high concentrations (Kortatsi, 2004). The mining activities in the study area also generate acid mine drainage, (AMD), that can leach trace metals into the groundwater, and could accounts for the low pH in the areas (Ahialey et al., 2010).

The differences in pH of the groundwater and underground mine water are directly linked to their chemistry, which is influenced by the geology, the chemical and biological processes occurring during infiltration and storage.

4.1.2 Temperature

Surface Water

Temperature for the surface water ranged from 24.10 to 27.35 ^{o}C (Table 4.1) for surface water. The temperature of surface waters is influenced by latitude, altitude, and season, time of day, air circulation and cloud cover. The lowest temperature for the surface water in the study area was recorded at BDU (Bondaye), the stream was under thick vegetation.

Groundwater and Underground mine water

The groundwater temperatures varied from 24.3 to 27.45 ^{o}C (Table 4.1), whilst for underground mine water the temperature varies between 22.0 and 26.05 ^{o}C (Table 4.1). Generally, the lowest temperature of 22.0 ^{o}C was recorded at UD-24C. The variations in temperature is attributed to several factors such as the season and also, different sampling time, the flow and well depth/ underground levels, nature of faults and structures associated with this Birimian Formation which the aquifers were found. Groundwater usually maintains a fairly constant temperature which, for surficial aquifers, is normally close to the mean annual air temperature; however, deep aquifers have higher temperatures due to earth's thermal gradient (Chapman and Kimstach, 1996).

Temperature affects pH, conductivity, redox potential and Total Dissolved Solids (TDS) of the water samples. Since pH is the –log [H^{+}], any dissociation of water at high temperatures causes a corresponding increase in pH. Also, since conductivities are dependent on the movement of electrons, any change in temperature causes a corresponding increase in conductivity. As water temperature increases, the rate of chemical reactions generally increases together with the evaporation and volatilization of substances from the water. Increased temperature also decreases the solubility of gases in water, such as O_2, CO_2, N_2, CH_4 and others (Chapman and Kimstach, 1996).

The sampling was carried out in the dry and early part of rainy seasons, most especially in the early mornings for underground sampling, late mornings and early evenings for the surface and groundwater samples.

4.1.3 Electrical conductivity (EC) and Total Dissolved Solids (TDS) Surface water

The electrical conductivity and total dissolved solids in surface water ranged from 19.89 to 4460.00 µS/cm and 23.45 to 2460.00 mg/L respectively (Table 4.1). The lowest TDS was recorded at BDSt2 (Bondaye), which is 73 meters above sea level. This suggests that the spring is recharged from nearby sources of water and it indicates the extent of fracture within the sampling area. The surface waters with the exception of PUWF, PUWM, PUME, BDU and BDWF, which were pumped underground mine water flowing as streams, were observed to have generally low TDS, ARaWT(US) increases as the river flows downstream ARaWM (DS). This is attributed to the long distance the river flows, runoffs from domestic and industrial waste and the dissolution of certain minerals (calcite, dolomite and gypsum) associated with Brimian formation, through which the Ankobra River flows, as well as the inter-mixing of PUME (Prestea) closer to mid-stream (ARaWM) (Himan) accounts for this trend.

For surface water, TDS and Conductivities are also affected by inputs from anthropogenic activities (Farming, quarrying and sand winning) (Davies and Dewiest, 1996). Lower TDS and Conductivities of surface water the in the study area, showed that the water is unable to react with rock matrix to equilibrium, indicating short resident time.

Groundwater and Underground mine water

The electrical conductivity and TDS values for groundwater ranged from 86.37 to 863.35 µS/cm and 66.37 to 454.30 mg/L, respectively (Table 4.1). For underground mine water, EC and TDS range from 720.00 to 5650.00 µS/cm and 400.00 to 3110.00 mg/L waters

respectively (Table 4.1). It was also observed that the TDS and Conductivities of groundwater were generally lower than underground mine water. This is attributed to deeper depth of the gallaries (Stopes), and this may also be as a result of significant weathering occurring at shallow depth and as increased hydraulic conductivity induced by mining activities expose large surface area of the rocks underground and the subsequent dissolution of mineral salts (halites and evaporites) along its path. This critical observation is in accordance with groundwater in discharge areas, hence there is a higher degree of water-rock interactions.

Groundwaters are classified on the following categories, based on TDS: Fresh water (0-1000 mg/L), brackish water (1000-10000 mg/L), saline water (10000-100000 mg/L), and brine water (> 100000 mg/L). Low TDS values are normally associated with recharge areas and referred to as young waters, while high TDS values are associated with discharge area and referred to as old waters (Freeze and Cherry, 1979).

Water –rock interaction, the type of groundwater flow, weathering, dissolution of soluble salts in the soil before ground water recharge and chemical activities in the unsaturated zone, induce the dissolution of metals, are major causes of higher TDS and Conductivities in both the groundwater and underground mine water.

Thus, for any conductivity, the TDS value can be estimated. The whole set of data fits a straight-line graph with ($r^2 = 0.9984$) [Equation 4.4] (Freeze and Cherry, 1979):

$$KA = S \qquad \textbf{4.4}$$

where, **K** is the conductivity in µS/cm and **S** is the TDS in mg/L (Hem, 2002), and **A** is a constant, whose value determines whether a particular water type is high in bicarbonate, sulphate or chloride.

The difference in TDS and Conductivities in the study area, Table 4.1 are a result of disparities in the origin of the groundwater, since groundwater flowing from a long distance will have higher TDS and Conductivity.

The TDS and Conductivities values of surface water, groundwater and underground mine water are evidently different, indicating that surface and groundwater systems are relatively independent flow systems, and recharge amount from surface water to groundwater is very small or non exists, suggesting that groundwater and underground mine water are likely to be recharged by groundwater flow from a long distance away.

Based on the TDS classification above, all the surface and ground waters belong to fresh water categories whilst underground mine water is brackish.

4.1.4 Salinity

Surface water

The salinity for surface water ranges from 0.00 to 0.30 ‰. In River Ankobra and Assesre, other surface water bodies, domestic wastes and industrial effluents from ("galamsay") activities significantly influence the salinity of the water. South-west monsoon winds carry along seawater droplets as they move towards north, these droplets may fall and settle on the surface of the soil, which are then leached to the groundwater system. This phenomenon is more profound towards the coast. Salinity in the surface and spring waters were also observed to increase from upstream to downstream. As rivers flow through towns, human

activities such as swimming, dumping of domestic waste, faecal matter, industrial waste and the activities of small-scale artisanal gold miners, all enter these water bodies (Ankkobra and Assesre). These activities may increase the salt content of the water.

Groundwater and Underground mine water

The groundwater and underground mine water salinity varies from 0.04 to 0.19 ‰ and 0.04 to 0.70 ‰, respectively. A general rise in salinity was observed in the groundwater when moving from south to north of the study area. While it increases with depths, from one level to the next downwards. The groundwater salinity in the study area is therefore not attributed to sea aerosol spray due to observed trend of evaporation of water in the saturated and unsaturated leading to dissolution of halites and evaporites.

4.2 MAJOR IONS

Anions (sulphate, bicarbonate, chloride, nitrate and phosphate) and cations (calcium, sodium, potassium and magnesium) ions in water offered qualitative and quantitative study methods for investigating the generation and involvement of water bodies (surface water, groundwater and underground mine water) of Prestea and GSBPL (NCM). Hydrochemistry was under the influence of lithology and soil and rock characteristics of the Birimian formation, where water passed by, and evolvement of components was strictly controlled by various chemistry functions.

Thus, in combination with the topographical and geological conditions, water circulation paths in the study basin are investigated expressly.

4.2.1 Major Anions

The major anions determined are discussed are shown in Table 4.3:

4.2.1.1 Sulphate (SO_4^{2-})

Sulphate concentrations in the water samples were high. It ranged from from 3.00-49.30 meq/L for surface water 2.15-5.69 meq/L for groundwater and 5.48-78.98 meq/L for underground mine water. Sulphate can be derived from atmospheric deposition sources (wet and dry fallout), anthropogenic source such as fertilizers applications and sedimentary lithogenic sources. High sulphate values may be due to naturally occurring atmospheric sulphate derived from marine sources (sea spray) or volcanic sources (from post emission

oxidation of SO_2 and H_2S) deposited in the soil and sulphate minerals that have accumulated in the unsaturated zone. The sulphate ion is negatively charged and is only held loosely on the soil exchange sites, which are highly soluble in water and therefore unless sulphate is used by plants it can leach down in the soil through the unsaturated zone to the saturated zone. The high levels of SO_4^{2-} in the water in the study area could be attributed to the dissolution of sulphite minerals such as calcite ($CaSO_4$), dolomite [$CaMg(CO_3)_2$] and gypsum ($CaSO_4.2H_2O$) and anhydrite, oxidation of metallic sulphides are possible sources of sulphate in underground mine water. The oxidation of pyrite is illustrated in the equation 4.5.

$$FeS_2 + H_2O + \frac{7}{2}CO_2 \leftrightarrow FeSO_4 + 2H^+ + SO_4^{2-} \qquad \textbf{4.5}$$

Pyrite sulphate

Acid mine drainage may be a very important source for the elevated content of sulphate (Wu, 2006).

From the Pearson correlation analysis (Table 4.2), there was a strong correlation between calcium and sulphate ion. These sulphates –rich waters likely evolved from the gypsum ($CaSO_4^{2-}.2.H_2O$) and or anhydride dissolution.

Table 4.2: Pearson Correlation coefficient for physico-chemical parameters and Major ions at 95 % CI

	pH	*Temp/^{0}C*	*Cond/µS/m*	*TDS/mg/L*	*Na^+*	*K^+*	*Ca^{2+}*	*Mg^{2+}*	*SO_4^{2-}*	*Cl^-*	*HCO_3^-*	*NO_3^-*	*PO_4^{3-}*
pH	1												
Temp/^{0}C	-0.309	1											
Cond/µSm	**0.504**	-0.1418	1										
TDS/mg/L	0.496	-0.1499	**0.9988**	1									
Na^+	-0.076	0.1835	**0.6384**	**0.6359**	1								
K^+	0.203	0.1175	0.1420	0.1638	0.0703	1							
Ca^{2+}	**0.573**	-0.2165	**0.9600**	**0.9608**	**0.5231**	0.132	1						
Mg^{2+}	**0.649**	-0.2422	**0.9535**	**0.9562**	**0.5120**	0.228	**0.961**	1					
SO_4^{2-}	0.452	-0.0952	**0.9658**	**0.9665**	**0.6101**	0.162	**0.957**	**0.895**	1				
Cl^-	-0.218	0.1485	-0.2002	-0.2024	0.1751	-0.152	-0.189	-0.171	-0.2211	1			
HCO_3^-	**0.742**	-0.3641	**0.8162**	**0.8187**	0.3266	0.159	**0.885**	**0.914**	**0.7640**	-0.1141	1		
NO_3^-	-0.415	0.2216	-0.0780	-0.0863	0.3423	-0.398	-0.152	-0.177	-0.1276	0.3811	-0.212	1	
PO_4^{3-}	0.332	-0.1351	0.6948	**0.7061**	0.4853	0.252	**0.659**	**0.688**	**0.6456**	-0.0841	**0.657**	0.1859	1

4.2.1.2 Bicarbonates (HCO_3^-)

The concentration of bicarbonate for surface water varied from 0.94-9.02 meq/L (Table 4.3) and for groundwater and underground mine water, the values ranged from 0.28-2.38 meq/L and 2.22-8.02 meq/L (Table 4.3), respectively. Bicarbonates in ground water are mostly due to the dissolution of $NaHCO_3$ and $Ca(HCO_3)_2$ from the weathering of plagioclase feldspares. Another possible source of bicarbonates in groundwater is the decay of organic matter in the root zone to produce CO_2, which reacts with water to produce carbonic acid.

Furthermore, natural sources of HCO_3^- include processes such as dissolution of carbonate minerals in the soil and carbon dioxide gas (CO_2) from the atmosphere according to the equations 4.6 and 4.7.

$$CaCO_3 + CO_2 + H_2O \leftrightarrow Ca^{2+} + 2HCO_3^- \qquad \textbf{4.6}$$

$$CO_2 + H_2O \leftrightarrow H^+ + 2HCO_3^- \qquad \textbf{4.7}$$

The HCO_3^- concentration were unevenly distributed in the study area.The presence of limestone in the geology of the area suggests that the carbonate mineral dissolution may be the major sources of HCO_3^- in the groundwater samples. The surface waters were generally observed to have low values of HCO_3^-, with the exception of PUWF, PUWM, PUWE, BDU and BDUW. However, decomposition of organic pollutant is said to be the course of high bicarbonates in the rivers.

4.2.1.3 Chloride (Cl^-)

The chloride values in the underground mine water and groundwater ranged from 0.16 to 6.90 meq/L and 0.69 to 3.89 meq/L (Table 4.3), respectively. For surface water, these varied from 0.64 to 3.28 meq/L (Table 4.3). The major sources of chloride in groundwater are ancient seawater entrapped in sediments; dissolution of halite and other related minerals in evaporate deposites and finally from the atmosphere as sea aerosol spray. Other sources of chloride in the groundwater system may include infiltration by runoff from domestic activities and waste, also the decomposition of organic matter may be a contributing factor. The highest values of chloride (6.90 meq/L) were observed at UDB-3A and generally higher values were obtained in the groundwater and underground mine water. The Birimian formation is made up of quartzite, tuff schists, phyllite and argillite. Halite and other evaporates and these are likely to be the sources of the chloride.

Furthermore, the high content of chloride in the underground mine water samples could be due to the end point chemistry of the underground mine water. The observed low concentration of chloride should result from mixing with surface water or local shallow groundwater before the out flow of the underground water as springs.

4.2.1.4 Phosphate (PO_4^{3-})

Phosphate values in the underground mine water and ground water were generally low ranging from 0.10-3.23 meq/L and 0.01-2.00 meq/L, respectively. PO_4^{3-} also varied from 0.01 to 3.06 meq/L for surface water. The main natural source of phosphate in many water samples is mainly the weathering of phosphorus-bearing rocks and the breakdown of

organic matter. Domestic waste-waters (particularly those containing detergents), industrial effluents and fertilizer run-off contribute to elevated levels in surface waters. However, phosphate minerals often do not last long in readily available form and tend to quickly combine with other minerals in the water. At high pH (alkaline water), phosphorus is often present as calcium phosphates. In acidic soils, phosphorus readily reacts with aluminium and iron to form aluminium and iron phosphates. Therefore, phosphate is negatively charged ion and held to a limited extent by exchange sites on clays.

4.2.1.5 Nitrate (NO_3^-)

The nitrate concentrations were low in the water samples ranging from 0.08 to 0.43 meq/L for underground mine water; 0.01 to1.36 meq/L for groundwater; and between 0.01 and 0.17 meq/L for surface water. Nitrate is usually introduced into groundwater through wide spread of diffuse sources, commonly called non-point sources, which is hard to detect. These sources include, leaching of chemical fertilizers and animal manure, groundwater pollution from septic tank and sewage discharges. Nitrate concentration in groundwater is not limited to solubility constraints but due to its ionic form, nitrate is very mobile in ground water and that nitrate moves in groundwater with no transformation and litter or no retardation (Kortatsi, 2004).

In the Tarkwa-Prestea area, nitrate is likely to enter the groundwater system not only from the enumerated sources but from explosives use for mining and waste generation due to population increase (Kortatsi, 2004). In situations where nitrogen explosives are used extensively for mining and quarrying, residues of the explosives left in the underground

goldmines or spoils could oxidize to nitrate mobilize in groundwater and subsequently underground water (Kusimi, 2007).

Table 4.3: Concentration of Major Anions

Surface water

Sampling ID	Elevation (m)	SO_4^{2-} (meq/L)	Cl^- (meq/L)	HCO_3^- (meq/L)	NO_3^- (meq/L)	PO_4^{3-} (meq/L)	Sampling ID	Elevation (m)	SO_4^{2-} (meq/L)	Cl^- (meq/L)	HCO_3^- (meq/L)	NO_3^- (meq/L)	PO_4^{3-} (meq/L)
PSW	62.00	4.56	1.12	1.52	0.04	0.18	PUWF(US)	68.00	42.78	1.47	7.48	0.02	2.27
BDSt	86.00	3.04	0.64	0.94	0.01	0.22	PUWM(MS)	63.00	49.30	3.28	9.02	0.01	3.06
BDSt2	73.00	3.25	1.32	0.94	0.08	<0.01	PUWE(DS)	35.00	11.85	1.99	6.98	0.02	1.30
ASP	60.00	3.00	0.65	1.38	<0.10	0.64	BDU(US)	78.00	7.48	0.80	4.66	0.01	0.41
BSP	52.00	3.06	0.95	3.90	0.06	0.04	BDUWF(MS)	73.00	4.67	2.49	4.14	0.01	0.90
BST2	48.00	4.75	0.72	1.06	0.03	0.41	ARaWT(US)	34.00	3.52	0.79	1.38	0.17	0.08
ARWT(US)	35.00	3.68	1.30	1.44	0.05	0.03	ARaWM(MS)	33.00	5.62	0.92	1.78	0.03	0.07
HRWM(MS)	27.00	3.34	1.14	1.54	0.04	0.01	ARaWE(DS)	30.00	3.03	0.92	1.74	0.01	<0.01
Range		**SO_4^{2-} (3.0-49.3)**		**Cl^- (0.6-3.3)**		**HCO_3^- (0.94 - 9.02)**		**NO_3^- (0.01-0.17)**			**PO_4^{3-} (0.01 – 3.06)**		

US (Upper Stream) **MS** (Mid Steam) **DS** (Down Stream)

Table 4.3: Concentration of Major Anions (Continuation)

Groundwater							Underground mine water						
Sampling ID	Depth (m)	SO_4^{2-} (meq/L)	Cl^- (meq/L)	HCO_3^- (meq/L)	NO_3^- (meq/L)	PO_4^{3-} (meq/L)	Sampling ID	Depth (m)	SO_4^{2-} (meq/L)	Cl^- (meq/L)	HCO_3^- (meq/L)	NO_3^- (meq/L)	PO_4^{3-} (meq/L)
PW1	49.00	3.25	1.39	1.58	0.54	0.14	UD-3A	71.50	9.17	6.90	4.46	0.16	1.00
PW2	54.00	5.69	2.06	0.32	0.28	<0.01	UD-3B		6.47	0.68	3.14	0.13	0.11
PW3	58.00	3.29	3.89	0.98	1.36	0.11	UD-6B	175.80	16.59	1.12	2.46	0.15	0.10
PW4	59.00	3.40	2.06	1.02	0.45	<0.01	UD-6C		8.68	1.27	3.30	0.16	1.04
PW5	63.00	3.24	1.76	1.92	029	0.10	UD-6E		12.41	1.47	3.42	0.35	0.34
HW	27.00	3.58	1.82	1.64	0.14	0.01	UD-6F		5.89	0.96	2.22	0.11	0.18
BDW1	93.00	3.06	0.98	0.90	0.20	0.06	UD-6G		9.01	0.86	2.30	0.13	0.25
BDW2	85.00	3.18	1.61	1.26	0.06	0.02	UD-6H		9.04	0.71	2.42	0.25	0.17
BDW3	80.00	3.24	1.39	0.74	0.41	2.00	UD-9A	323.30	6.48	0.79	4.52	0.23	1.11
BDW4	78.00	3.46	1.55	1.82	0.10	1.75	UD-9B		5.48	0.98	4.18	0.15	0.29
BBH	39.00	3.96	0.81	0.78	0.40	0.09	UD-9C		5.52	0.82	4.70	0.15	1.59
ABH	36.00	3.10	0.75	2.38	0.03	0.41	UD-17A	597.30	39.19	0.88	6.64	0.21	0.73
HBH1	41.00	3.32	1.39	1.20	0.10	1.63	UD-17B		13.68	0.81	5.66	0.08	0.77
HBH2	41.00	3.20	1.31	0.96	0.23	0.39	UD-17C		8.55	0.96	3.32	0.43	0.57
PBH1	58.00	2.85	2.21	0.30	0.39	0.30	UD-17D		49.06	1.49	8.02	0.14	3.23
PBH2	59.00	3.05	1.14	1.64	0.31	0.10	UD-17E		22.63	0.76	7.10	0.15	1.86
PBH3	54.00	3.19	1.39	1.22	0.49	0.11	UD-17F		17.94	1.91	5.82	0.08	0.77

Table 4.3: Concentration of Major Anion (Continuation)

Groundwater							Underground mine water						
Sampling ID	Depth (m)	SO_4^{2-} (meq/L)	Cl^- (meq/L)	HCO_3^- (meq/L)	NO_3^- (meq/L)	PO_4^{3-} (meq/L)	Sampling ID	Depth (m)	SO_4^{2-} (meq/L)	Cl^- (meq/L)	HCO_3^- (meq/L)	NO_3^- (meq/L)	PO_4^{3-} (meq/L)
PBH4	60.00	3.19	0.78	1.04	0.11	0.05	UD-24A	888.80	37.37	1.10	6.60	0.11	2.21
PBH5	48.00	2.15	0.72	1.16	0.04	0.36	UD-24B		28.82	0.78	4.74	0.22	1.34
PBH6	45.00	3.04	0.69	1.00	0.01	0.09	UD-24C		78.98	0.36	7.04	0.24	2.28
PBH7	69.00	3.04	1.10	0.28	0.06	1.14	UD-24E		60.10	0.16	5.48	0.09	1.68
Range		**(2.15-5.69)**	**(0.68-3.89)**	**(0.28-2.38)**	**(0.01-1.36)**	**(0.01-2.00)**	**Range**		**(5.48-78.98)**	**(0.16-6.90)**	**(2.22-8.02)**	**(0.08-0.43)**	**(0.10-3.23)**

UD (Prestea underground) **UDB** (Bondaye underground) **BH** (Borehole) **W** (Hand-dug well) **BD** (Bondaye) **P** (Prestea)

4.2.2 Major Cation

4.2.2.1 Calcium (Ca)

Concentrations of calcium in the surface water ranged from 0.64 to 33.00 meq/L (Table 4.4). Ca in groundwater and underground mine water also varied from 1.01 to 5.39 meq/L and 5.91 to 43.00 meq/L (Table 4.4), respectively.

The presence of calcium in the study area is due to the Birimian terrain, the commonest minerals in the area are quartz, feldspars, mica and hornblende. Feldspars result in the release of calcium ions in the ground water, Calcium is an essential constituent of many igneous rock minerals, especially of the chain silicates pyroxene and amphiboles. Calcium in surface water can be derived from oceanic and inland dust sources, together with periodic materials from fires, and of acidic rain water, which can increase the leaching of calcium from soils.

Also, the presence of elevated calcium in the groundwater and underground mine water samples might be as a result of dissolution of calcic-rich minerals such as calcite ($CaCO_3$) and dolomite [$CaMg(CO_3)_2$] and gypsum($CaSO_4.2H_2O$) and weathering of calcic- rich components of plagioclase feldspars anorthite ($CaAl_2Si_2O_8$)

The decompositon of anorthite is represented by equation 4.8.

$$CaAl_2Si_2O_8 + H_2O + 2H^+ \leftrightarrow 2Al_2Si_2O_3(OH)_4 + Ca^{2+} + 4H_4SiO_4 \qquad \textbf{4.8}$$

The dissolution of calcite is also represented by equation 4.9.

$$CaCO_3 + 2H^+ \leftrightarrow CO_2 + H_2O + Ca^{2+} \qquad \textbf{4.9}$$

Table 4.4: Concentration of Major Cations

Surface water

Sampling ID	Elevation (m)	Na^+ (meq/L)	K^+ (meq/L)	Ca^{2+} (meq/L)	Mg^{2+} (meq/L)	Sampling ID	Elevation (m)	Na^+ (meq/L)	K^+ (meq/L)	Ca^{2+} (meq/L)	Mg^{2+} (meq/L)
PSW	62.00	2.98	0.14	2.45	1.29	PUWF (US)	68.00	4.31	0.11	28.21	10.41
BDSt	86.00	0.12	0.02	1.81	1.55	PUWM (DS)	63.00	5.59	0.24	33.00	18.87
BDSt2	73.00	0.14	0.01	0.64	0.44	PUWE (DS)	35.00	3.28	0.15	19.80	7.41
ASP	60.00	0.31	0.04	2.66	1.25	BDU (US)	78.00	0.41	0.03	6.01	4.38
BSP	52.00	0.18	0.02	1.65	0.80	BDUWF (MS)	73.00	0.40	0.08	12.24	4.70
BSt2	48.00	0.16	0.02	0.64	0.70	ARaWT (US)	34.00	0.73	0.04	2.66	0.79
ARWT(US)	35.00	0.49	0.08	1.76	0.93	ARaWT (MS)	33.00	0.80	0.11	3.19	4.43
HRWM (MS)	27.00	0.25	0.10	1.48	0.91	ARaWT (DS)	30.00	0.40	0.07	2.13	1.53
ARWE (DS)	29.00	0.65	0.16	3.73	0.88						
Range		**Na^+ (0.12 – 5.59)**		**K^+ (0.01 – 0.24)**		**Ca^{2+} (0.64 – 33.00)**		**Mg^{2+} (0.44 – 18.87)**			

Table 4.4: Concentration of Major Cations (Continuation)

Groundwater						Undergound mine water					
Sampling ID	Depth (m)	Na^+ (meq/L)	K^+ (meq/L)	Ca^{2+} (meq/L)	Mg^{2+} (meq/L)	Sampling ID	Depth (m)	Na^+ (meq/L)	K^+ (meq/L)	Ca^{2+} (meq/L)	Mg^{2+} (meq/L)
PW1	49.00	0.87	0.11	3.57	0.97	UD-3A	71.50	1.22	0.85	11.44	5.49
PW2	54.00	2.31	1.03	2.04	1.54	UD-3B		0.28	0.96	7.31	4.34
PW3	58.00	3.57	0.39	3.78	1.65	UD-6B	175.80	0.89	0.84	11.18	4.59
PW4	59.00	2.48	0.92	1.54	1.89	UD-6C		0.97	0.80	9.38	3.89
PW5	63.00	1.33	0.95	1.49	2.32	UD-6E		0.97	0.89	12.23	4.53
HW	27.00	0.97	0.18	5.39	0.76	UD-6F		0.49	0.84	5.91	3.61
BDW1	93.00	1.62	0.84	2.34	1.37	UD-6G		0.50	0.84	9.58	3.68
BDW2	85.00	1.88	1.06	2.29	1.46	UD-6H		0.39	0.83	7.12	3.89
BDW3	80.00	1.48	1.06	2.13	1.47	UD-9A	323.30	0.45	0.85	8.05	4.95
BDW4	78.00	0.73	0.88	4.32	1.57	UD-9B		0.28	0.83	6.98	4.32
BBH	39.00	1.04	0.83	2.51	1.28	UD-9C		0.44	0.83	7.44	4.58
ABH	36.00	0.61	0.82	4.31	1.77	UD-17A	597.30	0.88	0.85	27.94	6.90
HBH1	41.00	1.10	0.86	1.65	1.72	UD-17B		1.03	0.86	15.08	7.34
HBH2	41.00	1.11	0.84	1.01	1.69	UD-17C		1.05	0.86	9.23	4.57
PBH1	58.00	1.63	0.87	1.49	0.78	UD-17D		4.14	0.93	31.40	12.61
PBH2	59.00	1.27	0.82	1.74	1.21	UD-17E		1.47	0.88	24.88	11.61

Table 4.4: Concentration of Major Cations (Continuation)

Groundwater						Undergound mine water					
Sampling ID	Depth (m)	Na^+ (meq/L)	K^+ (meq/L)	Ca^{2+} (meq/L)	Mg^{2+} (meq/L)	Sampling ID	Depth (m)	Na^+ (meq/L)	K^+ (meq/L)	Ca^{2+} (meq/L)	Mg^{2+} (meq/L)
PBH3	54.00	1.41	0.85	2.00	0.94	UD-17F		1.35	0.91	20.15	9.03
PBH4	60.00	0.75	0.83	1.12	1.54	UD-24A	888.80	4.01	0.90	25.28	10.49
PBH5	48.00	0.75	0.82	1.12	0.82	UD-24B		2.50	0.86	26.88	11.08
PBH6	45.00	0.74	0.83	3.26	0.76	UD-24C		3.40	0.90	43.00	14.50
PBH7	69.00	1.09	0.88	2.13	0.80	UD-24E		2.69	0.88	35.72	14.30
Range		**(0.61-3.57)**	**(0.11-1.06)**	**(1.01-5.39)**	**(0.76-2.32)**	**Range**		**(0.28-4.14)**	**(0.83-0.96)**	**(5.91-43.00)**	**(3.61-14.50)**

UD (Prestea Underground) **UDB** (Bondaye Underground) **BH** (Borehole) **W** (Hand-dug well) **BD** (Bondaye) **P** (Prestea)

Ion-exchange reaction with some minerals such as montmorillonite and glauconite also serve as source of Ca^{2+}.

The reason for the high concentrations of calcium in the ground water and underground mine water is that, as depth increases, the water samples had enough time to dissolve calcic-rich mineral in its path and in the larger interfacial area of aquitards in between the aquifer hosting the water.

4.2.2.2 Magnesium (Mg)

Magnesium concentration varied from 0.44 to 18.87 meq/L (Table 4.4) for surface water, ranged from 0.76 to 2.36 meq/L for groundwater and in between 3.61 and 14.50 meq/L (Table 4.4) underground mine water. The common sources of magnesium in the hydrosphere are dolomite in the sedimentary rocks; hornblend, biotite, augite etc in igneous rocks and talc, tremolite and diopside in metamorphic rock (Davies and Dewiest, 1966). Also, the major sources of magnesium are the olivine, the pyroxenes, the amphiboles, and the dark-coloured micas, along with various less common species commonly found within the Brimian formation. Magnesium occurs in significant amounts in most limestones. The dissolution of these materials brings magnesium into solution and its concentration tends to increase along the flow path of groundwater and subsequently in underground water, until a rather high Mg and Ca ratio is reached.

The cation-exchange behavior of magnesium is similar to that of calcium. Both ions are strongly adsorbed by the clay minerals and other surfaces having exchange sites. Brindley et al. 1951; and Walker G.F.,1949; observed that high level of magnesium in groundwater

samples may be attributed to the weathering of biotite [$K(Fe,Mg)_3ALSi_3O10(F,OH)_2$], Junner and Hirst, 1946; attributed magnessium to the weathering of chlorite [$(Fe,Mg,Al)_6(Si,Al)_4O_{10}(OH)_8$], as shown in eaquation 4.10.

$$4K_2(Mg_2Fe_2Al_2)Al_2Si_6O_{20}(OH)_4 + 4H_2O + 10CO_2 \leftrightarrow 2Al_4SiO_{10}(OH)_8 + Mg_8Al_2(Al_2Si_2O_{10})(OH)_8 + 14SiO_2 + 8FeCO_3 + K_2CO_3 \quad \textbf{4.10}$$

Mg^{2+} variations in the groundwater and underground mine water show a significant incremental pattern with respect to depth. The surface water also shows relative high values of Mg^{2+} concentrations. These values are observed to increase steadily as rivers flow downstream, and assigned to anthropogenic sources.

4.2.2.3 Sodium (Na)

Sodium concentrations in surface water ranged from 0.12 to 5.59 meq/L (Table 4.4). For groundwater and underground mine water it varied from 0.61 to3.57 meq/L and 0.28 to 4.14 meq/L (Table 4.3), respectively. Albite dissolution, sea water intrusion, flow pattern and sea aerosol sprays are possible sources of Na^+ in surface, ground water and underground mine water. The dominant minerals present in these rocks are the plagioclase feldspars ranging in composition from albite ($NaAlSi_3O_8$) to anorthite ($CaAl_2Si_2O_8$) and K-feldspares.

Albite dissolution may be the probable source of the Na^+ in the water as supported by equation 4.11.

$$2NaAlSi_3O_8 + 9H_2O + 2H^+ \leftrightarrow Al_2Si_3O_5(OH)_4 + 2Na^+ + 4H_4Si_2O_4 \quad \textbf{4.11}$$

Albite Kaolinite Silica

The general irregular variations in Na^+ concentration as one move downwards can be attributed to the ground water and underground mine water flow patterns in the underground goldmine. It also suggests that, increase of Na with pH is the main factor determining the clay deflocculation at a given salinity levels. Sodium tends to remain in solution rather than be adsorbed onto the soil surface.

4.2.2.4 Potassium (K)

The concentration of K was the least prevalent cation, whose concentration ranged from 0.01-0.24 meq/L (Table 4.4) for surface water, 0.11-3.57 meq/L, for groundwater and 0.83-0.96 meq/L for underground mine water (Table 4.4).

The major sources of K^+ in groundwater are the weathering of orthoclase and inputs from fertilizers. The high concentration of K^+ in groundwater may be due to primary minerals such as alumisosilicates, K-feldspares, biotite and muscovite found in the study area. In natural cycle, potassium is leached into the ground by rains during the dormant season or made available by the gradual decay of organic material.

The sequence of order of major cation ions concentration in the study area showed that, Calcium has the highest cation concentration followed by magnesium, sodium and with potassium been the least shown the surface water, groundwater and underground water (Ca

> Mg > Na > K). For the anions, sulphate has the highest value with nitrate been the least in the water samples.

4.2.3 Determination of Charged-Balance Error (CBE) (groundwater and underground mine water).

One of the fundamental laws of nature is that aqueous solutions are electrically neutral. This means that in real solutions, the total sum of the positive charges (cations, in meq/L) must be equal to the sum of all the negative charges (anions, in meq/L) (Freeze and Cherry,1979):

$$Charge\ \ balance: \sum(Cations) = \sum(Anions) \qquad \textbf{4.12}$$

However, analytical errors and unanalyzed constituents in the chemical analyses cause electrical imbalances (Wrigley, 1997 and Freeze and Cherry, 1979). One measurement of this imbalance is the charge-balance error (CBE) in % CBE is used to verify the validity and quality of water analyses.

CBE was calculated using equation 4.13:

$$CBE = \frac{\sum(Cations) - \sum(Anions)}{\sum(Cations) + \sum(Anions)} \bullet 100\,\% \qquad \textbf{4.13}$$

A positive CBE indicates that one or more of the cations was over determined, or one or more of the anions was under-determined, or both. Conversely, negative CBE indicates that one or more of the cations was under-determined, or nor or more of the anions was over-determined, or both.

According to Freeze and Cherry, 1979; the acceptable water analyses have CBE of ± 5 %.

As shown in (Table 4.5), the CBE analyses in the study area has about one half of the water analyzed had for 24 % for groundwater and 24 % underground mine water CBE within the range of ± 5 %, Table 4.5. Freeze and Cherry, 1979; reported that, water analytical laboratories considered an ionic balance error of less than ± 5 % to be acceptable. According ro Guler et al., 2002; charge balance error of less than ± 10 % suitable for South Lahoton hydrologic database (SLHDATA). Booth and Berth, 1999; and Leroy et al., 1998; also set a charge balance error within ± 5-10 % in their studies. In this present study, (57 % for underground mine water and 48 % for groundwater) charge balances that were considered suitable were within the range of ± 10 % with the exception of few ions that deviated from the range (19 % for underground mine water and 28 % for groundwater).

Table 4.5: Ionic Balance for Groundwater

Sampling	Cations (meq/L)					Anions (meq/L)				Ionic
ID	Na^+	K^+	Ca^{2+}	Mg^{2+}	$(Na^+ + K^+ + Ca^{2+} + Mg^{2+})$	SO_4^{2-}	Cl^-	HCO_3^-	$(SO_4^{2-} + Cl^- + HCO_3^-)$	Balance (%)
PW1	0.87	0.11	3.57	0.97	5.52	3.25	1.39	1.58	6.88	-10.98
PW2	2.31	1.03	2.04	1.54	6.92	5.69	2.06	0.32	8.07	-7.67
PW3	3.57	0.39	3.78	1.65	9.39	3.29	3.89	0.98	9.63	-1.25
PW4	2.48	0.92	1.54	1.89	6.83	3.40	2.06	1.02	6.48	2.63
PW5	1.33	0.95	1.49	2.32	6.09	3.24	1.76	1.92	7.31	-9.11
HW	0.97	0.18	5.39	0.76	7.30	3.58	1.82	1.64	7.19	0.75
BDW1	1.62	0.84	2.34	1.37	6.17	3.06	0.98	0.90	5.20	8.51
BDW2	1.88	1.06	2.29	1.46	6.69	3.18	1.61	1.26	6.13	4.36
BDW3	1.48	1.06	2.13	1.47	6.14	3.24	1.39	0.74	7.78	-11.80
BDW4	0.73	0.88	4.32	1.57	7.50	3.46	1.55	1.82	8.68	-7.31
BBH	1.04	0.83	2.51	1.28	5.66	3.96	0.81	0.72	5.62	0.37
ABH	0.61	0.82	4.31	1.77	7.51	3.10	0.75	2.38	6.67	5.95
HBH1	1.10	0.86	1.65	1.72	5.33	3.32	1.39	1.20	7.64	-17.80
HBH2	1.11	0.84	1.01	1.69	4.65	3.20	1.31	0.96	6.05	-13.40
PBH1	1.63	0.87	1.49	0.78	4.77	2.85	2.21	0.30	6.24	-11.81
PBH2	1.27	0.82	1.74	1.21	5.04	3.05	1.14	1.64	6.40	-10.66

Table 4.5: Ionic Balance for Groundwater (Continuation)

Sampling	Cations (meq/L)					Anions (meq/L)				Ionic
ID	Na^+	K^+	Ca^{2+}	Mg^{2+}	$(Na^+ + K^+ + Ca^{2+} + Mg^{2+})$	SO_4^{2-}	Cl^-	HCO_3^-	$(SO_4^{2-} + Cl^- + HCO_3^-)$	Balance (%)
PBH3	1.41	0.85	2.00	0.94	5.20	3.19	1.39	1.22	6.40	-10.34
PBH4	0.75	0.83	1.12	1.54	4.24	3.19	0.78	1.04	5.17	-9.87
PBH5	0.75	0.82	1.12	0.82	3.51	2.15	0.72	1.16	4.43	-11.63
PBH6	0.74	0.83	3.26	0.76	5.59	3.04	0.69	1.00	4.83	7.26
PBH7	1.09	0.88	2.13	0.80	4.90	3.04	1.10	0.28	5.62	-6.87

Table 4.5: Ionic Balance for Underground mine water (Contiuation)

Sampling	Cation (meq/L)					Anions (meq/L)				Ionic
ID	Na^+	K^+	Ca^{2+}	Mg^{2+}	(Na^++ K^++ Ca^{2+}+ Mg^{2+})	SO_4^{2-}	Cl^-	HCO_3^-	(SO_4^{2-} + Cl^- + HCO_3^-)	Balance (%)
UDB-3A	1.22	0.85	11.44	5.49	19.00	9.17	6.90	4.46	21.69	- 6.62
UDB-3B	0.28	0.96	7.31	4.34	12.89	6.47	0.68	3.14	10.53	10.10
UD-6B	0.89	0.84	11.18	4.59	17.50	16.59	1.12	2.46	20.42	-7.71
UD-6C	0.97	0.83	9.38	3.89	15.07	8.68	1.27	3.30	4.45	2.08
UD-6E	0.97	0.89	12.23	4.53	18.62	12.41	1.47	3.42	17.99	1.73
UD-6F	0.49	0.84	5.91	3.61	10.85	5.89	0.96	2.22	9.36	7.39
UD-6G	0.50	0.84	9.58	3.68	14.60	9.01	0.86	2.30	12.55	7.57
UD-6H	0.39	0.83	7.12	3.89	12.23	9.04	0.71	2.42	12.59	- 1.46
UDB-9A	0.45	0.85	8.05	4.95	14.30	6.48	0.79	4.52	13.13	4.26
UDB-9B	0.28	0.83	6.98	4.32	12.41	5.48	0.98	4.18	11.08	5.64
UDB-9C	0.44	0.83	7.44	4.58	13.29	5.52	0.82	4.70	12.78	1.98
UD-17A	0.88	0.85	27.94	6.90	36.57	39.19	0.88	6.64	44.65	- 9.95
UD-17B	1.03	0.86	15.08	7.34	24.31	13.68	0.81	5.66	21.00	7.31
UD-17C	1.05	0.86	9.23	4.57	15.71	8.55	0.96	3.32	13.83	6.38
UD-17D	4.14	0.93	31.40	12.61	49.08	49.06	1.49	8.02	61.94	- 11.58
UD-17E	1.47	0.88	24.88	11.61	38.84	22.63	0.76	7.10	32.50	8.88
UD-17F	1.35	0.91	20.15	9.03	31.44	17.94	1.91	5.82	26.50	8.49

Table 4.5: Ionic Balance for Underground mine water (Contiuation)

Sampling	Cation (meq/L)					Anions (meq/L)				Ionic
ID	Na^+	K^+	Ca^{2+}	Mg^{2+}	$(Na^+ + K^+ + Ca^{2+} + Mg^{2+})$	SO_4^{2-}	Cl^-	HCO_3^-	$(SO_4^{2-} + Cl^- + HCO_3^-)$	Balance (%)
UD-24A	4.01	0.90	25.28	10.49	40.68	37.37	1.10	6.60	47.39	-7.62
UD-24B	2.50	0.86	26.88	11.08	41.32	28.82	0.78	4.74	35.90	7.02
UD-24C	3.40	0.90	43.00	14.50	61.80	78.98	0.36	7.04	88.90	-17.98
UD-24E	2.69	0.88	35.72	14.30	53.59	60.10	0.16	5.48	67.50	-11.49

4.3 COMPOSITIONAL RELATIONS AND HYDROCHEMICAL FACIES

4.3.1 Water types relationship (Hydrochemical Facies)

In order to understand the chemical character of surface water, groundwater and underground mine water and relationships between dissolved ionic constituents, the hydrochemical data has been plotted on Piper diagram. Graphical methods, like Stiff diagram, Durov plot, Piper diagram etc. provide visible interpretation of water chemistry.

In this study, the basic chemistry of surface water, ground water and underground mine water samples with respect to presence of some key cations (Ca^{2+}, Mg^{2+}, Na^{+} and K^{+}) and some important anions (SO_4^{2-}, HCO_3^{-} CO_3^{2-} and Cl^{-}) were determined by constructing Piper trilinear diagram (Piper, 1944). The diagram is shown in (Fig. 4.1).

4.3.1.1 Piper Trilinear Diagram

A Piper diagram consists of geometrical combination of two outer triangles and a middle or inner diamond-shaped quadrilateral. Here, relative abundance of cations is plotted on left cations' triangle, while relative concentration of anions is simultaneously plotted on right anions' triangle and the resultant points from the cation and anion triangular plots are placed over the inner diamond-like quadrilateral structure. The water types were designated according to the domain in which they occur on the quadrilateral plot. Each point represents one water type.

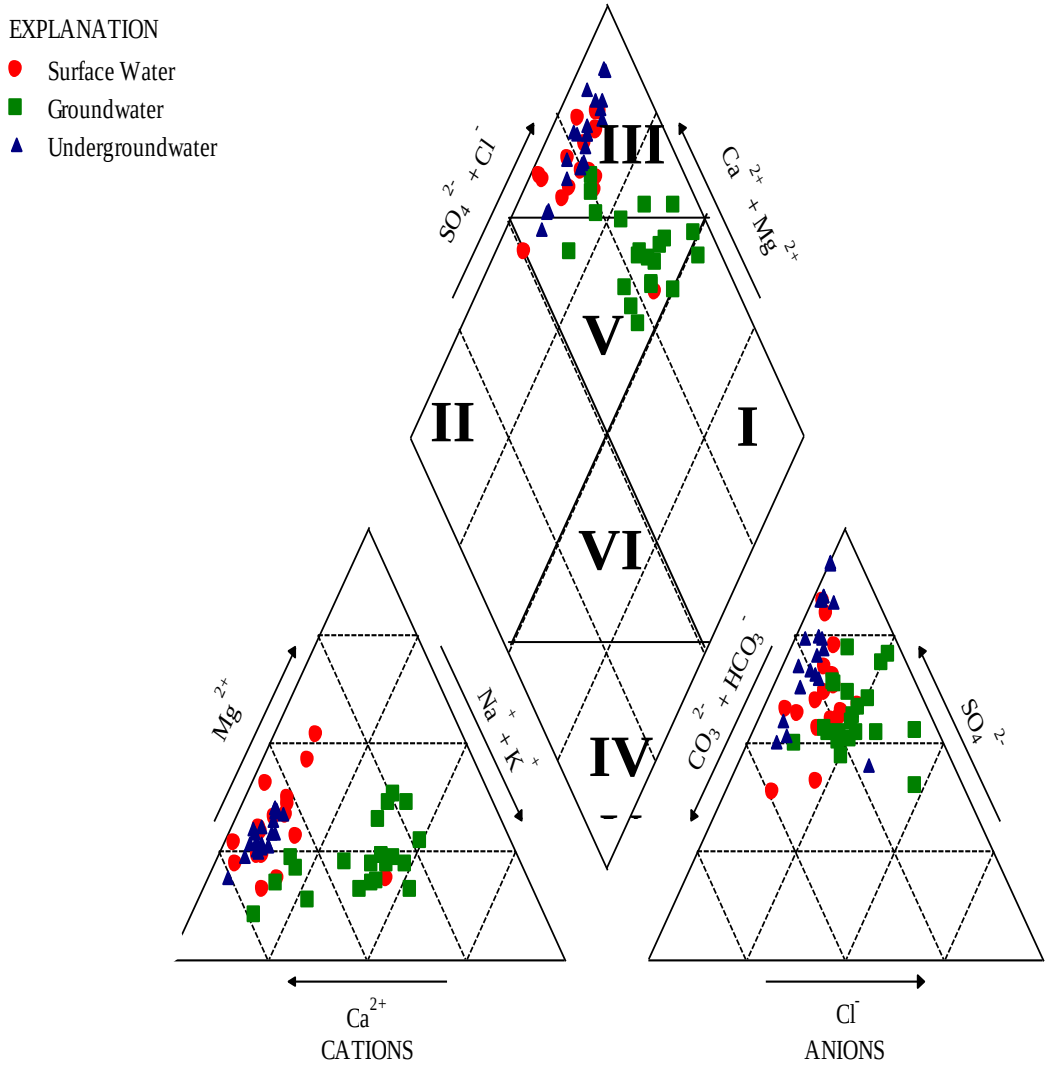

Fig.4.1: A Piper trilinear diagram showing the hydrogeochemical facies

Explaining the meaning of Sub-divisions I, II, III, IV, V and VI in the piper diagram as follow:

- Na-Cl or Na-HCO_3-Cl (Sub-division I),
- Ca-Mg-HCO_3 (Sub-division II),
- Ca-Mg-SO_4-Cl^- (Sub-division III),
- Na-HCO_3 (Sub-division IV),
- Ca-Mg-Cl-HCO_3 (Sub-division V) and
- Ca-Na-Cl-HCO_3 (Sub-division VI).

Figure 4.1 shows that the plotted points of the surface water, ground water and underground mine water fall in the sub-divisions I, III and V; indicating the dominance of alkaline earth (Ca^{2+} + Mg^{2+}) over alkalis (Na^+ + K^+); and strong acids (SO_4^{2-} + Cl^-) over weak acid (HCO_3^-). Three hydrochemical water types have been delineated:

Type I

These are Na-Cl or Na-HCO_3-Cl (Sub-division I) water and only about 5 % of the groundwater falls in this category. As discussed earlier, this water type might have evolved from combination of processes that include halite dissolution (from the quartzite, schists, soda feldspars, microline and orthoclase) from the unsaturated zone and evaporative concentration. Non-carbonate alkali (primary salinity) is the dominant.

Type II

The second water type is Ca-Mg-SO_4-Cl^- (Sub-division III). This water type is the dominant. About 90 % of surface water, 33 % of groundwater and 95 % of underground mine water make up this type in the study area. This water depicts rock-water interaction involving the dissolution of gypsum, dolomite, calcites and feldspars by the recharging ground water and underground mine water within the relatively permeable weathered zone above underlying rocks and oxidation of sulphur to arsenic sulphide (pyrite and arsenopyrite) in the rocks. Furthermore, non-carbonate hardness (secondary salinity) is responsible for permanent hard water and forms the majority.

Type III

The third is a mixed water type; Ca-Mg-Cl-HCO_3 (Sub-division V), about 10 % of surface water, 62 % of groundwater and 5 % of underground mine water make up this type. In this region, no Cation nor anion dominate

4.3.2 Correlation of physico-chemical parameters of groundwater and underground mine water

Correlation coefficient was used to show the degree of dependency of one variable on the other. From Pearson's correlation coefficient (Table 4.2), both EC and TDS are strongly correlated with SO_4^{2-}, HCO_3^-, Na^+, Mg^{2+} and Ca^{2+}. Ca^{2+} and Mg^{2+} are strongly correlated with SO_4^{2-} and HCO_3^-. A very weak correlation between Na^+ and Cl^- (r^2=0.1751), indicates the presence of low saline water in the study area. Strong positive correlation between SO_4^{2-} and HCO_3^- (r^2 = 0.7640) indicates that both groundwater and underground mine

water traverse through pyrite and arsenopyrite bearing shales, typically of Birimian formation, and thereby forming H_2SO_4, which interact with calcium carbonates, present in weathered zones, cementing materials of sandstone and shale to produce soluble calcium sulphate and carbonic acid (Equations 4.14 and 4.15).

$$H_2SO_4 + CaCO_3 \rightarrow H_2CO_3 + CaSO_4 \qquad \textbf{4.14}$$

$$2CaAl_2Si_3O_8 + 4H_2CO_3 + 2H_2O \rightarrow Al_4Si_6O_{10}(OH)_8 + 2Ca^{2+} + 4HCO_3 + 8SiO_2 \qquad \textbf{4.15}$$

Furthermore, a very strong correlation exist between Ca^{2+} and SO_4^{2-} (r^2= 0.9547), Ca^{2+} and HCO_3^- (r^2= 0.8865), Mg^{2+} and SO_4^{2-} (r^2= 0.8998), Mg^{2+} and HCO_3^- (r^2= 0.9104), Ca^{2+} and Mg^{2+} (r^2= 0.9651). These show that calcite, dolomite and gypsum are the main possible sources of these ions and are derived from the same sources. Similar reactions may also affect calcium feldspare and in the process different clay minerals and dissolve Ca^{2+} will form along with the dissolved silica.

In both groundwater and underground mine water, due to dilution of minerals, the interaction is temporarily ceased. Ca^{2+}, Mg^{2+}, SO_4^{2-} and HCO_3^- are highly interrelated among themselves indicating that the hardness of both the groundwater and underground mine water is permanent in nature. These types of significant direct relationships confirm the well-known behavior of alkali metals to be readily soluble and remain solution with several anions rather than to take part in important precipitations like calcium and magnesium (Hem, 1959). The high concentration of Ca^{2+}, Mg^{2+} and Na^+ in both ground and underground mine waters is due to the presence clay minerals such as montmorillonite, illite and chlorite (Garrels, 1976).

4.3.3 Geochemical Evolution of Groundwater and Underground mine water (Solute Acquisition Processes)

A number of factors control chemical compositions of groundwater and each groundwater system in any area has a unique chemistry due to chemical alteration of meteoric water recharging the aquifer system [Drever, (1988); Hem, (1991)]. The alterations in chemical quality of meteoric water depends on composition of infiltrating rainwater, geological structure and mineralogical composition of aquifer, duration of water-rock interaction, dissolution and precipitation of mineral species and seawater and anthropogenic influences[Hounslow, (1995); Datta and Tyagi, (1996); Andre et al., (2005)].

Compositional relations among dissolved species (Na^+, Mg^{2+}, K^+, Ca^{2+}, HCO_3^-, Cl^-, PO_4^{3-} ,SO_4^{2-} and NO_3^-) can reveal origin (meteoric, paleo-water or seawater) of solutes and process that generated the observed water compositions [Jalali, (2007); Singh et al., (2008)].

The geochemical evolution of groundwater and underground mine water from the study area is discussed on the basis of ion exchange process, leaching and dissolution of minerals (weathering), evaporation and oxidation-reduction in the following sections.

4.3.3.1 Ion exchange process

The ion exchange between the groundwater and its host environment during residence or in movement process is the most important controlling factor for groundwater and underground mine water composition. The process depends on replacement of adsorbed ions on the exchange complex by ions in solution. The ions of different elements have

different tendencies to be adsorbed or desorbed. The tendency for adsorption amongst the major cations in natural waters is as follows:

(Strongly adsorbed) $\mathbf{Ca^{2+} > Mg^{2+} > K^{+} > Na^{+}}$ (weakly adsorbed)

4.3.3.1.1 Chloro-alkalinity Index (CAI):

Schoeller (1977) proposed chloro-alkaline indices (CAI) to understand the ion exchange between the groundwater and underground mine water in the mines and their host geology. CAI is given as in equations 4.16 and 4.17.

$$CAI-1 = \left[Cl^- - \left(\frac{Na^+ + K^+}{Cl^-}\right)\right] \qquad \textbf{4.16}$$

$$CAI-II = \frac{\left[Cl^- - \left(Na^+ + K^+\right)\right]}{\left(SO_4^{2-} + HCO_3^- + CO_3^{2-} + NO_3^-\right)} \qquad \textbf{4.17}$$

The chloro-alkaline indices can either be positive or negative, depending on whether exchange of Na^+ and K^+ is from water with Ca^{2+} and Mg^{2+} in rock/ soil or vice versa. If Na^+ and K^+ are exchanged in water with Ca^{2+} and Mg^{2+}, the ratio will be positive, indicating a base-exchange phenomenon. The negative values of the ratio will indicate chloro-alkaline disequilibrium and the reaction as a cation-anion exchange reaction. During this process, the host lithology is the primary source of dissolved solids in the water.

In the present study (Fig. 4.2**)**, about 62 % of ground water and about 86 % underground mine water samples have negative values showing chloro-alkakine disequilibrium (reverse ion) and the reaction as a cation-anion exchange reaction. About 6 % of the ground water

and 6 % of the underground mine water samples have values that are positive indicating a base-exchange reaction. The rest of the samples (both groundwater and underground mine water) showed no variation. Groundwater and underground mine water with a base-exchange reaction in which alkaline earths have been exchanged for Na^+ ion (HCO_3^- > Ca^{2+} + Mg^{2+}) may be referred to as base-exchanged temporary (soften) water, and those in which Na^+ ions have been exchanged for the alkaline earths (Ca^{2+} + Mg^{2+} > HCO_3^-) referred to as base exchanged permanent (Hardened) water.

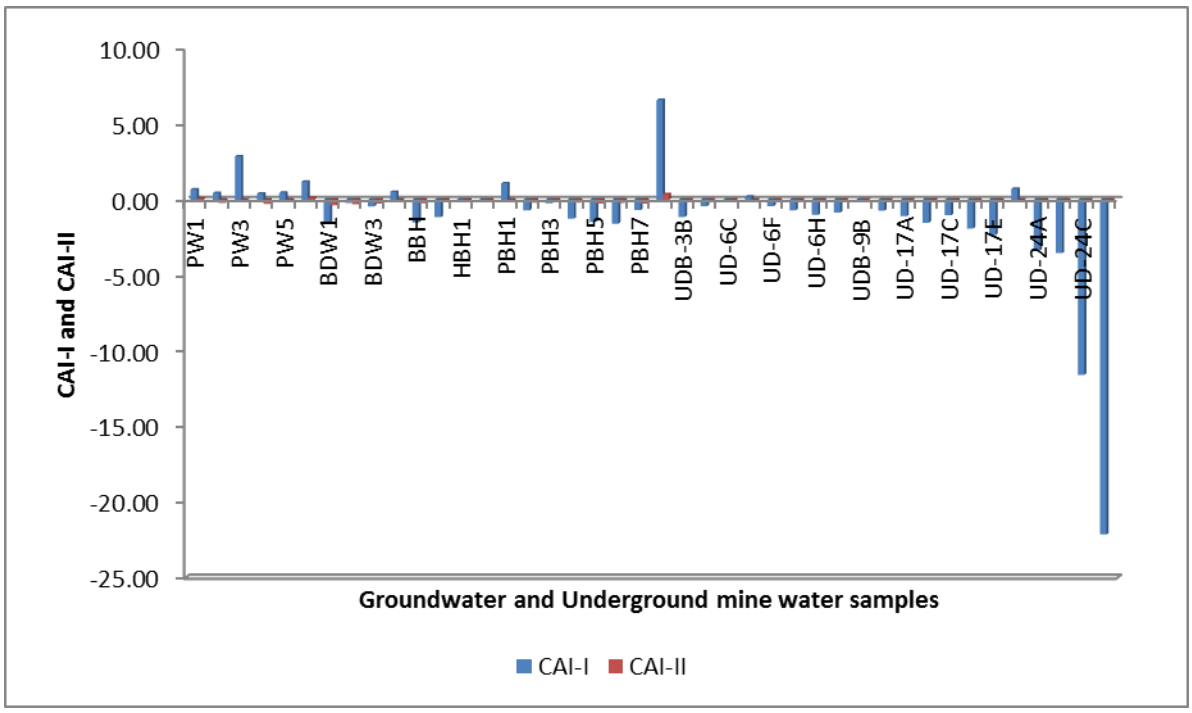

Fig. 4.2: Bar diagram of Chloro-Alkaline Indices (CAI-I and CAI-II) in Groundwater and Underground mine water samples.

In this study, about 95 % groundwater and about 98 % underground mine water have higher alkaline earths (Ca^{2+} + Mg^{2+}) than HCO_3^- (Ca^{2+} + Mg^{2+} > HCO_3^-), indicating exchange of alkaline earths for Na^+ and the water as base exchanged permanent (hardened) water.

The evidence of cation exchange can also be verified by the bivariate plot of (Ca^{2+} + Mg^{2+}) vrs (SO_4^{2-}+ HCO_{3-}) (Fig. 4.3).

4.3.3.1.2 Cation-Exchange Reaction

Cation exchange is a regulation factor of ionic concentration in water that plays a role as temporary buffer when the ionic contents are variable, causing non-steady conditions (Gimenez and Morell, 1997). The exchangeable cations on exchange sites tend to compensate for the variations of the chemical composition of waters, modifying considerably the cationic concentrations (Appelo and Postma, 1993).

a. The plot of (Ca^{2+} + Mg^{2+}) versus (SO_4^{2-} + HCO_3^-) (Fig. 4.3) will be close to the 1:1 line if the dissolutions of gypsum, ($MgSO_4.2H_2O$), calcite, ($CaCO_3$) and dolomite, [$CaMg(CO_3)_2$] are the dominant reactions in a system. Ion exchange tends to shift the points to right due to an excess of SO_4^{2-} + HCO_3^- [(Cerling et al., (1989); Fisher and Mulican, (1997)]. If reverse ion exchange is the process, it will shift the points to the left due to a large excess of Ca^{2+} + Mg^{2+} over SO_4^{2-} + HCO_3^-. Therefore in the study area, the plot of Ca^{2+} + Mg^{2+} versus SO_4^{2-} + HCO_3^- in (Fig. 4.3) shows that about 71 % of underground mine water samples of GSBPL (NCM) exceeded the 1:1 line, indicating reverse-ion exchange except for few samples distributed on both sides of line that indicate no ion exchange . On the other hand, the points falling along the equi-line (Ca^{2+} + Mg^{2+} = SO_4^{2-} + HCO_3^-) suggest that, these ions have resulted from weathering of silicates of igneous rocks [Datta et al., (1996); Rajmohan and Elango, (2004); Kumar et al., (2006)].

Underground mine water points, which are placed in the Ca^{2+} + Mg^{2+}over SO_4^{2-}+ HCO_3^- side, indicate that carbonate weathering is the dominant hydrogeochemical process in the underground goldmine.

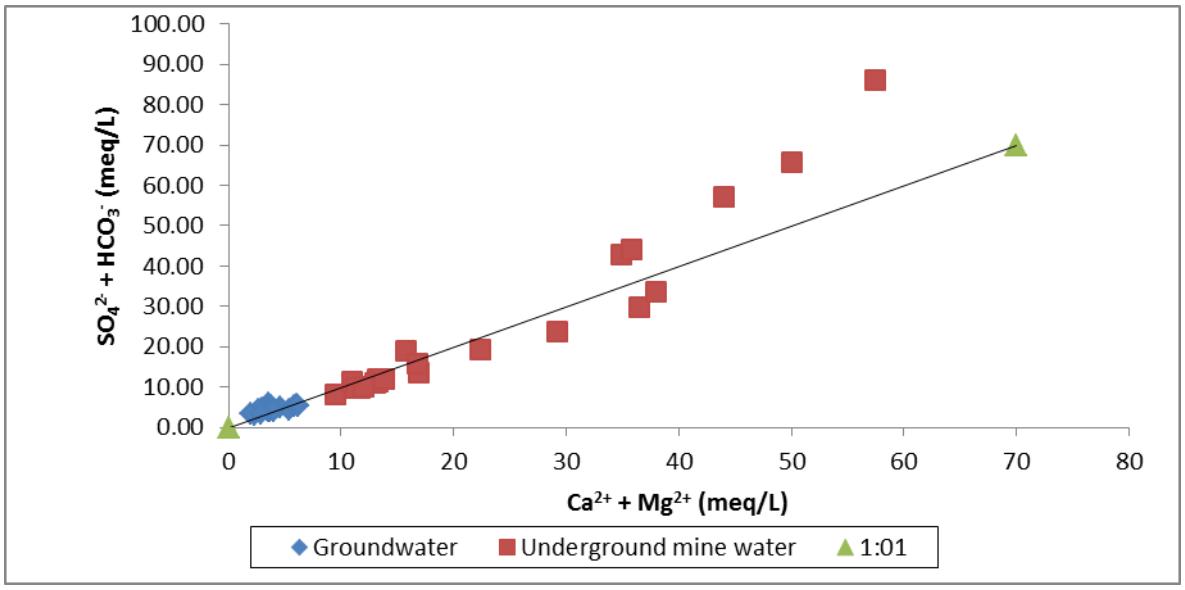

Fig. 4.3: A bivariate plot of Ca^{2+} + Mg^{2+} vrs SO_4^{2-}+ HCO_3^-

However, about 55 % of groundwater samples plot a little below the 1:1 line, which is placed in the SO_4^{2-}+ HCO_3^- over Ca^{2+} + Mg^{2+} side. It is evenly distributed on both sides but reverse ion tends to dominate over ion-exchange.

b. The evidence for cation exchange reaction can be verified by bivariate plot of [(Ca^{2+} + Mg^{2+}) - (HCO_3^- + SO_4^{2-}) as a function of [(Na^+ + K^+) - Cl^-] as shown in (Fig. 4.4). [(Na^+ + K^+) - Cl^-] represents the amount of Na^+ + K^+ gained or lost relative to that provided by Chloride salt dissolution; while [(Ca^{2+} + Mg^{2+}) – (HCO_3^- + SO_4^{2-})] represents the amount of (Ca^{2+} + Mg^{2+}) gained or lost relative to that provided by gypsum, calcite and dolomite dissolution.

If cation exchange reaction were an important composition controlling process in the study area then, the relation between these parameters would be linear with slope of – 1(Mclean et al., 2000). The bivariate plots for groundwater and underground mine water indicate a decrease in $Na^+ + K^+$ relative to increase in $(Ca^{2+} + Mg^{2+})$ or a decrease in $(HCO_3^- - SO_4^{2-})$. The plotted points are not closer to a straight line (r^2= 0.0987) with a slope of – 0.4 (Fig. 4.4). This indicates that almost all the $(Ca^{2+} + Mg^{2+})$ and Na^+ did not participate in the ion exchange reactions (Garcia et al, 2001). This confirms that cation exchange was not a significant processs occurring in groundwater and underground mine water in the study area.

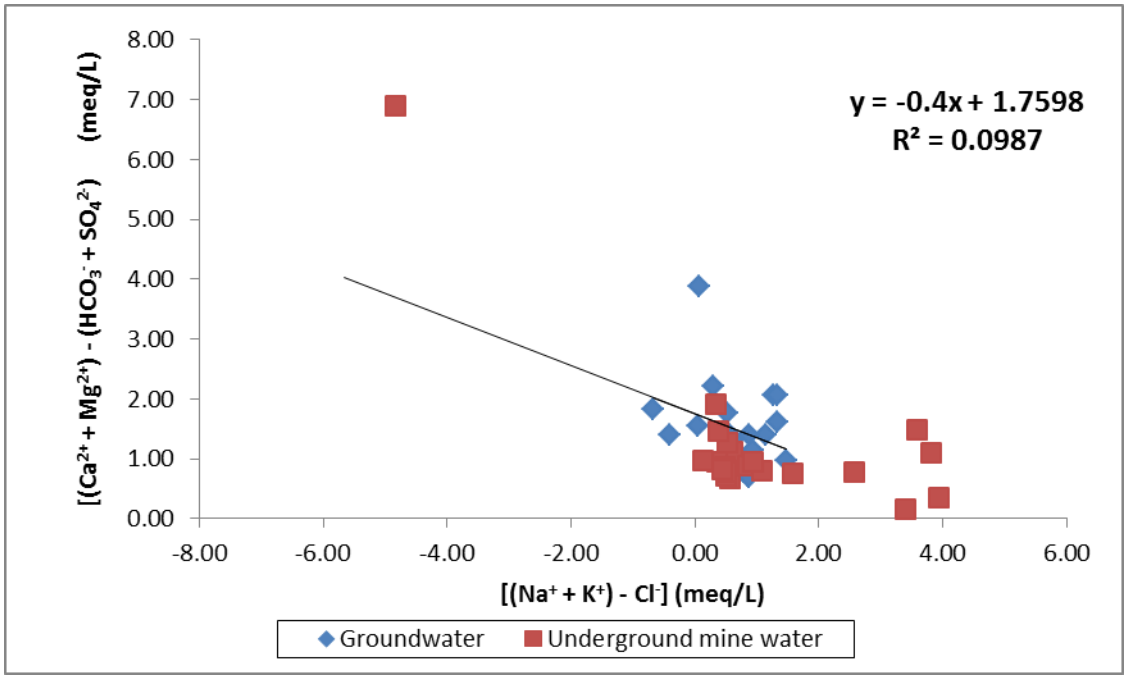

Fig. 4.4: Bivariate plot between $[(Ca^{2+} + Mg^{2+}) – (HCO_3^- + SO_4^{2-})$ vrs $(Na^+ + K^+) - Cl^-]$

4.3.3.2 Leaching and Dissolution of Weathering Minerals

Mineral weathering can contribute to the groundwater and underground mine water chemistry. The equiline (1:1) ratio would be maintained between total cation (Bivariate) and alkalinity when all the mineral weathering is the major process affecting the groundwater and underground mine water chemistry (Kim et al., 2004). The reactivity and abundance of feldspars and carbonates in the earth's crust are the major important minerals regulating the chemistry of natural waters [Bowser and Jones, (1993); Kenoyer and Bowser, (1992)].

In addition, carbonate minerals such as calcite, dolomite and gypsum largely influence the water chemistry, if they are present in the geological material, due to their dissolution rates are up to six orders of magnitude faster than those of aluminosilicate minerals (Lasaga, 1984).

4.4.3.2.1 Carbonate Weathering and Dissolution

Ca^{2+} and Mg^{2+} are the dominant cations in the groundwater and underground mine water samples collected from the area under study, with their average contributions of 64 % to the total cations. On the other hand, HCO_3^- has an average of 19 % contribution to the total anions in groundwater and underground mine water. The calcite, dolomitic limestone (the lime carbonate rocks) and gypsum are the major sources for carbonate in the area and are usually associated with Birimian formations. The carbonates from these sources might have been dissolved and added to the groundwater and underground mine water systems with recharging water during rainfall or leaching and mixing processes.

a. In Ca^{2+} + Mg^{2+} versus SO_4^{2-} + HCO_3^- scatter diagram (Fig. 4.3), the point falling along equiline (1:1) (Ca^{2+} + Mg^{2+} = SO_4^{2-}+HCO_3^-) suggests that, these ions have resulted from weathering of carbonates and silicates [Datta et al, (1996); Rajmohan and Elango, (2004); Kumar et al., (2006)]. Most of the point which are placed in the Ca^{2+} + Mg^{2+} versus SO_4^{2-}+ HCO_3^- plot indicate that carbonate weathering is the dominant hydrogeochemical process in the underground goldmine, while those placed below the (1:1) line are indicative of silicate weathering for the groundwater.

b. The plot of Ca/Mg ratio of the groundwater and underground mine water (Fig. 4.5) suggests the dominance dissolution of calcite and dolomite present in the aquifers. That is, if the ratio Ca/Mg = 1, dissolution of dolomite should occur, whereas a higher ratio is indicative of greater calcite contribution (Maya and Loucks, 1995). Higher Ca/Mg molar ratio (>2) indicates the dissolution of silicate from igneous minerals, which contribute calcium and magnesium to groundwater and underground mine water. It can be seen from (Fig. 4.3) that, 24 % of the groundwater samples in the study area, plot below and closer to the line (Ca/Mg = 1) indicate dissolution of dolomite. However, 38 % of the groundwater and 29 % of the underground mine water plot above the (Ca/Mg = 1) indicating greater calcite contribution. Furthermore, 38 % of the remaining groundwater and 71 % of the underground mine water plot above ratio line (Ca/Mg > 2), indicating the weathering effect of silicate minerals (igneous including granite rocks).

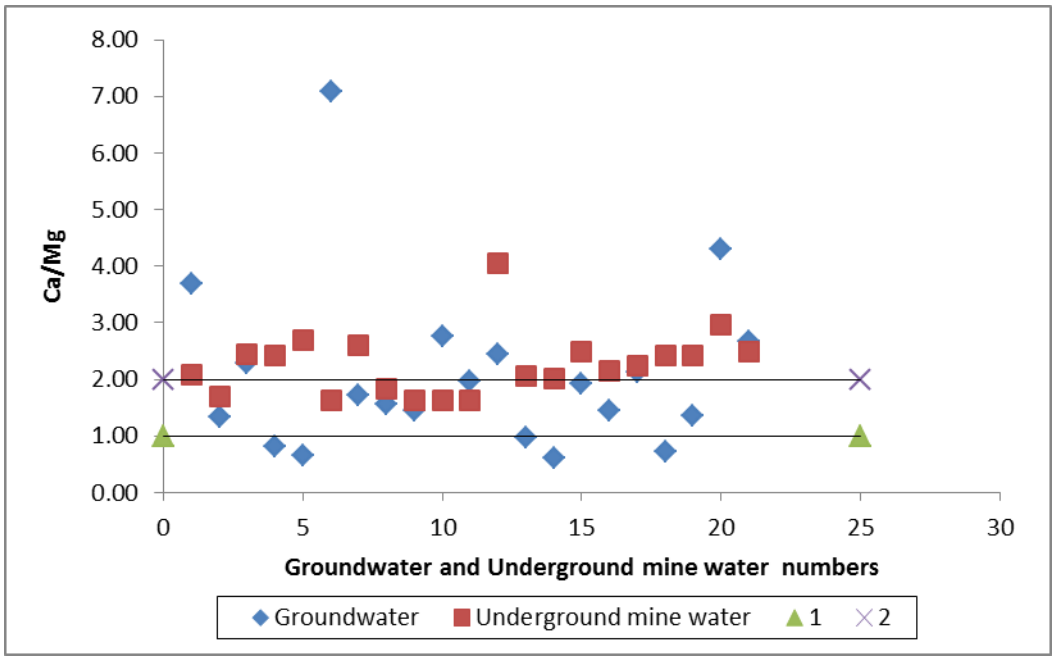

Fig. 4.5: A plot of Ca^{2+}/Mg^{2+} vrs Groundwater and Underground mine water numbers

The weathering reaction is enhanced by the presence of carbonic and sulphuric acids. If the weathering of carbonates is by carbonic acid, the equivalent ratio of dissolved Ca^{2+} and HCO_3^- in the groundwater and underground mine water resulting from calcite weathering is 1:2, whereas for dolomite weathering, it is 1:4 (Garrels and Mackenzie, 1979). If sulphuric acid is the weathering agent, then Ca^{2+}: SO_4^{2-} ratio is almost 1:1(Das and Kaur, 2001).

c. In Ca^{2+} against HCO_3^- scatter diagram (Fig. 4.6 A) almost all (80 %) groundwater and majority of underground mine water (68 %) fall along the 1:2 line and (98 %) of the underground mine water lie below 1:1 line. Furthermore, the Ca^{2+} versus SO_4^{2-} scatter diagram (Fig. 4.6 B) show that, more number about 60 % of groundwater and about 76 % underground mine water samples fall above the 1:2 line and again, these water samples trend along the 1:1 equiline $Ca^{2+} = SO_4^{2-}$, with the exception of few deviations from the

underground mine water samples. This clearly indicates the dominance of calcite weathering in the presence of sulphuric acid rather than dolomite (Garrels and Mackenzie, 1979). It also indicates the presence of dissolution of gypsum ($CaSO_4.2H_2O$) in both the groundwater and underground mine water.

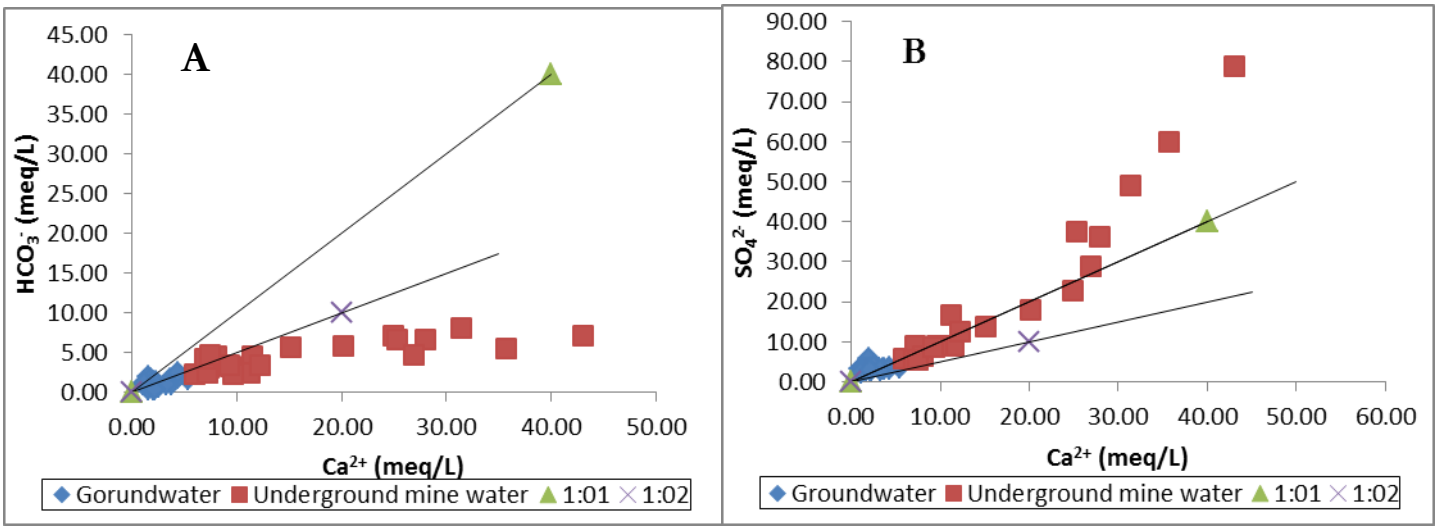

Fig 4.6 :[(A: plot of Ca^{2+} vrs HCO_3^-) (B: A plot of Ca^{2+} vrs SO_4^{2-})]

The sources of Ca and Mg in groundwater and underground mine water can be deduced from the (Ca^{2+} and Mg^{2+})/HCO_3^- ratio (Fig 4.7). Ca^{2+} and Mg^{2+} are added to solution at a faster rate than HCO_3^- ratio, which is evident from the majority of groundwater and underground mine water samples which are above one. If Ca^{2+} and Mg^{2+} originate solely from the dissolution of carbonates in the aquifer materials and from the weathering of accessory pyroxenes and amphibole minerals associated with the Birimian terrain, this ratio would be about 0.5 (Sami, 1992). Therefore the abundance of Ca^{2+} and Mg^{2+} in groundwater and underground mine water of the study area can be attributed to mainly gypsum and carbonate weathering (Sharma et al., 1998). The carbonate alkalinity in few

samples can be balanced by the alkalis Na^+ and K^+ through either silicate weathering or dissolution of alkaline soil salts. The calcium and magnesium in aquifer material exchanged with in the water is explained by the equation 4.18 below:

$$2Na^+ + Ca\ (Mg)\,Clay \leftrightarrow Na - Clay + Ca^{2+}\ (Mg^{2+}) \qquad \textbf{4.18}$$

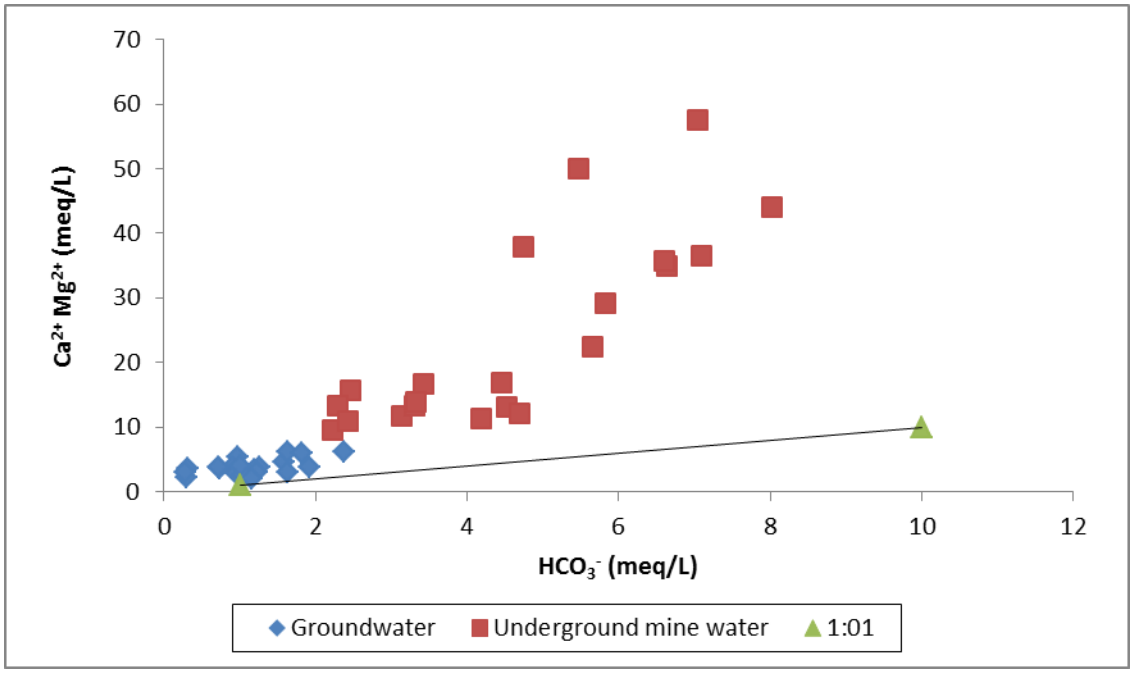

Fig. 4.7: A bivariate plot of Ca^{2+} + Mg^{2+} against HCO_3^-

4.3.3.2.2 Silicate Weathering

Silicate weathering is one of the keys for geochemical processes controlling major ion chemistry of groundwater and underground water, especially in hard rock aquifers [Mackenzie and Garrells, (1965); Rajmohan and Elango, (2004); and Kumar et al. 2006)].

a. Evidence of silicate weathering can be explained by the relationship of $Ca^{2+} + Mg^{2+}$ versus HCO_3^- (Fig. 4.7). The plot shows that, most of the ground and underground mine water samples data points fall above the equiline (1:1) (excess $Ca^{2+} + Mg^{2+}$). This situation requires part of the HCO_3^- alkalinity to be balanced by the alkalis ($Na^+ + K^+$).

b. The $Ca^{2+} + Mg^{2+}$ versus total cation (TZ^+) plot (Fig. 4.8) shows that the data points lie below the equiline 1:1. Silicate weathering can be understood by estimating the ratio between ($Na^+ + K^+$) and total cations (TZ^+), (Fig. 4.9) also shows that data points lie below the equiline (1:1) reflecting the involvement of silicate weathering in the geochemical processes, which contributes mainly sodium and potassium ions to the groundwater (Stallard and Edmond, 1983).

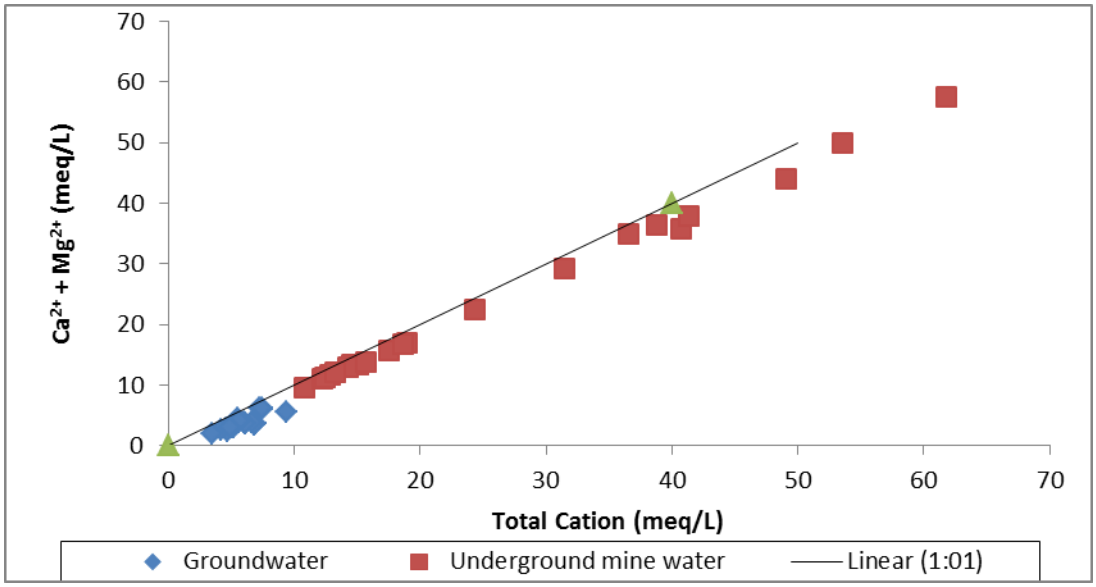

Fig.4.8: A scatter plot of ($Ca^{2+} + Mg^{2+}$) versus Total Cation (TZ^+)

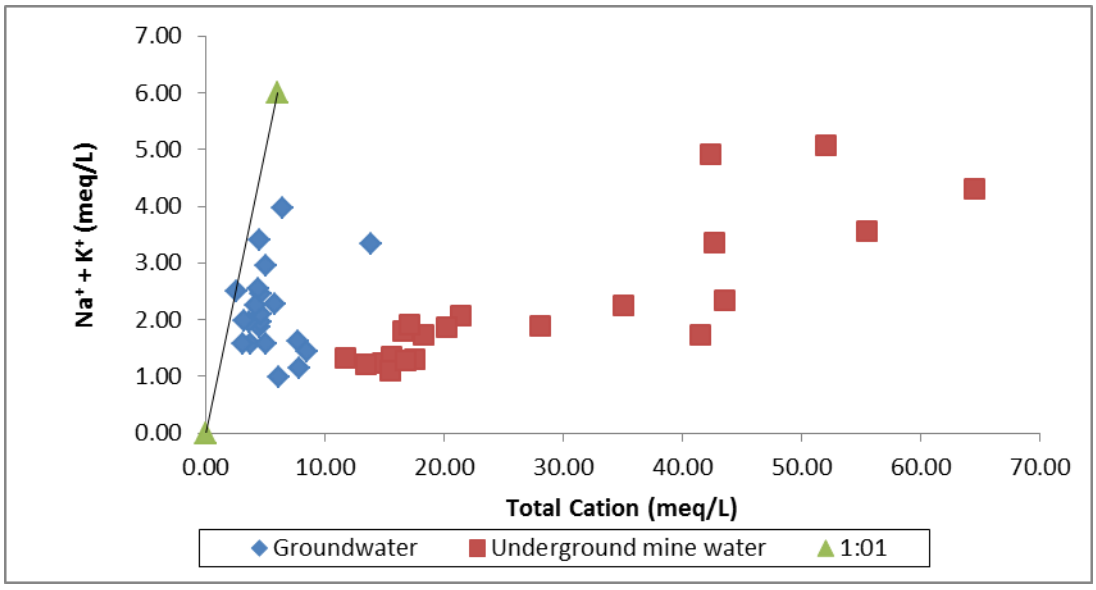

Fig. 4.9: A bivariate plot between ($Na^+ + K^+$) and Total Cations (TZ^+)

Furthermore, weathering of soda feldspar (albite) and potash feldspars (orthoclase), which are common in the Birimian formation, may contribute Na^+ and K^+ ions in groundwater and underground mine water. Feldspars are more susceptible to weathering and alteration than quartz in silicate rocks. This relatively high contribution of $Na^+ + K^+$ to the total cations is an indication of silicate weathering [Mohan et al., (2000); Rajmohan and Elango, (2004)].

c. The molal Na/Cl (Fig. 4.10) ratio greater than one (> 1), is typically interpreted as reflecting Na release from silicate weathering reactions (Meyback, 1987). The molal Na/Cl, about 81 % of groundwater and about 67 % of underground mine water samples pointed below the line. However, only a handful of about 19 % groundwater lie a little above the ratio line, while about 33 % of underground mine water, lie above the ratio line, indicating that, Na released from silicate weathering occurs in this region, in addition to

carbonate dissolution. Silicate dissolution is the probable source of Na in study area, because water that derives solutes primarily by silicate weathering could have elevated concentration of HCO_3^- as an abundant anion (Fisher and Mullican, 1997).

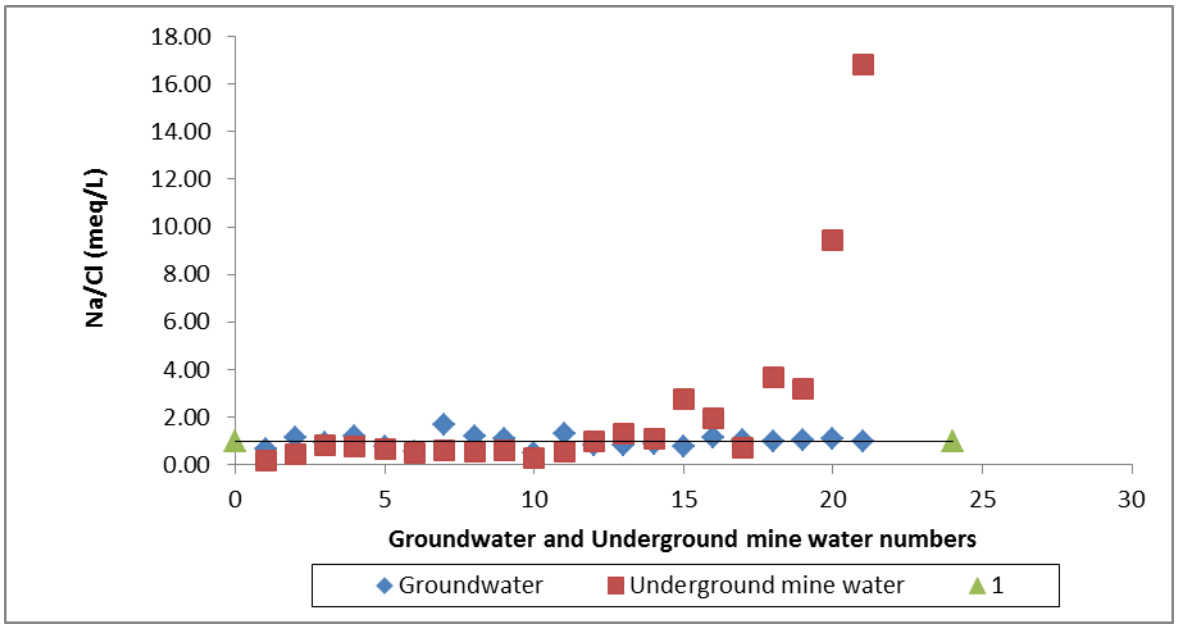

Fig. 4.10: The bivariate plot of Na/Cl vrs Groundwater and Underground mine water numbers

This is due to the reaction of feldspar minerals with carbonic acid in the presence of water, which releases HCO_3^-, Elango et al., 2003; as illustrated by the equation 4.18 below

$$2NaAlSi_3O_8 + 2H_2O + CO_3 + 9H_2O \rightarrow Al_2Si_2O_5(OH)_5 + 2Na^+ + 2HCO_3^- + 4H_4SiO_4 \qquad \textbf{4.18}$$

Albite Kaolinite

The primary silicate minerals, such as calcic-plagioclase feldspars, amphiboles and clinopyroxenes associated with Birimian rock formation, can be dissolved and weathered to kaolinite (H_4SiO_4) and cations (Na^+, Ca^{2+} and Mg^{2+}) (Guo and Wang, 2004).

The high concentration of HCO_3^- and pH less than 8.00 clearly indicates the intense chemical weathering processes taking place in this study area.

In concluding, either carbonate or silicate weathering is the dominant reaction. A plot (Fig. 4.11) of (Ca^{2+} + Mg^{2+}) versus (Na^+ + K^+) suggested both the groundwater and underground mine water data pointed towards the Ca^{2+} and Mg^{2+} region and reveals carbonate weathering as the major source of calcium and magnesium.

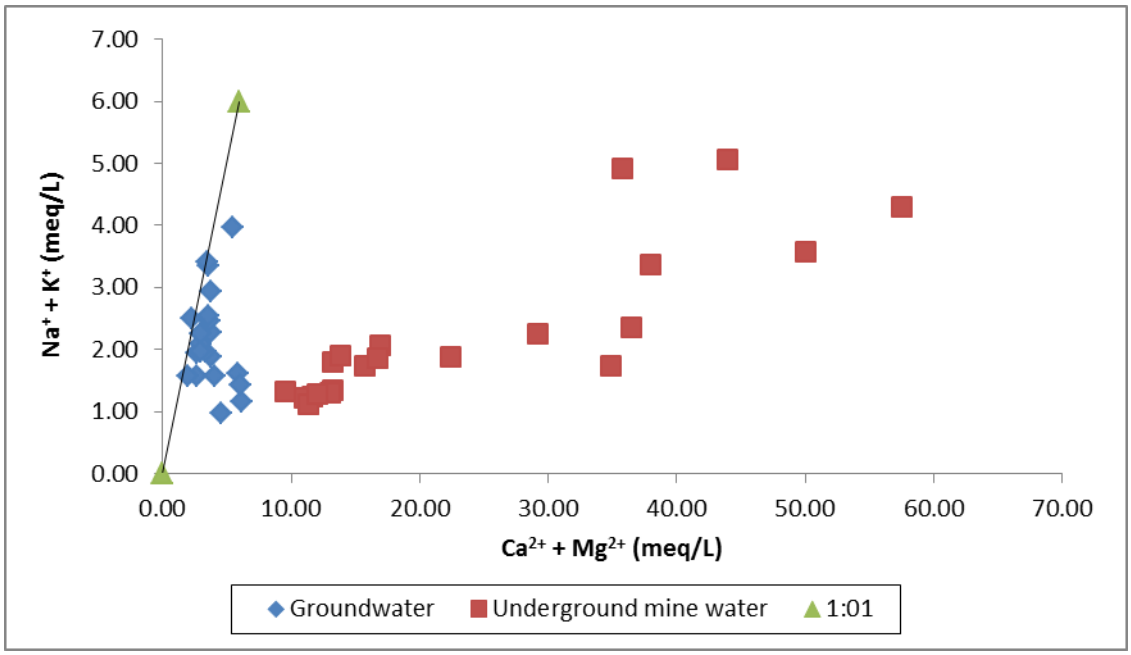

Fig. 4.11: A plot of (Ca^{2+} + Mg^{2+}) versus (Na^+ + K^+)

In the groundwater and underground mine water, K^+ is not as abundant as that of Na^+. This is expected due to the predominance of Na together with the positive of K in 2:1 of clay minerals. The levels of K in both groundwater and underground mine water are a consequence of its tendency to be fixed by clay minerals and precipitate in the formation of secondary minerals.

4.3.3.3 Evaporation (Salinity)

In general, the evaporation process causes an increase in concentrations of all species in water. If the evaporation process dominates, assuming that no mineral species are precipitated, the Na+/Cl- ratio would be unchanged (Jankowski and Acworth, 1997).

a. Hence, the plot of Na+/Cl- versus EC (Fig. 4.12) would give a horizontal line, which would then be an effective indicator of concentration by evaporation and evapotranspiration. If halite dissolution is responsible for sodium, the Na^+/Cl^- molar ratio should be approximately equal to one, whereas a ratio greater than one is typically interpreted as Na released from a silicate weathering reaction (Mayback, 1987).

The dissolution of halite in water releases equal concentration of Na^+ and Cl^- into the solution and the resulting Na^+/Cl^- molar ratio will be approximately one (Hounslow, 1995). The molar ratio of Na^+/Cl^- for groundwater samples generally ranges from 0.47 to 1.65, and for underground mine water, varied from 0.18 to 16.81. Most groundwater samples (about 43 %) have Na^+/Cl^- a molar ratio below one indicating that halite dissolution is the minor process, This is substituted by silicate weathering in the rest of the ground water samples (about 57 %) at few locations, where ratio is above one. While most underground mine water samples (about 52 %) of the underground goldmine have Na^+/Cl^- ratio trend below one, suggesting that, halite dissolution is the major process, which is replaced by silicate weathering in the rest of underground mine water samples (48 %) at few locations where the data point is above one. The lower molar Na^+/Cl^- ratio (< 1), in the rest of groundwater (about 43 %) and underground mine water (about 52 %) water samples are probably from ion exchange of Na^+ for Ca^{2+} and Mg^{2+} in clays.

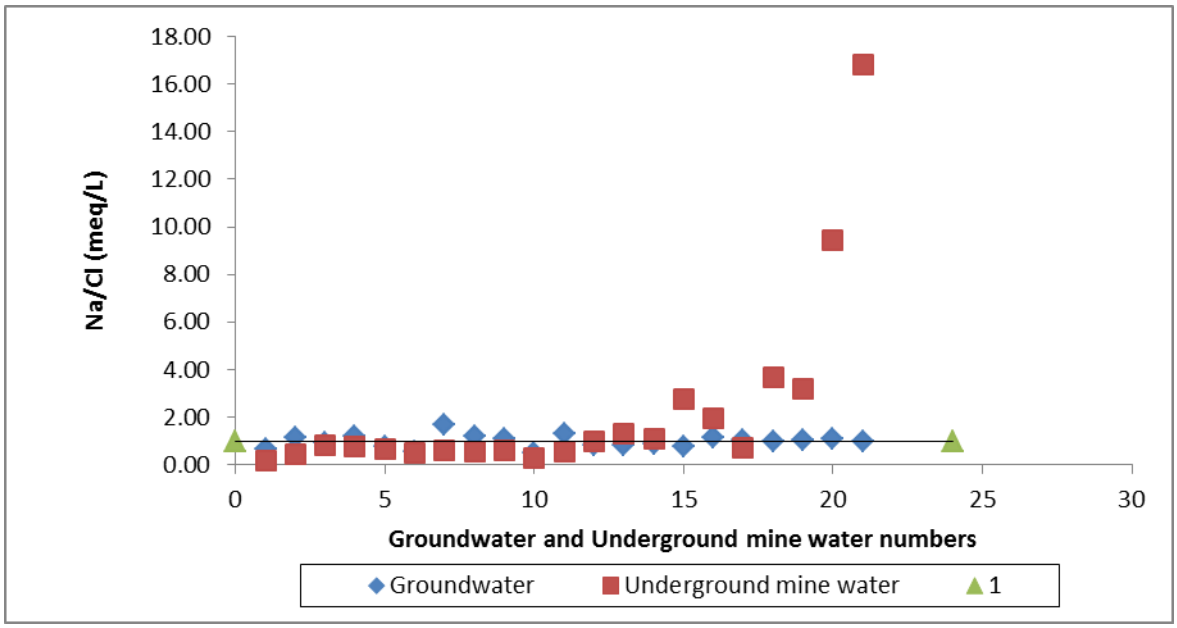

Fig. 4.12: A plot of Na/ Cl molal ratio vrs Groundwater and Underground mine water numbers

b. The trend of EC versus Na+/Cl- scatter diagram (Fig. 4.13) of the groundwater samples shows that the trend line is inclined, which indicates that evaporation may not be the major geochemical process controlling the chemistry of groundwater and underground mine water.

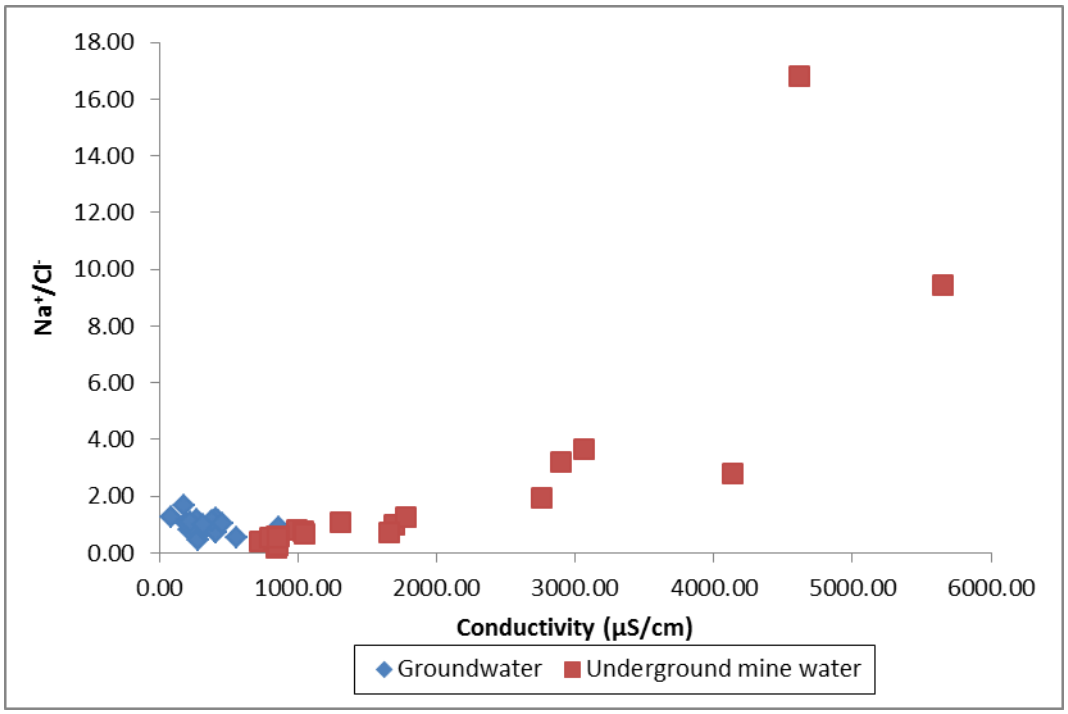

Fig. 4.13: A plot of Na^+/Cl^- vrs EC

c. The bivariate plot of Na^+ versus Cl^- diagram (Fig. 4.14) shows that, about 43 % of the total groundwater samples are lying below line1:1 and cluster along the line suggesting the same source. This indicates that the addition of Cl^- may be due to water level rise, which causes more salt dissolution from the matrix of the aquifer. Na concentration is also decreased by ion exchange. Hence, Na^+ and Cl^- do not increase simultaneously and the decrease of Na^+ is attributed to silicate weathering (Stallard and Edmond, 1983).

Underground mine water samples (about 23 %) show a wide variation, lying closer to the 1:1 line. However, few data point plotted away from the 1:1 line, indicating that evaporation occurs at the underground goldmine to a large extent.

The relationship between Na^+ and Cl^- have been used to identify the mechanism for acquiring salinity in semi arid and arid regions and to quantify atmospheric contribution [Sarin et al., (1989); Sami, (1992); Singh et al., (2005). The observed higher Na^+/Cl^- ratio in the groundwater and underground mine water as compared to Sea (marine) aerosol [Na^+/Cl^- = (0.86-1)] suggests limited contribution from atmospheric precipitation and reveals that high levels of major ions are derived most likely from the weathering of rock forming minerals of the Birimian Formation.

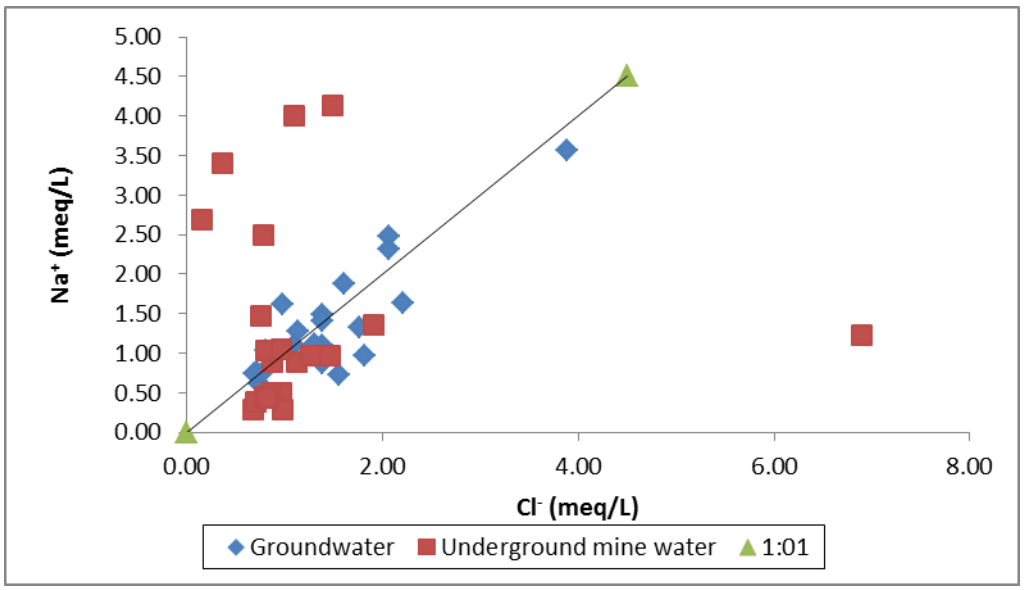

Fig. 4.14: A scatter plot of Na^+ against Cl^-

4.3.3.4 The Evolution of Ions (Mechanisms controlling groundwater and underground mine water)

Ingress of air-carrying oxygen deep into the mines provides an oxygenated environment to the subsurface rocks which triggers new set of geochemical and biogeochemical reactions of weathering. These new sets of reactions change the geochemistry of groundwater and

underground mine water through dissolution and precipitation reactions between aquifer materials and moving oxygenated groundwater and underground mine water.

Formation of clay minerals by weathering of feldspar, amphiboles and pyroxenes in new geo-environmental setting deep into the Preastea underground goldmines may take place. Release of heavy metals from surrounding rocks to groundwater and underground mine water may also take place under new regime.

To confirm the identity and hydrogeochemical processes, the diagrams of Gibbs, 1970; were done to show the hydrochemical processes of the chemical components of waters from their respective aquifer lithologies. Log (TDS) versus $(Na^+ + K^+)/(Na^+ + K^+ + Ca^{2+})$ and Log TDS versus $Cl^-/(Cl^- + HCO_3^-)$ were plotted for ground and underground mine waters of the study area.

The Gibbs diagram is a useful platform to evaluate relationships between water composition and aquifer lithological characteristics (Gibbs, 1970). The Gibbs diagram is composed of three distinct fields namely: precipitation dominance, rock dominance [water–rock interaction (leaching and dissolution of rock weathering)] and evaporation-crystallization dominance.

The results (Fig. 4.15) and (Fig. 4.16) indicates that, about 100 % of the ground water and 62 % of the underground mine water samples are laid in the water–rock interaction area. The other underground mine water data (38 %) pointed outside the plot. This may be due to anthropogenic or chemical activities that are taking place in the underground operations, and around the abandoned shafts (Alpha, Ankobra and Tuapin) as point of entry of surface water collected in the underground gold mine.

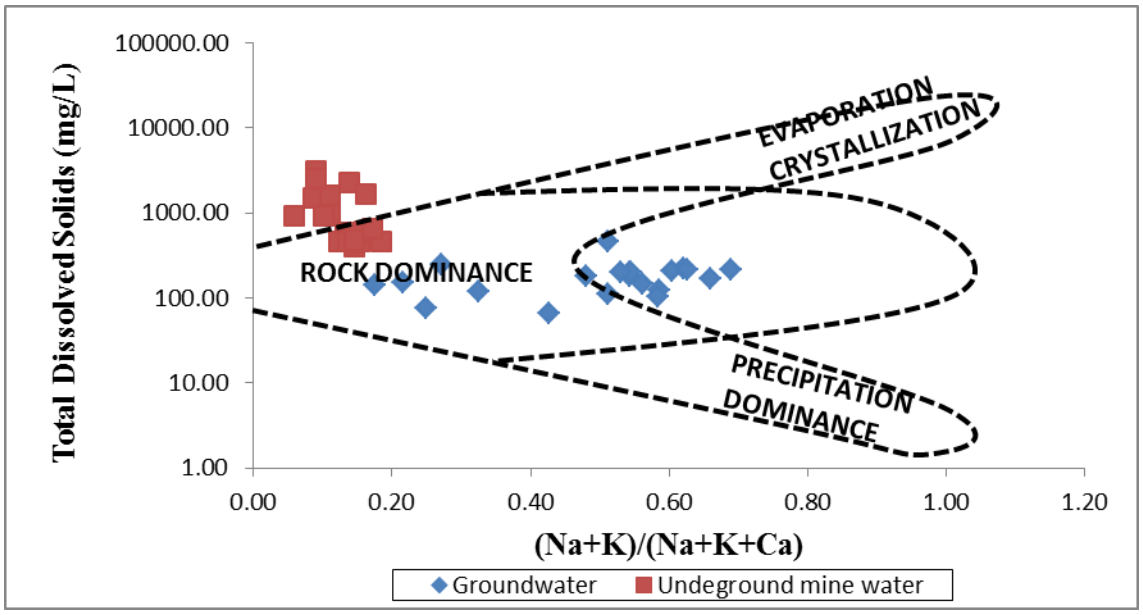

Fig. 4.15: A plot of Log (TDS) versus $[(Na^+ + K^+)/(Na^+ + K^+ + Ca^{2+})]$

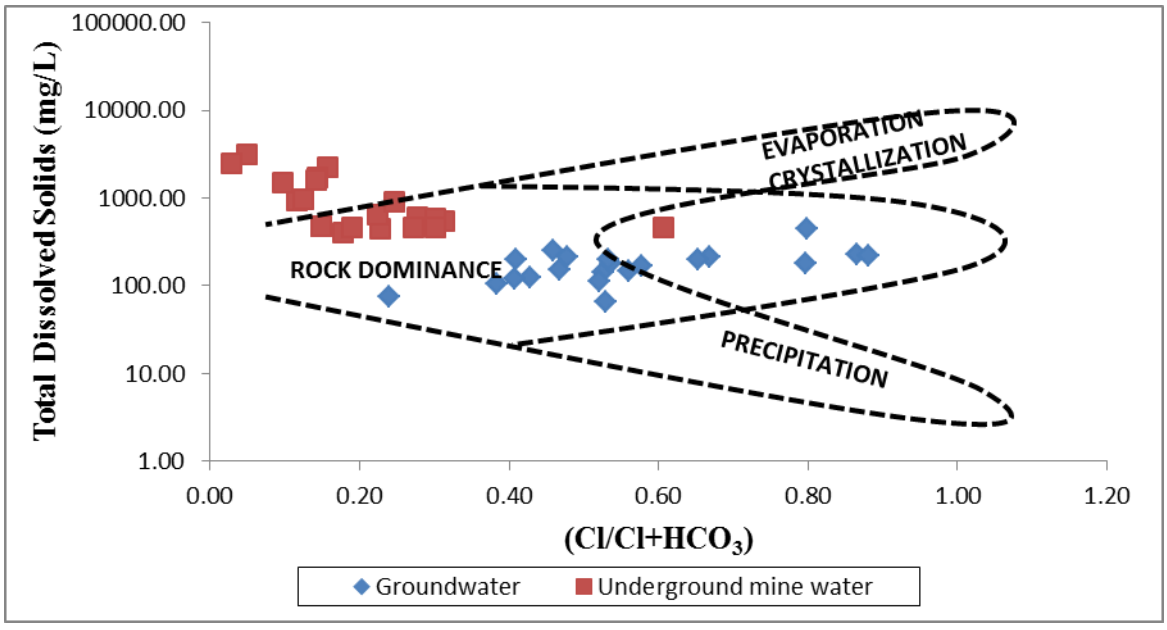

Fig. 4.16: A Bivariate plot of Log TDS versus $[Cl^-/(Cl^- + HCO_3^-)]$

4.3.3.4.1 Oxidation-Reduction Processes:

The chemistry of groundwater and underground mine water is also likely to be significantly influenced by other chemical processes, such as oxidation-reduction. This process is one of the suggested reasons for the deviation from the mineral dissolution lines (Gibbs diagram).

Oxidation reactions usually take place at the surface near the atmosphere, where O_2 is readily available. Sulphides carried to groundwater and underground mine water aquifers are oxidized to sulphates. On the other hand, the sulphate-reducing bacteria gain the upper hand under anaerobic conditions.

In the study area, this geochemical reaction is important because sulphides (pyrite and arsenopyrite) are detected in large concentrations, enough to be oxidized in the different water bearing Birimian formations.

From the above discussions, the hydrochemical processes that mostly influence the species of groundwater and underground mine water chemistry are leaching and dissolution of weathered rocks of the Birimian rocks with some influence of reverse and ion exchange water-rock interaction. Also, the evaporation and oxidation-reduction hydrochemical processes have a slight effect, if any, on the chemistry of groundwater and underground mine water of the study area.

4.4 TRACE ELEMENTS IN THE WATER SAMPLES

Trace element may be defined as an element which is present in matrix in concentration of less than 0.1 wt %. Trace elements are dissolved metallic elements that occur or can be

present in groundwater often at concentration well below 0.1mg/L, but occasionally higher (Kortatsi, 2004). Sometimes, trace elements will form mineral species on their own right but most commonly they substitute for major elements in the rock forming minerals (Hugh Rollison). Trace elements make up of only 1 % of naturally-occurring dissolved constituents in ground water.

Trace elements that are going to be discussed include arsenic, cadmium, copper, iron, lead, manganese and zinc.

4.4.1 Concentration of Elemental Compositions

Arsenic (As)

Arsenic concentration of surface water varied from <0.001 to 0.19 mg/L, ranges from <0.001 to 0.03 mg/L for groundwater and between <0.001 and 0.69 mg/kg for underground mine water (Appendix VI). The highest As concentration (0.69 mg/L) was detected at UD-24A (Prestea Central Shaft). Interestingly, 19 %, 20 % and 33 % arsenic concentrations in surface water, groundwater and underground mine water samples, respectively, were however low, non-existence or below detection limit in most of the aquifers except where negligible traces were encountered (Fig. 4.17).

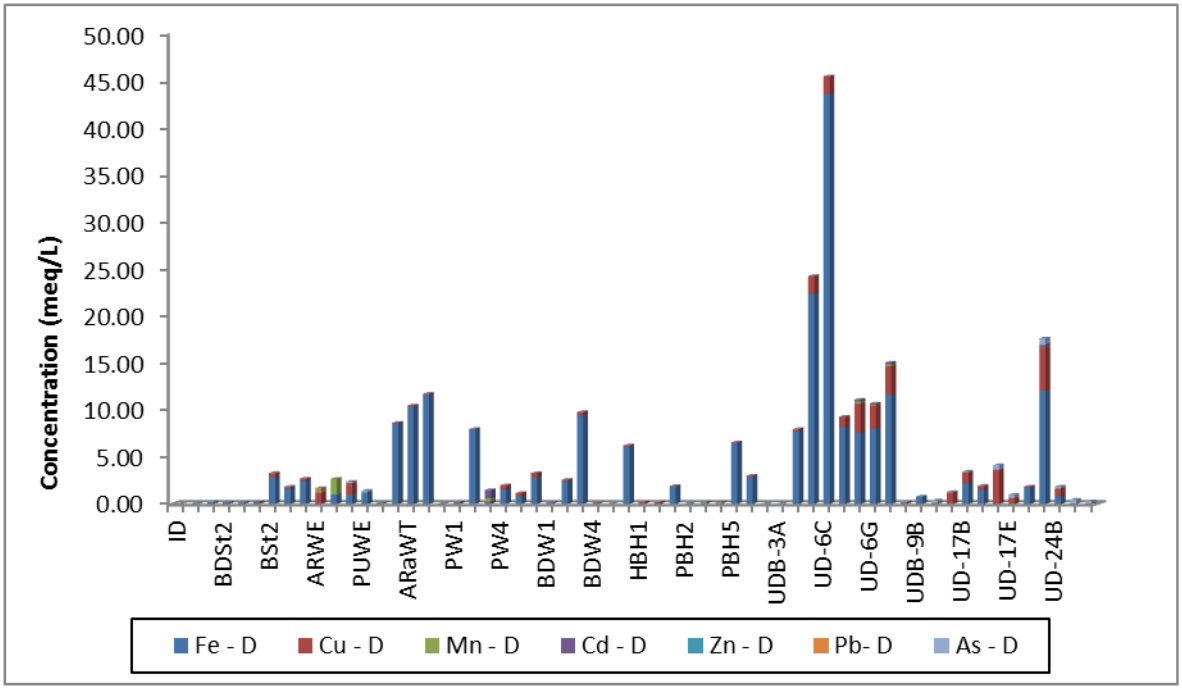

Fig. 4.17: Trend in the concentration of trace elements

The primary source of arsenic in nature is the oxidation of arsenic sulphides like arsenopyrite (FeAsS), and pyrite (FeS_2) (Bhattacharya et al., 2004). Other sources include anargite (Cu_3AsS_4), tennanite [$(CuFe)_{12}As_4S_{13}$)], realgar (As_2S_4), orpiment (As_2S_3) and arsenides of silver and lead (Kesse, 1985). These minerals can be oxidized by O_2, Fe^{3+} and NO_3^-. Conversion of NO_3^- to NH_4^+ is a common phenomenon in reducing environments and a positive correlation between As (III) and NH_4^+ signifies its importance in mobilizing arsenic in the ground aquifers (Bhattacharya et al., 2004). Irrespective of whether mining has taken place or not, arsenic bearing ores can therefore be oxidized to produce arsenic in water, however, mining activities increases the surface area of rocks and exposes rocks to rapid weathering. Inorganic arsenic can occur in the environment in several forms but in

natural waters it is mostly found as [trivalent arsenite, As (III) or pentavalent arsenate, As (IV)].

In the Tarkwa-Prestea, area arsenic occurs in aquifers underlain by Birimian rocks as a result of the oxidation of pyrite and arsenopyrite, which is hastened by mining activities. With increase in residence time of groundwater and underground water, arsenic concentration tends to increase (Kortatsi, 2004). This explains the presence of arsenic in the lower Birimian at Bondaye (southern part of the study area). Mining has generally low impact on arsenic concentrations as there are no seasonal variations in levels (Kortatsi, 2004).

Cadmium (Cd)

Concentration of Cd in the surface water varied from <0.005 to 0.01 mg/L, ranges from <0.005 to 0.89 mg/L for groundwater and <0.005 to 0.28 mg/L (Appendix VI) for underground mine water. Cd contents in 95 % of surface water, 86 % of groundwater and 18 % of underground mine water samples were below the detection limit. The detailed result is presented in (Appendix VI). The observed trend in the concentration of Cd in most of the underground mine water samples is due to the large surface areas of the host rock induced by the mining activities. Most importantly, the water has long residence time to react with rock matrix at equilibrium.

Cadmium naturally occurs as accessory elements in zinc ore (sphalerite, ZnS) (largest industrial sources), CdS; and $CdCO_3$ (rare). Anthropogenic sources of Cd are industrial wastes. Almost zinc concentration in the study area were below the detection limit (<0.001 mg/L), suggesting that, Cd could have occurred as accessory element of Zinc ore

(sphalerite, ZnS). The other natural sources [rare ($CdCO_3$)] could have contributed to the concentration of cadium in the Prestea underground gold mine.

Copper

Concentration of copper varies from <0.003 to 0.50 mg/L for surface water (Appendix VI). For groundwater, ranges from <0.003 to 1.24 mg/L and for underground mine water, it is between <0.003 to 4.60 mg/L (Appendix VI).

Copper occurs naturally in the environment and spreads through natural and artificial phenomena (Nayaka et al., 2009). Natural sources can be: decaying vegetation, potash from ashes and sea aerosol. Phosphate fertilizer production is another means of artificial phenomena that generate copper into the environment. Most of the colloidal materials of soil (oxides of Mn, Al, and Fe, silicate clays and humus) adsorb Cu^{2+} strongly, so as to raise the pH (McBride, 1994). Furthermore, Cu has a much lower mobility in reducing conditions. The increasing trend of copper, as observed in the underground mine water samples, indicated the surface exposure of rocks and the extent of time for water-rock interaction taking place within the host aquifer.

Iron (Fe)

The range of iron (Fe) in the water sample concentration was from <0.01 to 11.55 mg/L (Appendix VI) for surface water, varied from <0.01 to 0.93 mg/L for ground water, and for underground mine water; it was between 0.02 and 43.53 mg/L (Appendix VI). However, concentrations in 19 % of surface water, 5 % of both groundwater and underground mine

water samples were below detection limit. The highest level of Fe concentration was detected at UD-6C, suggesting the intense exposure of the rock to water due to intense mining activities and further showing that iron concentration increases with exposure of mafic minerals to aquifers

Iron occurs naturally in aquifers but levels in groundwater and underground mine water can be increased by the dissolution of ferrous boreholes and hand-pumped components. (Lenntech, 2005). In groundwater systems, iron occurs in one of the two oxidation states, reduced soluble divalent ferrous iron (Fe^{2+}) or oxidized insoluble trivalent ferric iron (Fe^{3+}) (Vance, 2002). The chemical processes of iron occurrence in groundwater involves hydrolysis and precipitation of hydroxides, solution and precipitation carbonates, oxidation and reduction reactions, solution and precipitation of sulphides and formation of complex ions and chelation. These processes are interrelated and may act simultaneously (Kortatsi, 2004).

Pyrite and arsenopyrite are associated with the underlain geology of the Tarkwa-Prestea area (Kesse, 1985). The presence of iron in ground water and underground mine water is explained by the chemical weathering (oxidation) of iron bearing rocks by weak carbonic acids formed either in the air or soil. The variations in iron levels in the aquifers can be attributed to the geology as wells within the Birimian Formation having higher levels than those within the Tarkwaian. Kortatsi (2004); suggested that, the Birimian System is much impregnated with iron bearing ores of pyrite, limonite, arsenopyrite than the Tarkwaian System (Kesse, 1985). Iron concentration in Tarkwa-Tarkwaian was high because of higher iron minerals in the rocks (Kuma, 2003). Iron in the groundwater could be derived from the leaching of iron from amphiboles and pyroxenes as a result of carbon dioxide

attack on rock matrix (Kortatsi, 2004). Amphiboles and pyroxenes are common minerals in the silts and dyke intrusion of the Tarkwaian and Birimian Formation (Kesse, 1985).

Manganese (Mn)

Manganese concentrations varied from <0.002 mg/L to 1.69 mg/L (Appendix VI) for surface water, between <0.002 and 0.32 mg/L for groundwater and ranges from <0.002 to 0.24 mg/L underground mine water respectively, (Appendix VI).

Manganese can be found in rocks such as granites, schists and sandstones but in minute quantities. Manganese ores in commercial quantities exists as oxides and hydroxides as pyrolusite (MnO_2), psilomelane, manganite (MnO_2H), braunite (Mn_2O_3) and hausmannite (Mn_3O_4). Minute occurrences include carbonate and silicate ores (Kesse, 1985).

Manganese found in groundwater is probably most often the result of solution of manganese from soils and sediments aided by bacteria. Like iron, manganese occurs in more than one oxidation. The oxidation states of manganese in groundwater are the bivalent (Mn^{2+}) and the quadrivalent (Mn^{4+}) (Kusimi, 2007) Manganese can also occur in more highly oxidized states (Mn^{6+} and Mn^{7+}), but it is not normally encountered in these in natural water. Under reducing conditions, manganese can be taken into solution in groundwater containing carbon dioxide in a manner analogous to iron. In quadrivalent forms as manganic hydroxide [$Mn(OH)_4$], manganese is a nearly insoluble, and it is carried in colloidal suspension in a manner similar to ferric hydroxide. Manganese usually occurs with iron as redox couple as shown in equation 4.17.

$$2Fe^{2+} + Mn^{2+} \leftrightarrow 2Fe^{3+} + Mn \qquad \textbf{4.17}$$

where, the $\mathbf{Mn^{2+}}$ is reduced to **Mn**, and **Fe** is oxidized to $\mathbf{Fe^{3+}}$.

In the Tarkwa-Prestea area, manganese occurs as manganese and manganiferous oxides particularly in Birimian rock terrains (Kortatsi, 2004). Manganese exists in the Upper Birimian in three forms; magniferous phyllites, spessartite-quartz rocks in association with biotite-paragneiss, biotite schists and amphibolite and oxides of the two. Mobility of this mineral is also independent of mining activities since there are no seasonal variations in concentration levels (Kusimi, 2007).

Lead (Pb)

Lead concentration for surface water was between <0.01 and 0.22 mg/L and varied from <0.01 to 0.22 mg/L for ground water samples (Appendix VI). Furthermore, 62 % of surface water, 95 % of and underground mine water samples were below instrumental detection limit (<0.01 mg/L).

Lead occurs in small amounts in the earth's crust. The main minerals of the lead are the sulphate galena (PbS), anglesite ($PbSO_4$), pyromorphite ($3Pb_3P_2O_3PbCl_2$), jamesonite ($2PbSSb_2S_3$) and sulphenite ($PbMoO_4$) (Kesse, 1985). The movement of lead into groundwater is unlikely, unless the water is acidic, a common problem is the acid mine drainage areas.

Like arsenic, lead concentration levels are very low. The highest concentration detected was 0.22 mg/L at PUWF (Prestea); this may be due to the dissolution of underground water in the lead pipes as it is being pumped from underground onto the surface.

High concentrations occur at Birimian rock terrains particularly in the Bogoso-Prestea area (Kortatsi, 2004). Its relatively high occurrence in the Lower Birimian implies that concentration levels are directly related to residence time.

In Tarkwa-Prestea, lead occurs with sulphide ores in the form of boulangerite ($Pb_5Sb_4S_3$), which i about 0.01 %, bournonite (Pb_5CuSbS_3) approximately 0.01 %, galena (PbS) about 0.006 % (Kortatsi, 2004). The humic acid waters leach these minerals into groundwater. The lower pH values of the Tarkwa-Prestea groundwaters have been attributed to high rainfall and vegetation regime of the area, which produces high levels of carbonic and organic acids resulting in intense leaching (Kuma, 2003).

Zinc (Zn)

Zinc concentration varied from <0.001 to 0.01 mg/L for groundwater [(BDW4) (5 %)] (Appendix VI)**.** However, all the surface and underground mine water sample were low and even below detection limit (Appendix VI).

Zinc is one of the most common elements in the earth's crust and its ore sphalerite (ZnS) usually occurs in association with lead (Kesse, 1985). Most of the zinc in water bodies, such as lakes or rivers, settles on the bottom. However, small amounts may remain either dissolved in water or as fine suspended particles. The level of dissolved zinc in water may

increase as the acidity of water increases. Most of the zinc in soil is bound to the soil and does not dissolve in water, with present study being no exception. However depending on the characteristics of soil or rock, some of the zinc may reach ground water and subsequently through hydraulic conductivity induced by mining processes (exploration), it may reach underground. In the Tarkwa-Prestea area, zinc is found mainly in sphalerite (ZnS) and tennalite [(Cu, Fe, Zn) As_4S], which forms 0.03% of the sulphide ore in the Prestea underground goldmine (Kortatsi, 2004).

4.4.2 Elemental Relationship

The correlations matrix, (Table 4.6) of the elements in the samples demonstrate excellent correlation between elemental pairs for Cd and Mn with their corresponding correlation coefficient for both ground water and underground mine water and suggest common sources of these elements into the groundwater and underground mine water, likely resulting from the geology of the study area. However the rest exhibited poor correlation and indicates different source of origins of the trace elements.

However, the low detectability of some of the trace elements in the samples may have masked the true relationship between the elements. Trace elements also show the correlation between Cd and Mn, and the dominant element to be Fe in the study area and correlates very well with Sulphate.

Table 4.6: Pearson correlation coefficient for ground and underground mine water at 95% CI

	Fe	*Cu*	*Mn*	*Cd*	*Zn*	*Pb*	*As*
Fe	1.0000						
Cu	0.4543	1.0000					
Mn	0.0194	0.3082	1.0000				
Cd	0.0662	0.2888	**0.8269**	1.0000			
Zn	-0.0424	-0.1750	-0.1615	-0.1200	1.0000		
Pb	-0.0336	-0.2110	0.1827	0.2727	-0.1262	1.0000	
As	-0.0740	0.4718	-0.1269	0.0819	-0.1284	-0.1580	1.0000

4.5 ENVIRONMENTAL ISOTOPES DEUTERIUM (δ^2H) AND OXYGEN-18 ($\delta^{18}O$)

Deuterium and oxygen-18 isotopes are influenced by processes affecting the water, rather than the solutes and can help identify waters that have undergone evaporation, recharge under different climatic conditions than present, migration pathways and mixing of waters from different sources [Fontes, (1976); Sacks and Tihansky, (1996)].

4.5.1 Stable Isotope Composition in Surface water, Groundwater and Underground mine water

The composition of oxygen-18 and deuterium of the surface water, hand-dug wells, borehole and underground water are presented in (Table 4.7).

The stable isotope data are expressed as per mil deviations from VSMOW standard. The stable isotopes compositions ($\delta^{18}O$ and δ^2H) for surface water, groundwater (hand-dug wells and borehole) and underground mine water are discussed in the following.

Table 4.7: Stable Isotopes [δ^2H (‰) and $\delta^{18}O$ (‰)]

Underground mine water			Groundwater			Surface water		
Sample ID	δ^2H (‰)	$\delta^{18}O$ (‰)	Sample ID	δ^2H (‰)	$\delta^{18}O$ (‰)	Sample ID	δ^2H (‰)	$\delta^{18}O$ (‰)
UDB-3A	-4.73	-1.99	HW	-1.32	-1.31	ASP	-2.74	-1.12
UDB-3B	-4.67	-1.98	PW1	-6.48	-1.82	BSP	-4.93	-2.16
UD-6B	-4.44	-1.79	PW2	-4.29	-1.62	BSt2	-5.32	-1.83
UD-6C	-4.97	-1.77	PW3	+0.42	-1.59	BDSt	-5.12	-2.05
UD-6E	-6.57	-1.59	PW4	-6.05	-1.75	BDSt2	-3.83	-1.08
UD-6F	-6.43	-1.88	PW5	-6.12	-1.67	PSW	-4.71	-1.96
UD-6G	-7.63	-1.83	BDW1	-4.10	-2.28	ARaWT (US)	-0.93	-0.63
UD-6H	-6.20	-2.14	BDW2	+0.53	-1.63	ARaWM (MS)	+0.21	-0.49
UDB-9A	-8.54	-2.07	BDW3	- 2.93	-1.68	ARaWE (DS)	-2.21	-0.50
UDB-9B	-5.65	-2.03	BDW4	-2.27	-0.87	HRWT (US)	+1.73	-0.24
UDB-9C	-5.98	-1.91	BBH	-5.70	-2.06	APWM (MS)	+3.02	+0.47
UD-17A	-4.96	-2.10	ABH	-6.43	-2.16	ARE (DS)	+2.85	-0.90
UD-17B	-3.26	-1.18	HBH1	-2.53	-1.43	PUMF (US)	-6.66	-1.78
UD-17C	-3.68	-2.00	HBH2	-1.68	-0.48	PUWM (MS)	-2.08	-1.15
UD-17D	-4.74	-2.17	PBH1	-2.71	-1.51	PUWE (DS)	-1.07	-1.01
UD-17E	-4.94	-2.22	PBH2	-4.44	-2.19	BDU (US)	-1.84	-0.79
UD-17F	-1.00	-0.95	PBH3	-5.00	-1.50	BDUW (MS)	-3.29	-0.98
UD-24A	-6.10	-2.17	PBH4	-8.88	-2.23			
UD-24B	-3.01	-1.83	PBH5	-5.62	-2.08			
UD-24C	-5.04	-2.03	PBH6	-2.41	-1.71			
UD-24E	-2.71	-1.63	PBH7	-2.99	-0.66			

4.5.2 The ($\delta^{18}O$ and $\delta^{2}H$) Correlation in Water Samples

Stable isotope composition of surface water, hand-dug wells, boreholes and underground mine water collected were plotted, as shown in (Fig 4.18), from different locations of the study area.

Two meteoric water lines have been inserted. These include that obtained by (Craig, 1966)

$$\delta^{2}H = 8\delta^{18}O + 10 \qquad \textbf{4.19}$$

Which is the Global Meteoric Water Line (GMWL); and Local Meteoric Water Line equation (LMWL)(Akiti, 1980) written as:

$$\delta^{2}H = 7.86\delta^{18}O + 13.6 \qquad \textbf{4.20}$$

The work by Akiti (1980) was in the Accra plains in the South-Eastern part of and the Upper Regions of Ghana. Coincidently, Prestea, the study area, lies in the South-Western part of Ghana, Akiti Meteoric Water Line was the adequate paramater for the studies.

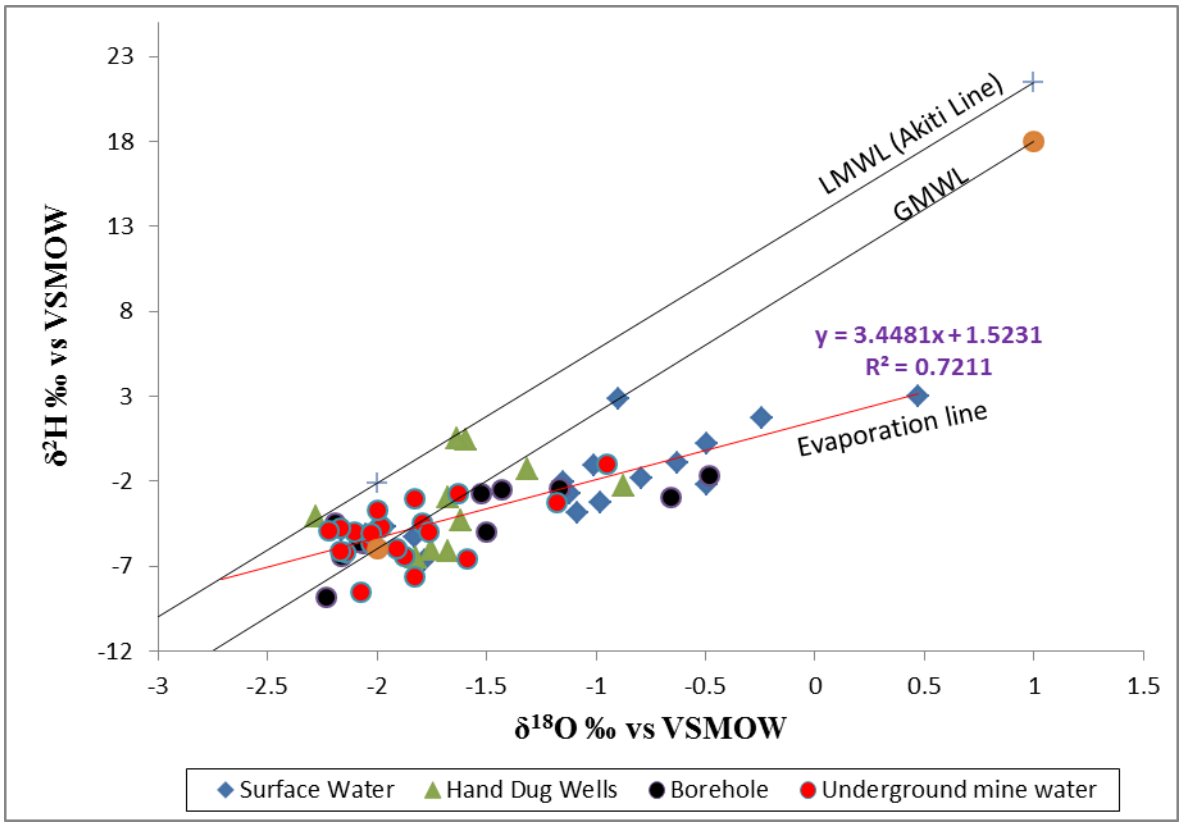

Fig. 4.18: Relationship between δ^2H ‰ vrs VSMOW and $\delta^{18}O$ ‰ vrs VSMOW

Figure 4.18 shows the relationship between surface water, hand-dug wells, and boreholes from the catchment area and underground mine water from GSBPL (NCM). Some of the water samples plotted on and near the Local Meteoric Water Line (Akiti line), with majority of the water samples clustering around the global meteoric water line. Those that were plotted closer to or on the GMWL, in (Fig 4.18) are in direct equilibrium with GMWL and confirm that local rainfall is capable of recharge. Evaporation line (red line) is drawn to account for those that plotted away from the GMWL, it showed little or much enrichment pattern that could be attributed to either evaporation of meteoric water before and/ or prior to groundwater (hand-dug well and borehole) and underground mine water recharge.

Stable isotopes of surface water

Values of $\delta^{18}O$ for surface water in the Prestea catchment area were between – 2.16‰ vs VSMOW and + 0.43 ‰ vs VSMOW , and ranged from -6.66 ‰ vs VSMOW to + 3.02 ‰ vs VSMOW for $\delta^{2}H$ for seventeen (17) samples (Table 4.18). These values are more depleted for $\delta^{18}O$ and enriched for $\delta^{2}H$ relative to sea water ($\delta^{18}O$ = 0 ‰ and $\delta^{2}H$ = 0 ‰) and suggests a meteoric origin for the surface water. The most depleted surface water sample ($\delta^{18}O$ = -2.16 ‰; and $\delta^{2}H$ = -4.93 ‰) occurs at BSP (Brumase), the northern part of the study area (Fig. 3.2)**.** The values were narrowly spread indicating that surface water bodies within the catchment area were homogenous.

When plotted on the conventional diagram of $\delta^{18}O$/ $\delta^{2}H$ diagram (Fig 4.18), about 10 % of the surface water samples fall between Local Meteoric Water Line (Akiti Line) and Global Meteoric water line (GMWL). This lends support to the presence of non-evaporated waters, likely originating from rapid direct rainfall. About 10 % of surface water fall under the GMWL, showing enrichment pattern that could be attributed to evaporation of meteoric water from the local climatic conditions. About 52 % of the surface water samples plot along the Evaporation line defined by the linear regression (r^2 = 0.721).

$$\delta^2 H = 3.45\delta^{18}O + 1.52 \qquad \textbf{4.19}$$

The slope is less than the 8 of GMWL. Such lower slopes are normally associated with contribution from evaporative processes such as open surface evaporation from large surface water and to some extent could reflect the integration of isotopic composition of the surface water samples especially River Ankobra and Assere and their tributaries (PUWE).

Ground water (hand-dug well and borehole)

Hand-dug well

Ten hand-dug wells were sampled for the analysis of stable isotope composition. The $\delta^{18}O$ for most hand-dug wells in the study area ranges from -2.22 ‰ vrs VSMOW to -0.87 ‰ vrs VSMOW and for $\delta^{2}H$, it was between -6.48 ‰ vrs VSMOW and +0.58 ‰ vrs VSMOW (Table 4.7). The most depleted hand-dug well is located at Bondaye (BDW1) at the southern part of study area. This means the water is recharged by long distance sources of water other than those nearby.

About 40 % of the hand-dug wells fall between the Global Meteoric Water Line and Local Meteoric Water Line (Akiti line), revealing the existence of non-evaporated waters, mostly originating from a fast infiltration of direct rainfall. However, about 50 % of the others fall below the GMWL, indicating an enrichment trend that could be attributed to either evaporation of meteoric water from the local climatic condition before and or prior to groundwater recharge (Allison, 1982). The linear aspect of regression ($r^2 = 0.721$) in this equation suggests that few hand-dug wells (about 10 %) slightly deviate from the Akiti line along relatively low slope (3.45). These variations certainly indicate the action of combined local processes such as selective infiltration, direct percolation through preferential channels that do not alter the isotopic character of the original rain, some degree of fractionation both on land surface and in the unsaturated (vadose) zone, most probably surface water contribution and mixing mechanisms by anthropogenic actions like irrigation, evaporation of recharge water before infiltration.

Boreholes

Table 4.18 showed that eleven (11) borehole values had $\delta^{18}O$ ranging from -2.22 ‰ vrs VSMOW to -0.48 ‰ vrs VSMOW and $\delta^{2}H$ values varying from -8.88 ‰ vrs VSMOW to -1.68 ‰ vrs VSMOW. The most depleted borehole ($\delta^{18}O$ = -2.22 ‰ and $\delta^{2}H$= -8.88 ‰) is (PBH4) at Prestea, central part of the part of the study area. These values were comparatively more depleted and may be due to the absence of considerable evaporation underground. The boreholes are tapping the deeper part of the fractured aquifer. The wells are deeper than 40 meters.

About 36 % of the borehole samples are situated between GMWL and Akiti line (Fig. 4.18). This accounts for the existence of non-evaporated ground waters, likely originating from rapid rainfall that drives the local climate condition of Prestea. Also, about 36 % borehole samples fall under the GMWL, suggesting that the groundwater originated from local precipitation with possibility of evaporative enrichment. Furthermore, about 28 % of the boreholes deviated from the GMWL showing an evidence of isotopic enrichment by evaporation process in the unsaturated zone before recharge. This signifies that the meteoric water recharging the groundwater system is homogenous and smooth with evaporation playing an insignificant role on the infiltration water. In semi- arid regions, the isotopic composition of groundwater can be considerably modified from that of the rainfall due to the strong isotopic enrichment in water during evaporation. Groundwaters that have undergone evaporation display systemic enrichment in stable isotope, resulting in divergence from the LMWL along evaporation lines that have slopes of usually 4 - 6 (Gibson et al., 1993). The trend in groundwater samples reveals this phenomenom in (Fig. 4.18). They are characterized by enrichment in isotopes.

Underground mine water

Twenty-one percent underground water samples had the isotopic composition values of $\delta^{18}O$ varying from -2.22 ‰ vrs VSMOW to -0.95 ‰ vrs VSMOW, and for $\delta^{2}H$ ranges from -8.54 ‰ vrs VSMOW to -1.00 ‰ vrs VSMOW. The most depleted underground mine water sample ($\delta^{18}O$ = -2.22 ‰ vrs VSMOW and $\delta^{2}H$= -4.74 ‰ vrs VSMOW) was recorded in UD-17E at a depth of 597.3 meters.

When plotted on the conventional $\delta^{18}O$/ $\delta^{2}H$, (Fig. 4.18)**.** About 29 % of underground mine water samples fall below the GMWL, showing an enrichment pattern that could be attributed to either evaporation of meteoric water before or prior to groundwater recharge (Allison, 1982). About 21 % of the sample plot on the GMWL indicating that direct infiltration of meteoric water from the Prestea local climatic condition. About 52 % plot between the Akiti line and the GMWL; this shows the existence of depleted waters likely originating from infiltration of rainfall. About 9 % of the underground mine water deviated and plot on the evaporation line, showing degree of enrichment.

The $\delta^{18}O$ concentration shows a homogenous content compared to the boreholes and the $\delta^{18}O$ depleted value (-2.22 ‰ vrs VSMOW) is comparable to the value of the borehole. It is observed from current study that a strong leakage zone probably exists in the underground gold mine, either at the Bondaye or Prestea. Underground mine water travelling through the high-permeability fractured rocks rapidly collects in the sumps/dams intensively faulted runoff zone and recharge the underground mine water. Furthermore, mining and exploration activities underground, induce the large size of macrospores of the rocks, thus increasing hydraulic conductivity

Electrical Conductivity (µS/cm) vrs $\delta^{18}O$ ‰ vrs VSMOW

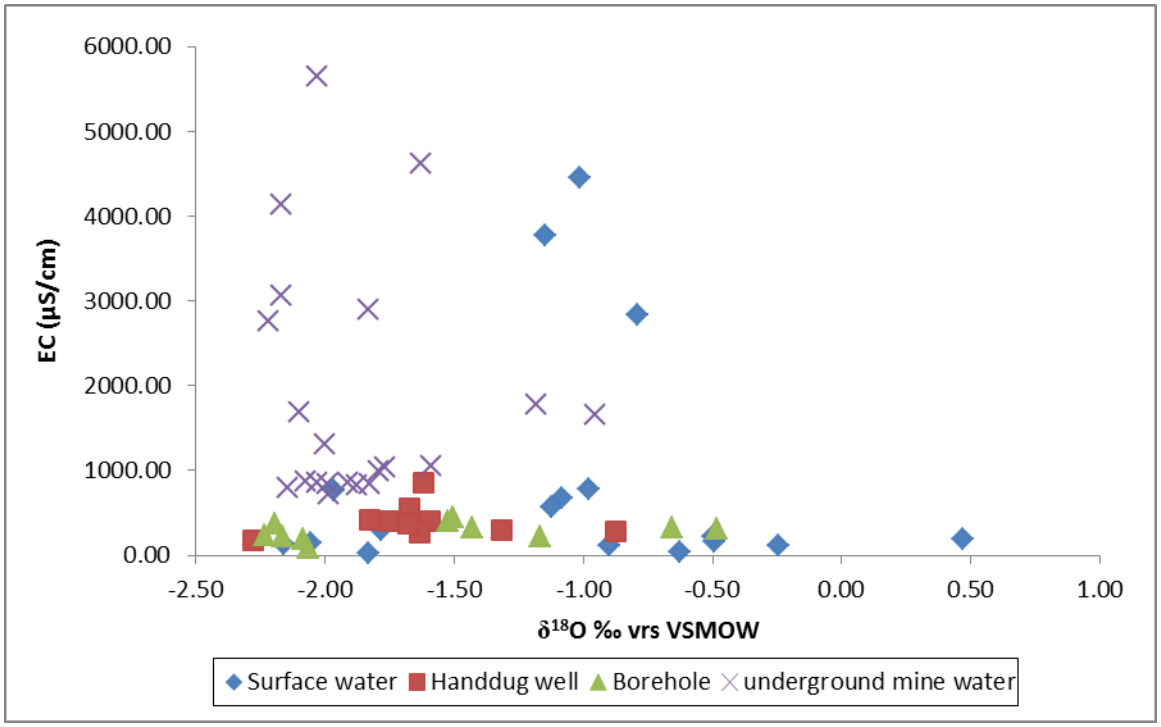

Fig. 4.19: EC against $\delta^{18}O$ ‰ vrs VSMOW

Surface water

In Figure 4.19, the plot of EC vrs $\delta^{18}O$ ‰ shows a relationship that the surface waters are undergoing tremendous enrichment $\delta^{18}O$ with a constant electrical conductivity, suggests recharging or intermixing of fresh water from runoffs and some of the pumped underground mine water within the catchment area confirming direct infiltration of water from rainfall.

However only three samples [PUME(DS), PUWM(DS) and (BDU)] indicate a high level of conductivity (4460, 3770 and 2840 µS/cm, respectively) due to the long distances these

surface water travel and finally, due to vegetation cover under which they flow, evaporation is minimal.

Hand-dug well

The plot shows (Fig. 4.19) clearly that these wells are recharged from surface or other nearby groundwater, and also indicates clearly the shallow nature and the deep fractures within the unsaturated zone and that evaporation plays an insignificant role in their recharging and mixing of fresh water (rainfall or other surface water) is the cause of low conductivity trend observed in these hand dug well.

Borehole

The boreholes also show a trend similar to the hand-dug wells (Fig. 4.19) and because boreholes are deeper than the wells, the possibilities of direct hydraulic connections exist and the deep fractures within the underlain geology, indicate a high degree of well-borehole mixing pattern recharging the boreholes and accounts for their low conductivities.

Underground mine water.

The plot of EC against $\delta^{18}O$ ‰ vrs VSMOW (Fig. 4.19) shows that about 43 % of underground mine water are depleted with $\delta^{18}O$ values. These are located in UD-24C, UD-24E, UD-17D, UD-24A, UD-17E, UD-24B, all at the Prestea underground gold mine.

Water samples from these boreholes also depict higher electrical conductivities of 5650, 4615, 4140, 3065, 2755, 2900 µS/cm, respectively. This shows that, the underground mine water has travelled longer distances (high residence time). This also confirms that the more depleted $\delta^{18}O$ do not necessarily correspond to increased EC values. This further confirms dissolution of rock minerals.

Finally, ground water undergoing evaporation will have a positive correlation between EC vrs $\delta^{18}O$ ‰ vrs VSMOW values. It is observed that a negative correlation was obtained with (r^2= 0.08)

Salinitisation (Evaporation)

Stable isotope can provide an independent variable which can assist in identifying the salinization mechanism. Salinitisation arising from leaching of salts is not accompanied by changes in stable isotope composition of the leaching water, while salinitisation as a result of evaporation is accompanied by enrichment of the stable isotope.

Surface water

The mechanism for salinitisation of surface water of the catchment area is illustrated in (Fig. 4.20). In these waters, it is shown that there are two kinds of waters;

The first group (A) are the waters in which leaching of salts (anothite) lead to salinitisation, so there are no differences in their isotopic composition. About 35 % of the surface waters make up this group.

The second group (B) is those affected by both evaporation and leaching of salts. Together, about 65 % of surface waters are in this group, confirming that industrial and domestic wastes are major factors in the salinitisation processes of the surface waters of the study area.

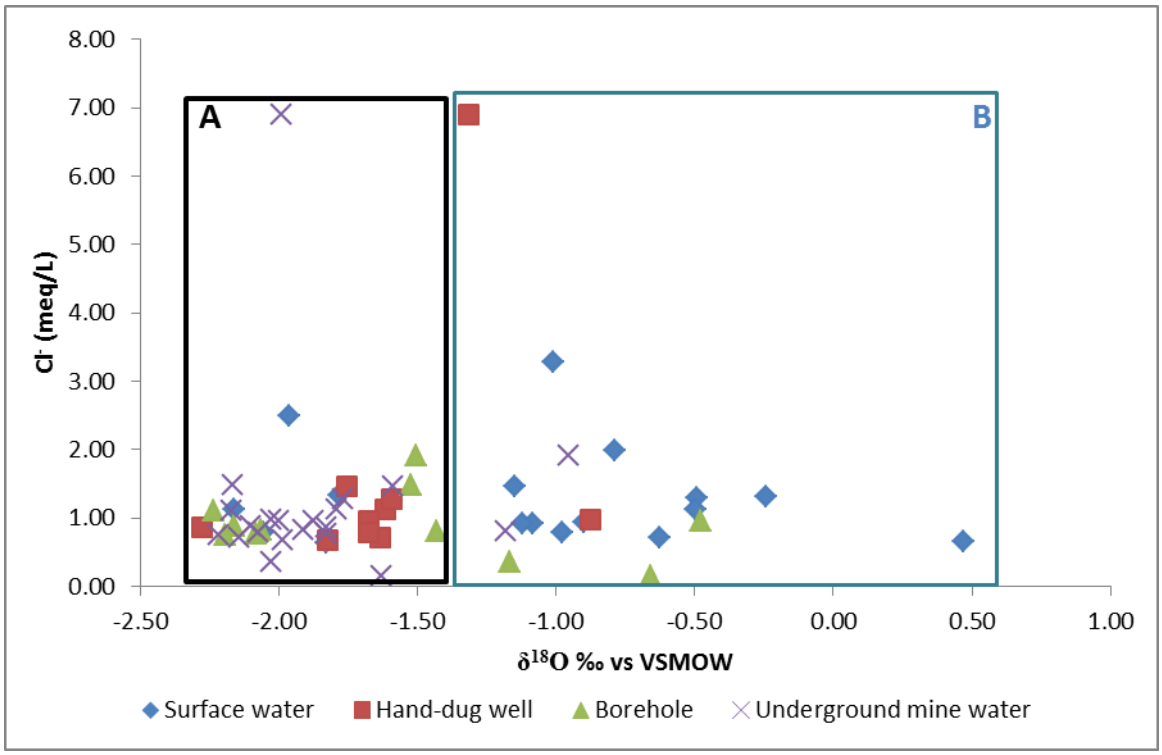

Fig. 4.20: $\delta^{18}O$ ‰ vrs Cl^- (meq/L)

Hand-dug wells

About 70 % belong to group (A), showing that only leaching of salt causes salinitisation and other 30 % belongs to group (B), indicating both evaporation and leaching and due to close proximity to the surface and direct hydraulic connection (faults) may exist and the quick intermixing of fresh water either from direct rainfall or other sources.

Borehole

About 73% of the boreholes belong to group (A), suggesting leaching of salt. The remaining 27 % belong to both evaporation and leaching of salt of group (B) character.

Underground mine water

About 90 % of underground mine water samples exhibit group (A) characteristics indicating leaching of salt as a major process of the dominant reaction, while about 10 % of underground mine water samples show both group (B) qualities of evaporation and leaching of salts.

In conclusion, the leaching of salts confirms that, leaching is the major sources of minerals that water-rock interaction as the dominated reaction confirmed at the hydrogeochemistry discussion, and evaporation plays an insignificant role in the GSBPL (NCM) mines, the study area.

Interrelationship between Surface waters, Hand-dug wells, Borehole and Underground mine water

The water stable isotope content is a maker of the water origin. When combined with the water ionic content, it offers a powerful tool to study the mixing between water masses of different salinities and to track the origin of salinity. Oxygen-18 (^{18}O) and deuterium (^{2}H) were used to assess the genesis and evolution of surface waters, hand-dug wells, boreholes and underground mine waters. The relationship trend between $\delta^{18}O$ and $\delta^{2}H$ (Fig 4.18) were compared with the others and the following observations were made;

Surface water and Borehole

From (Fig. 4.18), one surface water, River Ankobra with the sample ID [(ARaWE)(DS)($\delta^{18}O$ = -0.50 ‰ vrs VSMOW and $\delta^{2}H$= -2.21 ‰ vrs VSMOW)] is found to be recharging a borehole at Himan with ID [(HBH2)($\delta^{18}O$ = -0.48 ‰ vrs VSMOW and $\delta^{2}H$= -1.68 ‰ vrs VSMOW)]. These sampling points are not quite far from each other, the homogeneous nature of ^{18}O and $\delta^{2}H$ value suggests that the degree of fracture and the nature of fault in the rocks within the Birimian Formation, the undulating nature of Prestea topography, runoffs from heavy rainfall within these catchment area accounts for the main reason why recharging is smooth and fast, considering the extent of depletion of the both $\delta^{18}O$ and $\delta^{2}H$.

Surface water and Underground mine water.

Surface water with sampling ID [PUWF (DS) ($\delta^{18}O$ = -1.01 ‰ vrs VSMOW and $\delta^{2}H$= -1.07 ‰ vrs VSMOW)] and underground mine water with sampling ID (UD-17F ($\delta^{18}O$ = -0.95 ‰ vrs VSMOW and $\delta^{2}H$= -1.00 ‰ vrs VSMOW)]. This surface water is pumped underground mine water that flows like a stream, however, it is not quit far from its tributary closer to River Ankobra (MS) situated at Himan. This surface water recharges UD-17F by infiltrating into the NCM underground goldmines and collected at this level. One interesting revelation is the particular zone within which these surface water bodies are identified in the catchment area. (Fig. 4.3**)** it confirms the fracture and the nature of fault within geology of the area, especially along the banks of River Ankobra (Himan).

Surface water, Borehole and Underground mine water

Surface water with ID [ASP ($\delta^{18}O$ = -1.12 ‰ vrs VSMOW and $\delta^{2}H$= -2.74 ‰ vrs VSMOW) and [PUWM (MS) $\delta^{18}O$ = -1.15 ‰ vrs VSMOW and $\delta^{2}H$= -2.08 ‰ vrs VSMOW)], Borehole ID [PBH6 ($\delta^{18}O$ = -1.17 ‰ vrs VSMOW and $\delta^{2}H$= -2.41 ‰ vrs VSMOW)] and Underground mine water with sample ID [UD-17B ($\delta^{18}O$ = -1.18 ‰ vrs VSMOW and $\delta^{2}H$= -3.26 ‰ vrs VSMOW)]

The relationship between these water samples indicates a greater degree of recharging in a particular trajectory, because PUWM (MS) is also pumped underground water flowing like a stream through Prestea town, and so is the borehole, PBH6. Due to the relatively short distance between [PUWM (MS) and PBH6] is not great, it indicates recharging is fast and smooth with high hydraulic conductivities, and further reveals the deep fracture and the nature of fault connecting these sampling points. Furthermore, the UD-17B (Prestea Central Shaft) could also be as a result of induced mining activities; is also in the trajectory and also affirms the recharging from the borehole via the stream. The underground mine water collected at level UD-17B strongly greatly how deep the fracture and trend of the fault are and alludes the extent of level of systematic depletion of $\delta^{18}O$ and $\delta^{2}H$ relative fractionation processes taking place in ground and subsequently in underground gold mine. Additionally, ASP at Ankobra, is a spring water at the northern part of Prestea, few minutes' walk from Himan.

However, it shows either the PUWM recharging it or is underground mine water but conclusively, the principal suspect is the PUWM, since both PUWM (MS) and ASP are within the zone of River Ankobra or vice versa.

$\delta^{18}O$ ‰ vrs VMOW against Depth (m)

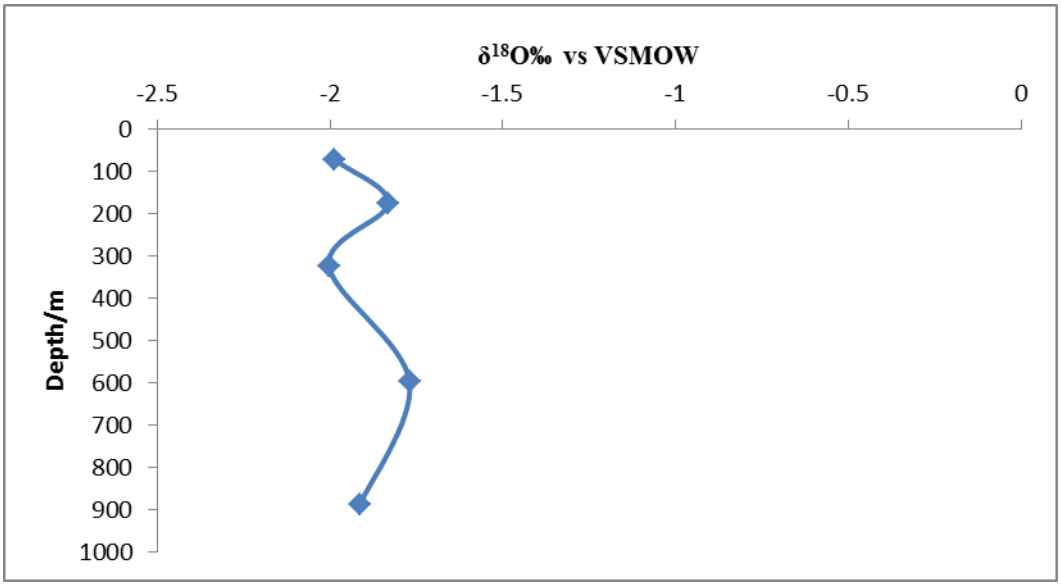

Fig. 4.21: Average $\delta^{18}O$ vrs depth (Underground mine water)

The $\delta^{18}O$ ‰ and $\delta^{2}H$ ‰ composition of underground mine water samples measured at different levels is expressed in per mil units relative to Vienna Standard Mean Ocean Water (VSMOW). Vertical profiles of underground gold mine and $\delta^{18}O$ ‰ were investigated to determine the movement of underground mine water with depth (m) in the study area (Fig. 4.20). The average isotopic composition for the underground gold mine [UDB-3L ($\delta^{18}O$ = - 1.99 ‰ and $\delta^{2}H$ = -4.70 ‰), UD-6L ($\delta^{18}O$ = -1.83 ‰ and $\delta^{2}H$ = -6.04 ‰), UDB-9L ($\delta^{18}O$ = -2.00 ‰ and $\delta^{2}H$ = -6.72 ‰), UD-17L ($\delta^{18}O$ = -1.77 ‰ and $\delta^{2}H$ = -3.76 ‰) and UD-24L ($\delta^{18}O$ = -1.92 ‰ and $\delta^{2}H$ = -4.22 ‰)]. The depth showed isotopic enrichment (-1.99 ‰) for $\delta^{18}O$ at the top (71.5 m), which indicating high evaporation near the surface, due to little vegetation cover and exchange of oxygen bearing minerals. Below 71.8 m, the isotopic contents become depleted with the heavy isotope. The depletion of the

isotopic composition with depth is not homogenous with the average, because the $\delta^{18}O$ at 175.8 m is -1.83 ‰ vs VSMOW and that for 323.3 m and 888.8 m are $\delta^{18}O$ = -2.00 ‰ vrs VSMOW and $\delta^{18}O$ = -1.92 ‰ vrs VSMOW respectively. Thses indicate depletion with depth at these points, and that for 597.3 m are $\delta^{18}O$ = -1.77 ‰ vs VSMOW show enrichment trend and could be attributed to mixing pattern of sueface water with other underground mine water either within a neighboring aquifer with different isotopic compositions. The net effect of evaporation is an enrichment of heavy isotopes ($\delta^{18}O$ ‰) near the shallow depth.

CHAPTER FIVE

CONCLUSIONS AND RECOMMENDATIONS

5.1 Conclusions

The study determined the hydrogeochemistry of underground mine water at Golden Star Bogoso/Prestea Limited (GSBPL) New Century Mine (NCM) and the sources of recharge and discharge, as well the water types. Physico-chemical parameters of water (pH, TDS, Cond., Alkalinity, HCO_3^-, Cl^-), major and trace elements (Ca, Mg, Na, Pb, Cd, Hg, As) and the stable isotope (δ^2H and $\delta^{18}O$) composition of the studied waters were determined. Data generated from the study will serve as a baseline data on which further studies and monitoring could be undertaken.

The study revealed that, the physico-chemical analysis of water samples with the pH ranges [surface water (5.37-7.94) groundwater (3.36-6.59) and underground mine water (6.10-7.96)] from Golden Star Bogoso/Prestea (New Century Mines) was generally acidic to mildly basic.

Electrical conductivity values in the study varied greatly for the water sample systems [surface water (86.37 to 863.35 µS/cm), groundwater (19.89 to 4460.00 µS/cm) and underground mine water (720.00 to 5650.00 µS/cm)]. TDS values of surface water (23.45 to 2460.00 mg/L), groundwater (66.37 to 454.30 mg/L) and underground mine water (400 to 3110 mg/L) for the study area was also determined. The water types are mostly fresh with the exception of underground mine water that is brackish.

The high values of pH, EC and TDS of the surface water, groundwater and underground mine water suggest that water infiltration in the study area is top-down movement,

dissolving the accumulated mineral salts as it moves from the surface and makes its way to underlying aquifers and find their way into the various levels of the underground gold mines; indicating the presence of a deep fracture within the study zone.

Ca was the most dominant cation in water systems (underground mine water, groundwater and surface water). The dominance of Ca may be attributed to the dissolution of calcic-rich minerals such as calcite ($CaCO_3$), dolomite [$CaMg(CO_3)_2$] and gypsum($CaSO_4.2H_2O$) and weathering of calcic- rich components of plagioclase feldspars anorthite ($CaAl_2Si_2O_8$). The variation of surface water, groundwater and underground mine water hydrogeochemistry revealed the dominance of $Ca^{2+} > Mg^{2+} > Na^{+} > K^{+}$ as relative abundance of cation,

SO_4^{2-} is the most dominant anion content determined. The sources were attributed to the dissolution of sulphite minerals such as calcite ($CaSO_4$), dolomite [$CaMg(CO_3)_2$] and gypsum ($CaSO_4.2H_2O$) and anhydrite, oxidation of metallic sulphides are possible sources of sulphate in underground water. The variation of surface water, groundwater and underground mine water hydrogeochemistry revealed the dominance of $SO_4^{2-} > HCO_3^{-} > Cl^{-} > PO_4^{3-} > NO_3^{-}$ as the order of dominance of relative anions. The determined strong correlation between SO_4 and HCO_3 gives an insight into the hydrogeochemical mechanisms in the study area indicating the processes of formation of clay minerals, dissolved ions from feldspars present in the rocks.

The correlation between these ions showed an increasing trend with increasing depth from the surface water to groundwater and then the underground mine water system in the area

The Piper diagram used in the study to determine the hydrochemical facies of the water types indicated that the water types were, [Type I (Na-Cl or Na-HCO_3-Cl), [Type II (Ca-

Mg-SO_4-Cl^-)] the major hydrochemical species in GSBPL (NCM) and [Type III (Ca-Mg-Cl-HCO_3)]. However, substantial presence of other hydrochemical species leads to the conclusion that mixing of groundwater and underground mine water derived from different sources occurs in the catchment area. This principal water type [Type II (Ca-Mg-SO_4-Cl^-)] depicts rock-water interaction in which there is the dissolution of rock minerals within the relatively permeable weathered zone above the underlying rocks.

The bivariate plots confirmed different hydrogeochemical processes such as simple ion exchange, dissolution, weathering of carbonates, silicate weathering evaporation and oxidation-reduction as the key factors in the variation of geochemistry of groundwater and underground mine water, which was over casted by leaching and dissolution processes and cation exchange.

The trend of Na/Cl vrs EC indicates evaporation may not be a major geochemical process controlling the geochemistry of groundwater and underground mine water.

Gibbs diagram confirms also that a considerable portion of cations might have been derived from sources other than the aquifer material.

The trace elements concentrations (mg/L) were found to be in the order Fe > Cu > Mn > Pb > As > Cd > Zn. The high Fe concentrations in groundwater (<0.01-11.55 mg/L) and underground mine water (0.02 – 43.53 mg/L) may be attributed to Iron in the groundwater and underground mine water could have been derived from the leaching of iron from amphiboles and pyroxenes as a result of carbon dioxide attack on rock matrix. The concentration of Pb and Zn (< 0.002 mg/L), Pb, As and Cd (<0.001 mg/L) levels were below the detection limit. This shows that the groundwater and surface water are not

heavily polluted with respect to heavy metals despite the growing human activities such as metal works, scrap dealers, and farming activities through the application of agro-chemicals and the activities of the small scale artisanal gold miners in the study area.

Stable isotopic composition of (δ^2H and $\delta^{18}O$) measurements revealed that the stable isotopes (δ^2H and $\delta^{18}O$) in underground mine water samples from GSBPL (NCM) clustered closely along the global meteoric water line (GMWL) suggesting an integrative and rapid recharge from meteoric origin. Consequently, surface water hand-dug well and boreholes in the GSBPL (NCM) are mainly meteoric water with little or no isotopic variation.

Stable isotopic compositions of (δ^2H and $\delta^{18}O$) data were used to determine the relationship between surface water, hand-dug wells; borehole and underground mine water in identifying the origin of recharge was identified. The slope and intercept of the evaporation line was lower than the GMWL, indicating an evaporation effect of large surface water bodies. In comparing $\delta^{18}O$ values in water samples from hand-dug well and borehole and underground mine water, it was observed that evaporation was the cause of enrichment of isotopes at the surface and groundwater (hand-dug well and borehole) causing departure to the right-side of GMWL. Water from the hand-dug well and borehole show a mixture of recent rainfall and water already in saturated zone.

Last but not least, the interrelationship between these water bodies borehole at Himan (HBH2) and River Ankobra [(ARaW(DS)], a spring water (ASP) at Ankobra, a stream at Prestea (PUWF), UD-17F, PUMM(MS) and PBH6 revealed the recharging processes of one another form the meteoric water line and the depth of the isotope further confirms both depletion and enrichment patterns with respect to depth.

5.2 RECOMMENDATIONS

Based on the study conducted, the following recommendations are proposed:

(a). Continuous monitoring of the waters in the PBH3 should be encouraged, especially in Prestea where the waters were slightly acidic (pH 3.36)

(b). Although, the study revealed that surface water, groundwaters and underground mine water in the district are mainly from meteoric origin, the existence of hydraulic connection between surface water and groundwater, [based on only the similarities in the stable isotopes ($\delta^{2}H$ and $\delta^{18}O$) composition] could not be established. Therefore, future work on water from the GSBPL (NCM) should also include rain water samples taking seasonal variability into account in order to establish the recharge regime.

(c) Sampling should include both dry and rainy seasons, to take into account seasonal variation of results.

(d) The scope of the area should be extended to other areas beyond Prestea to identify waters that infiltrates into the underground mines

(e) The pumped underground stream should be diverted to avoid re-entrying into the underground mines

(f) The use of other isotope techniques such as carbon-14, tritium should be included to identify the time of recharging.

(g) Silicate analysis should be incorporated in the future research work, to cater for serious geochemical processes happening in the study area.

REFERENCES

Abouchami W., Boher, M., Michard A. and Albarede, F. (1990). A major 2.1 Ga event of mafic magmatism in West Africa: an early stage of crustal accretion, Journel of Geophysical Research, 95, 17605 – 17649.

Acheampong S.Y.,Owusu D., Gyau-Boakye P., and Ayibotele N.B., (1985). Groundwater utilization in the Afram Plains. Internal Report, Water Resources Research Institute, Counsel for Scientific and Iindustrial Research., Accra, 40p

Acheampong S.Y. and Hess J.W., (2000). Orin of the Shallow Groundwater System in the Soutern Voltain Sedimentary Basin of Ghana. Hydrogeology Journal: 6: 527-537.

Aggarwal, P. K., Gat, J., Froehlich, K. (Eds.), Isotopes in the Water Cycle. Springer, Dordrecht, Netherlands (2005).

Agomor A.K. (1987). Geological Indications and Prospecting Guide to Rere Metalmineralisation of Birimian Granite Pegmatite of Ghana, Proceeding of the International Conference on the Geology of Ghana with Empasis on Gold, Geological Survey Department, Volume 1, B-2-B-24.

Ahmed , S.M., Blay P.K. and Castor S.B. (1977). The Geology of ¼ fields Sheets No 33, Winneba N.E, 59, 61, and 62, Accra S.W.N.W, and N.E., Ghana Geological Survey Bulletin 32, Ghana.

Ahialey E.K., Serfo-Armah Y., amd Kortatsi B.K., (2010). Hydrochemical Analysis of Groundwater in the lower Pra Basin of Ghana. Water Resources and Protection:2, 864-871.

Akiti T.T., (1980). Geochemical and Isotopic Studies of groundwater in Upper West Region of Ghana. Unpublished PhD Thesis. Universitie′ de Paris Sud, Laboratoires hydrologic et de geochemic Isotopique.

Akiti T.T., (1985). Environmental isotopes study of the groundwaters of the Island of Santiago. Mission report to the UNDP for the government of Cape Verde.

Akiti T.T., (1986). Environmental Isotope Study of Groundwater in Crystalline rocks of the Accra Plains, Ghana. 4th working meeting. Isotope in nature, proceedings of an advisory group meeting. Pp. 107-121, Leipzig.

Aldalla O.A.E. (2009) Groundwater recharge/discharge in semi-arid regions interpreted from isotope and chloride concentrations in North White Nile Rift, Sudan. *Hydrogeol J* 17(3):679-692

Allen S.K., Allen J.M., Lucas S., (1996). Concentration of contaminantsin surface water samples collected in west-central Indiana impacted by acid mine drainage, *Environ Geol* 27**,** 34–37.

Asiedu, D.K., Dampare, S.B., Sakyi, P.A., Banoeng-Yakubo, B., Osae, S., Nyarko, B.J.B. and Manu J. (2004). Geochemistry of Paleoproterozoic Metasedimentary Rocks from the Birimian Diamondiferous Field, Southern Ghana; Implications for Provance and Crustal Evolution at the Archean-Proterozoic Boundary, Geochemical Journal, 38.215-228.

Allison G.B., (1982). The relationship between ^{18}O and deuterium in water and sand columns undergoing evaporation. J Hydro 76: 1-25.

American Public Health Association (APHA), (1995). Standard methods for the examinations of water and waste water, 17th ed. Washington DC, USA.

AOAC International, Association of Official Analytical Chemist International, (2001). Official Methods of Analysis of AOAC International. 18th edition.

APHA, AWWA, WPCF (American Public Health Association, the American Water Works Association and the Water Pollution Control Federation) (1995) Standards methods for the examination of water and wastewater, APHA, AWWA, WPCF, Washington, DC.

Appello C.A.J. and Postma D., (1993). Geochemistry, Groundwater and Pollution. A.A Balkema. Rotterdam (4th Ed). Brookfield: Rotterdam.

Appelo C.A.J., C., (1994). Cation and proton exchange, pH variations and carbonates reactions in a fresh aquifer. *Water Resources Res*. 30, 2793-2805

Appiah H. Norman D.I. (1991) The Geography of the Prestea and Ashanti Goldfields: A comparative Study: in Ladeira EA (Ed), Brazil Gold 91 Balkema, Rotterdam pp 247-255.

Aragaus-Aragaus L., Froehlich, K., Rozanski, K., (2000). Deuterium and oxygen-18 isotope composition of precipitation and atmospheric moisture. Hydrological Processes. Journal of Hydrology:168,159-171.

Attoh, K., Evans, M.J. and Bickford, M.E. (2006): Geochemistry of an Ultramafic-rodingite Rock Association in the Paleoproterozoic Dixcove Greenstone Belt, Southwestern Ghana, Journal of African

Aravena R. Suzuki O. (1990) Isotopic evolution of river water in the northern Chile region. *Water Resour Res* 26(12):1887-1895.

Banner J.L., Wasserburg G.J., Dodson P.F., Carpenter A.B. and Moore C.H., (1989). Isotopic and trace-element constraints on the origin of saline groundwaters from central Missouri. Geochim Cosmochim Acta 53:383-398.

Banoeng-Yakubu, K.B., (1989) occurrence of groundwater in basement complex rocks of the Upper Region of Ghana. M.Sc. Thesis, Obafemi-Awolowo University, Geology Department.187p.

Barbieri M., Boschetti T., Pettita M et al.,(2005) Stable isotope(^{2}H,^{18}O and $^{87}S/^{86}S$) and hydrochemistry monitoring for groundwater hydrodynamics analysis a karst aquifer (Gran Sasso, Central Italy*). Appl Geochem* 20:2063-2081.

Barnes C.J. and Turner J.V., (1998). Isotope exchange in soil water. In: Isotope tracer in catchment hydrology, C. Kendall and McDonnell, J.J., ed., Elsivier, Amsterdam, 137-162.

Bhattacharya H.N., Bhattacharya B., (2006). A permo- carboniferoustide- storm interactive system: Talchir Formation, Raniganj Basin, India, *Journal of Asian Earth Science*, 27, 303- 311

Borella, P., Bargellini, A., Caselgrandi, E., Menditto, A., Patriarca, M., Taylor, A. and Vivoli, G. (1998). Selenium determination in biological matrices. *Microchemical Journal*, 58:325-336.

Bowser C.J., and Jones, B.F., (1993). Silicate mass balances of natural waters, dissolution kinetics, clay products, and the calcium problem. Proc 10th Int Clay Conf. Adelaide, Australia. Brown, GJ. Soil Sci.5 (1954). 145-155

Brown R.L., Parizek R. R.,(1971). Shallow groundwater flow systems beneath strip and deep coal mines at two sites. Clear field Co.PA. Coll. *Earth and Min. Sci Spec. Res. Repot*. SR. 84 Penn Stat Uni. Pp 216.

Buckley D.K., (1986). Report on advisory to wateraid in Ghana. Unpublished Report, British geological Survey, Hydrogeology Research Group. Wilingford, 55pp

Burdon, D.J., (1958). Metasomatism of groundwater at depth. UNESCO course on Hydrology, Desert Institute, Cairo, Egypt.

Cedestorm D.J.,(1945) Genesis of groundwater in the central plains of Virginia. *Eco Geol*41:218-245.

Cerling, T.E., B.L. Pederson and K.L.V. Damm, (1989). Sodium-Calcium ion exchange in the weathering of shales: implications for global weathering budgets. Geology, 17: 552-554.

Chebatarev II (1995). Metamorphism in the central waters in the crust of weathering. Part 1-3, *Geochim cosmochim Acta* 8:22 48, 137-170, 119- 212.

Clark I.D., Fritz P. (1997). Environmental isotope tracers in subsurface hydrogeology. CRC, Boca Ranton, FL.

Coplen, T.B., (1996). New reporting of stable hydrogen, carbon, and oxygen isotopic abundances. *Geochimica at Cosmochimica Acta* 60, 3359–3360.

Data P.S., Bhattacharya S.K., and Tyagi S.K., (1996). ^{18}O studies on recharge of phreatic aquifers and groundwater flow-paths of mixing in the Delhi area. J Hydrol 176:25-36.

Dampare, S.B., Shibata, T., Asiedu, D.K., Osae, S., Banoeng-Yakubo, B. (2008). Geochemistry of Paleoproterozoic metavolcanic rocks from the southern Ashanti volcanic belt, Ghana: petrogenetic and tectonic setting implications. Precambrian Research 162, 403–423.

Domenico, P.A., (1972). Concepts and Models in Groundwater Hydrology. McGraw-Hill, New York, U.S.A.

Daviest S.N., and Turk, L.J., (1964) Optimun depth of wells in crystalline rocks. Groundwater, volume 2, no. 2, pp.6-11

Daviest S.N., and Dewiest R.G.M., (1996). Hydrology New York, John Willey and sons. 463pp

Dickson K. and Benneh G.(1995). A New Geography of Ghana. Longman U.K. pp

Dickson K. B., and Benneh G. (1998).A New Geography of Ghana. Longman Group Limited. Longman House, Burnt Mill, Harlow, Essex, England. Pg 25-52.

Domenico P.A., (1972). Concepts and models in groundwater hydrology. N.Y: Lewis.

Domenico P.A., Schwartz F.W., (1990). Physical and Chemical Hydrogeology. Wiley, New York

Domenico, P.A., (1972). Concepts and Models in Groundwater Hydrology. McGraw-Hill, New York, U.S.A.

Drever J.I., (1988). The Geochemistry of natural waters. Prentice-Hall. Englewood Cliffs NJ.

Duan Y. C., Hei L., Xie G.X., (1994). Application of environmental isotopes in the drain test of Xingtai Mine (in Chinese). *Coal Geol Explor* 22(1):33-37.

Elango L. Kannan R. and Senthilkumar M., (2003). Major ion chemistry and identification of processes of groundwater in the part of Kancheepuram dictrict. Tamilnadu India: Environ. Geocsi.10(4) 157-166.

Elango L., Subramani T., and Rajmohan N., (2010). Groundwater geochemistry and identification of hydrogeochemical processes in hard rock region, Southern India. Envirn Monit Assess 162:123-137.

Emunds W.M., (2009). Geochemistry's vital contribution to solving water resources problems. App Geochem 24(6):1058-1073.

Fisher R.S., and Mullican III W.F., (1997). Hydrochemical evolution of of Na-SO_4 and Na-Cl groundwater beneath the northern Chihuahua desert, Trans-Pecos, Texas, USA: *Hydrogeol. J* 5(2) 4-16.

Fontes J.C., (1980) Environmental isotopes in groundwater hydrology. In: Fritz P, Fontes JC (eds) Handbook of environmental isotope geochemistry. *Elsevier*, Amsterdam, pp 75–140.

Fonts J.Ch (1976). Isotopes du milieu dans les eaux naturelles. La Houille Balache 314: 205-221.

Foster M.D., (1950) The origin of high sodium bicarbonate water in the Atlantic and Gulf Coastal Plains. *Geochim Cosmochim Actal*: V. 1. Pp 33-48.

Freeze, R.A. and Cherry J.A., (1979). Groundwater. Prentice-Hall, Englewood Cliffs, 604.

Gamels R.M. and Christ C.L., (1965). Solutions, Minerals, and Equilibria (p 458). New York.Harper and Row.

Ganyaglo S.Y., (2006). Hydrochemical and isotopic characterization of groundwater in some rocks in the Easten region of Ghana.

Garcia M.G., Hidalgo M. and Blesa M.A., (2001). Geochemistry of groundwater in the alluvial plain of Tucuman province , Argent Hydrogeol J 9:597-610.

Garrels R.M. and Mckenzie F.T., (1971). Evolution of sedimentary rocks. WW Norton, New York.

Gast R.G (1979). In Encyclpaedia of soil Sciences eds. Fairbridge, R.W., and Finki, C.W. Dowden, Hutchson and Ross, Stroudfburg Pa. 148-158.

Gibbs, R.J., (1970). Mechanisms controlling world water chemistry. Science, 170: 1088-1090.

Gibrilla A. Osae S. Akiti T.T., Adomako D., Ganyaglo S.Y., Bam E.P.K., and Hadisu A. (2010). Hydrogeochemical and Groundwater Quality Studies in the Northern Part of Densu River Basin OF Ghana. *J. water Resources and Protection*, 2, 1071-1081.

Gibson J.J., Edwards T.W.D. and Bursey G.G. (1993). Estimating evaporation using stable isotopes: quantitative results and sensitivity analysis for two catchments in northern Canada. Nord Hydrol 24:79-94

Gimenez E. and Morell I. (1997). Hydrogeochemical analysis of salinitization processes in the coastal aquifer of Oropesa (Catellon, Spain). Environmental Geology, 29 (1/2), 118-131.

Glover E.T., Akiti T.T., and Osae S., (2012). Major ion chemistry and identification of hydrogeochemical processes of groundwater in the Accra plains. Elixir Geoscience 50(2012). 10279-10288.

Geological Survey Department of Ghana, SDG (2009): Geological Map of Ghana.

Gonfiatini R., (1986). Environmental isotopes in the lake studies. In Handbook of Environmental Isotope Geochemistry: Vol 2, The Terrestrial Environment, A. P. Fritz and J.C Fontes (Eds), Elsevier, Amsterdam, The Netherland. 113-168.

Gui H.R., Chen L.W. Song H.M., (2006) Features of oxygen and hydrogen stable isotopes in deep groundwater in mining area of northern Anhui. *J Harbin Int Technol* 37(1):111-114.

Guo H., and Wang Y., (2004). Hydrogeochemical processes in shallow quaternary aquifers northern part of Datong Basin, China; *Appl. Geochem.* 19(1) 19-27.

Harrington G.A., Cook P.G., Herczeg A.L.,(2002) Spatial and temporal variability of groundwater recharge in central Australia: a tracer approach. *Ground Water* 40(5):518-528.

Hem J.D., (1991).Study and interpretation of the chemical characteristics of natural water,*US Geological Surv. Water- Supply Paper* 2254, Scientific Publishers, India.

Hem, J.D., (1989). Study and interpretation of the chemical characteristics of natural water. U.S. Geol. Survey, water supply, paper 2254. 3rd. edition, third printing, pp: 248.

Herczeg A.L., Barns C.J., Macumber P.G. Olley J.M. (1992) A stable isotope investigation of groundwater-surface water interactions at Lake Tyrrell, Victoria. *Chem Geol* 96:19-32.

Hill J.G., Price D.R.,(1983). The impact of deep mining on an overlying aquifer in western Pennsylvania. Groundwater Monitoring Review V-3, nol, pp 138-143.

Hirdes, W., Davis, D.H. and Eisenlohr, B.N. (1992): Reassessment of Proterozoic Granitoid Ages in Ghana on the Basis of U/Pb Zircon and Monazite Dating, Precambrian Research, 56, 1–2

Hobba W.A. Jr (1981). The effect of Underground mining and mine collapse in the hydrology of selected basin in Western Virginia. W.V. *Geol and econ. Survey, Repot*. Inv.33

Hodson, M .E., (2002). Experimental evidence for mobility of Zr and other trace elements in soils. Giochemica et Cosmochemica Acta 66, 819-828.

Hoeing M., Baeten H., Vanhentenjik S., Vassileva E., Quevauviler P.H. (1998). Critical discussion on the need for an efficient mineralization procedure for the analysis of

plant material by atomic absorption spectrometric methods. *Analytica Chemica Acta* 358, 85-94.

Hounslow A.W., (1995). Water quality data: analysis and interpretation. CRC Lewis Publ, New York, USA, p.396.

Hu W.W., Ma Z.Y., Cao H.D., et al(2010) Application of isotope and hydrogeochemical methods in distinguishing mine bursting water sources(in China). *J Earth Sci Environ* 32(3):268-271.

Huddart P.A., Longstaffe F.J., Crowe A.S. (1999) D and ^{18}O evidence for inputs to groundwater at wetland coastal boundary in the southern Great Lakes region of Canada. *J Hydrol* 214(1-4):18-31.

IAEA [International Atomic Energy Agency] (2009). Laser Spectroscopic Analysis

Issawi, B. and E. Zaghloul, (1994). Quaternary sediments and the hydrogeological conditions of Wadi Feiran, South Sinai. VIII IWRA World Congress on Water Resources: 21-25 Nov. Cairo. Egypt. Jacks, G., 1973. Chemistry of groundwater in a district in Southern India. J. Hydrol., 18: 185-200.

Isaac A.O, (2013), Study of the origin of salinity in the unsaturared zone of using chloride profiles and stable isotope at Ekumfi Akwakrom and Ekumfi Asorkwa ,Mankessim Municipality of the Central Rrgion of Ghana. Mphil Thesis Submitted to University of Ghana.

Jalali M. (2007). Hydrochemical identification of Groundwater Resources and their Changes Under the impacts of Human Activity in the Chah Basin in Western Iran. *Environ Monit Assess.* 130, 347-364.

Jankowski J. Acworth R.I., (1997). Impact of debris-flow deposites on hydrogeological process and the development of dry land salinity in the Yass River catchment, New South Wales, Australia. Hydrogeol J 5(4): 71-88

Junner N.R. and Hirst T. (1946). The geology and hydrogeology of the Volta Basin. Memoir 8, GoldD Coast Geological Survey.

Kandall C., McDonnell J.J., (1980) Isotope tracers in catchment hydrology. *Elsevier*, Amsterdam, pp 203-204.

Kenkel J., (1994). Analytical Chemistry for Technicians. Lewis Publishers, Boca.

Kenoyer G.J., and Browser C.J., (1992). Groundwater chemical evolution sandy silicate aquifer in Northern Wiscontin, I. Patterns and rates of Change. Water Resour Res 28(2):579-589.

Kermensky G.N., (1958) Hydrochemical zoning in the distribution of undergroundwater. In: Proceedings of the Symposium on Groundwater 1955.Central Board of Geophysics. Temple press. Calcutta, Pub No pp 281- 292.

Kesse G.O. (1985). The mineral and rock resources in Ghana. Balkema, Rotterdam, PP 13-26, 40-67.

Kesse G.O. (1995). The Mineral and Rock Resources of Ghana.(1st ed).Balkema, Rotterdam.Netherland.

Kim.K., Rajmohan N., Kim H.J., Hwang G.S., and Cho M.J., (2004). Assessement of groundwater chemistry in a coastal region (Kunsan, Korea) having complex contaminant sources: Astoichio approach. Environmental Geology, 46, 763-774.

Kortatsi B.K., (2004). Hydrochemisrty of Groundwater in the Mining Area of Tarkwa-Prestea, Ghana-University of Ghana, Legon.

Kortatsi B.K., (2006). Concentration of Trace Metals in Boreholes in the Ankobra Basin,Ghana. West Africa Journal of Applied Ecology 10.

Kortatsi B.K., Tay C.K., Anornu G., Hayford E., and Dartey G.A., (2007). Hydrogeochemical Evaluation of Groundwater in the Lower Offin Basin, Ghana.

Kortatsi B.K., Tay C.K., Anornu G., Hayford E., Dartey G.A., (2007). Hydrogeochemical Evaluation Groundwater in the lower Basin of Offin Basin, Ghana. Evniron. Geol. 53: 1651-1662.

Kumar M., Ramanathan A.L., Rao M.S., and Kumar B., (2006). Identification and evaluation of hydrogeochemical processes in the groundwater environment of Delhi, india. J Environ Geol 50:1025-1039.

Kusimi J.M., (2007). Groundwater Hydrogeochemistry and Landcover Change in the Wassa West District of Ghana.(Mphil thesis work). Royal institute of Technology, Stockholm, Sweden. pp. 11-23.

Lasaga A.C., (1984). Chemical kinectics of water-rock interactions. Journal of Geophysical Research, 89(B6), 4009-4025

Leap D.I., (1999). Geological occurrence of groundwater, p 40-43. In: J. Delleur (ed) The handbook of groundwater engineering. CRC Press LLC and Spinger-Verlag.

Leube A. and Hirdes W., (1986). The Birimian Supergroup of Ghana – depositional environment, structural development and conceptual model of an early Proterozoic Suite. Rep. Arch. BGR, 99529:260p.

Leybourne M.I., Clark I.D., Goodfellow W.D. (2006). Stable isotope geochemistry of ground water and surface water associated with undisturbed massive sulfide

deposits; constraint on origin of waters and water- rock reactions. *Chem Geol* 231: 300-325.

Li X. D., Masuda H., Kusakabe M. Yanagisawa F., and Zeng H.A., (2006). Degradation of groundwater quality due to anthropogenic sulfur and nitrogen contamination in the Sichuan Basin, China; Geochem J. 40: 309-332.

Li W.P., Hao H,-B., Zheng Y,-J, et al., (2006).Regional environmental isotopic features of groundwater and thei hydrogeological explanation in the Tarim Basin. Earth Science Frontiers, 13(1),191-191(In Chinese).

Lu-Wang C., He-rong G. and Xiao Y. Monitoring of flow field based on stable isotope geochemical characteristics in deep groundwater. Environmental Monit Assess (2011) 179: 487-498

Long A.J., Putnam L.D., (2004) Linear model describing three components of flow in karst aquifers using ^{18}O data. *J Hydrol* 2296:254-270.

Mackenzie, F.J. and R.H. Garrells, (1965). Silicates: reactivity with water. Sci. J., 1505: 57-58.

Maclean W., Jankowski J. and Lanvit N., (2006). Groundwater quality and sustainability in an alluvial aquifer, Australia, In: O. Sililo et al. (Eds), Groundwater, past achievements and future challenges (pp. 567-573), Balkema, Rotterdam.

Mahapatra, S., Tripathi, R. M., Raghunath, R. and Sadasivan, S. **(2001)**. Daily intake of selenium by adult population of Mumbai, India. *Science of the Total Environment*, 277:217-223.

Mallari B., (1959). Preliminary study of geology and groundwater resources of Ghana. Ghana Water and Sewerage Corporation Report 200p.

Manu,J.(2004): Geochemistry of Paleoproterozoic Metasedimentary Rocks from the Birim

Mark S.K., (2012). Groundwater Quality Assessment in the Krachi West District of the Volta Regoin of Ghana. Mpil Thesis Submitted to University of Ghana (unpublished).

Marifa A.M., Krishnamurthy R.V., Atekwanne E.A., et al (2003) Isotope and geochemical evolution of ground and surface water in karst dominated geological setting: a case study from Belize, Cenral America. *Appl Geochem* 19:973-946.

Matthess, G., (1982). The properties of groundwater. Wiley, New York, U.S.A., pp: 498.

Maya A.L., and Loucks M.D., (1995). Solute and isotopic geochemistry and groundwater flow in the Central Wastch Range, Utah. J Hydrol 172:31-59

Mayback, M., (1987). Global chemical weathering of surficial rocks estimated from river dissolved loads. Am. J. Sci., 287: 401-428 *Aust. J. Basic & Appl. Sci., 6(3): 638-654, 2012* 654

Mayboon, P. (1966). Groundwater studies in the Assiniboine River Drianage Basin: the evaluation of a flow system in south-central saskachewam. Geol. Surv. Can. Bull. 139, 65pp.

Mazor E., (1997). Groundwater and Isotopic Groundwater Hydrology. Third Edition: Marcel Decker, Inc. New York pp. 114-152

Mazor, E. 2004. Chemical and Isotope Groundwater Hydrology, 3rd edn. Maecel Dekker, New York.

McBride M.B., 1994. Environmental chemistry of soils, Oxford University Press, Inc., New York.

McSween H.Y.,Richardson S.M., and Uhle M., (2003). Geochemistry: pathways and processes. Columbia Uni. Press, 2nd edition.

Merlivat, L. and Jouzel, J. 1979. Global Climatic interpretation of the deuterium-oxygen-18 relationships for precipitation. J. Geophysic. Res., 84, 5029-5033.

MLGRD [Ministry of Local Government and Rural Development](2006). Western Region (Prestea-Huni valley District). Retrieved from **http://www.ghanadistricts.com.** Assessed on 12 December, 2013.

Mohan R., Singh A.K., Tripathi J.K., and Chowdhary G.C., (2000). Hydrochemistry and quality assessment of groundwater in Naini industrial area, Allahabad district, Uttar Pradesh: *J. Geol.Sci*. India 55: 77-89

Mook W.G., Klaus F., and Rozanski K., (2000).environmental isotope in the Hydrological Cycle Principles and Applications. International Hydrological Programma. 1 Technical Documents in Hydrology No.39, Vol. III.

Morren, A. A., Zachariadis, G. A., Anthemidis, A. N., Stratis, J. A. (2006). Investigation of four digestion procedures for multi-element determination of toxic and nutrient elements in legumes by inductively coupled plasma-optical emission spectrometry. *Analytica Chemica Acta*, 565:81-88.

Nayaka S.B.M., Ramakrishna, S. Jayaprakash and Delvi M.R., (2009). Imput of heavy metals on water, fish (Cyprinus carpio) and sediments from a water tank at Tumkur, India, Ocean Hydrobiol, Stu., 38(2): 17-28.

Nielen J., Vander Merwe, Practical coal mining strata control-A guide for manegers and Supervisors at All Levels, Johannesburg (1998)

Olmted F.H., (1962) Chemical and Physical character of groundwater in the National Reactor Testing Station. Idaho. U.S. Geo Survey IDO-22043-USGS.

Pan G. Y.,Wang S.N., Sun X.Y., et al.,(2009). Identification of the source of groundwater in cial mining district by applying isotope technique (in Chinese). *Min Saf Environ Prot* 36(1):32-34.

Parizek R.R., and Brown R. L., (1971). Shallow groundwater flow systems beneath strip and deep coal mines at two sites. Clearfield Co. PA. Coll. Earth and Min.Sci Spec Res. Rept. SR-84. Penn State Uni. Pp 216.

Palig-Ba K.B. (1987). Hydrochemical studies of groundwater, presented in some aquifers in the Upper Regions of Ghana, presented at the joint conference of the West African Scienecs Assoc, August 1987, Accra, Ghana.

Pelig-Ba K.B., Biney C.A., and Antwi L.A., (1991). Trace Metal Concentration in Borehole Waters from the Upper Regions and Accra Plains of Ghana. Water, Air, and Soil pollution 59,333-345.

Pelig-Ba K.B. (1996). Trace elements in Groundwater from crystalline Rocks in the Upper Regions of Ghana. Water, Air, and Soil Pollution 103: 71-89.

Ragnarsdottir K.V., Kapitulcinova D., Cockell C.S., and Hallam K.R.,(2010). The role of cyanobacteria in sheet silicate weathering: a laboratory study. Environmental minerology group researchin progress meeting (mineralogical society of Great Britain and Ireland), Keyworth, U.K.

Rajmohan, N. and L. Elango, (2004). Identification and evolution of hydrogeochemical processes in the groundwater environment in an area of the Palar and Cheyyar River Basins, Southern India. Environ. Geol., 46: 47-61.

Rao S., D.V. et al., (2007). Mine water –A sustainable resource in coal mining area, *National Seminar on Agriculture Development and Rural drinking water, Bhopal,* 1**,** 141- 148

Rollinson, H.R. (1993): Using Geochemical Data; Evaluatio, Presentation, Interpretation, Longman Group UK Limited, 1–314 pp.

Rowell D.L., (1981). The chemistry of soil processes eds. Greenland , D.J ans Hayes, M.H.B. John Wiley, Chichester. 401-462.

Rozanski K Aragaus-Aragaus L. and Gonfiantini R., (1993). Isotopic patterns in global precipitation. In: Swart PK et al (eds) Climate change in continental isotopic records. Geophysical Monograph Series, vol 78. AGU, Washington, DC, 1-36 pp.

Sacks L.A. and Tihansky A.B., (1996). Geochemical and isotopic compositions of groundwater, with emphasis on source of sulphate, in the upper floridan aquifer and

intermediate aquifer system in southwest Florida. US Geological Survey. Water-Resources Investigations: Technical Report 96-4146.

Sadashivaiah C. Ramakrishnaiah C.K. and Ranganna G (2008). Hydrochemical Analysis and Evaluation of Groundwater Quality in Tumkur Taluk, Karnataka, India, Int.J. Environ.Res. Public Health, 5(3 158-164).

Sami K. (1992). Recharge mechanisms and geochemical processes in a semi-arid sedimentary basin, Eastern Cape, South Africa. J Hydrol 139:27-48

Stallard, R.F. J.M. Edmond, (1983). Geochemistry of Amazon, the influence of geology and weathering environment on the dissolved load. J. Geophys. Res., 88: 9671-9688.

Sarin M.M., Krishnaswamy, S., Dilli K., Somayajulu B.L.K., and Moore W.S., (1989). Major ion chemistry of the Ganga-Brahmaputra river system: weathering processes and fluxes to the Bay of Bengal. Geochem.Cosmochim. Acta, Vol 53, pp 997-1009.

Schoeller, H., (1965). Hydrodynamique lans lekarst (ecoulemented emmagusinement). Actes Colloques Doubronik, I, AIHS et UNESCO, 3-20.

Schuh W.M., Klinekebiel D.L., Gardner J.C., and Mayar R.F., (1997). Tracer and nitrate movements to groundwater in the Norruem Great Plains. J Environ Qual 26:1335-1347

Serfo-Armah Y., Nyako B.J.B., Adotey D.K., Adomako D., and Akaho E.H.K., (2004). The impact of small-scale mining activities on the levels of mercury in the environment: The case of Prestea and its environs. Journal of Radioanalytical and Nuclear Chemistry 262, 685-690.

Sharma B.D., Mukopadhyay S.S., and Sidhu P.S., (1998). Microtopographic controls on soil formation in the Punjab region, India, Geoderma 81:635-368

Singh A. K., Mahato, Mukesh K., Neogi B., Mondal G.C., Singh K.K., (2010). Quality Assessment of Mine Water of the Raniganj Coalfield Area, India, *Mine Water Environ*, 29**,** 248- 262

Singh A. K., Mondal G. C., Singh P. K., Singh S., Singh T.B., and Tewary B.K., (2005). Hydrochemistry of reservoirs of Damador River Basin, India. Weathering processes and water quality assessement. Environ Geol., Vol 8, pp.1014-1028.

Singh A. K., Mondal G.C., Kumar S., Singh T.B.,TewaryB.K., Sinha A., (2008). Major ion chemistry, weathering process and water quality assessment in upper catchment of Damodar River basin, India, *Environ Geol*, 54, 745- 758

Song X. Liu X. Xia J. Yu J. and Tang C., (2006). A study of Interaction between Surface and groundwater using Environmental Isotope in Huaisha River Basin. Science in China Series D: Earth Science 2006 vol.49 No.12 pp1299-1310.

Song X.F., Yu J.J. International symposium summaries on Environmental Isotopic Hydrology and study countermeasures in China. *Hydrolgeol Eng Geol* (in Chinese), 2002, 1: 114-115

Sophacleous, Marios (2002). Interaction between groundwater and surface water: the state of the science. Hydrology Journel10:52-67 Bilcode: 2002HydJ… 10525.

Sposito G and Page A.L., (1985). Metal ions in biological systems. Vol 18 circulation of metals in the environment, ed. Siegel, H. Marcel Dekker, New York. 287-322.

Stallard R.F., and Edmond J.M., (1983). Geochemistry of Amazon, the influence of geology and weathering environment on the dissolved load. J Geophys Res 88:9671-9688.

Subba Rao N., (2006). Seasonal variation of groundwater quality in part of Guntur district, Andrahn Pradesh, India. Environ Geol 49:413-429 the east Midland Triassic sandstone aquifer Appl. Geochem. 15:737-752.

Subyani A.M. (2004) Use of chloride mass balance and environmental isotopes for evaluation of groundwater recharge in the alluvial aquifer, Qadi Tharad, Western Saudi Arabia .*Environ Geol* 46(6):741-749.

Taylor, P.N., Moorbath, S., Leube, A. and Hirdes, W. (1992): Early Proterozoic Crustal Evolution in the Birimian of Ghana; Constraints from Geochronology and Isotope Geochemistry, Precambrian Research, 56, 97–111.

Toth J.,(1984). The role of regional gravity flow in the chemical and thermal evolution of groundwater. Proceedings of the first Canadian/American conference on hydrology Banff, Alta.

Velbel M.A., (1993). Constancy of silicate-mineral weathering-rate ratios between natural and experimental weathering: Implication for hydrologic control of differences in absolute rates. Chemical geology 105,89-99.

Vengosh A., Spivack A.J., Artzi. Y. Ayalon A.,(1999). Geochemical and boron,strontium and oxygen isotopic costraints on the origin of the salinity in groundwater from the Mediterranean Coast of Isreal. *Isreal Water Res.*35, 1877-1894.

Wallick E.I. and J. Toth, (1976). Methods of regional groundwater flow analysis with suggestions for the use of environmental isotope and hydrochemical data in groundwater hydrology. IAEA, Vienna, 37-64.

Wang Y.M., Jao L.M., (2001) Identification of source of water inrush by applying water quality analysis methods in coal mining districts (in Chinese). Mine Saf 36(10):12-14.

White A.F. and Brantley S.L., (1995). Chemical weathering rates of silicates minerals, p1-22. In: white A.F. and Brantley S.L. (eds.) Reviews in minerology.

White D.E., Hem J.D., Waring G.A.,(1963) Chemical composition of subsurface water- In Data of geochemistry, 6th edn. U.S Geol Sur Prof pap 440-F: F1-F67.

Wikipidia(2013). Groundwater sampling. Retrieved from **http://groundwatersampling.org** Assessed on 13th may, 2013.

Windhorst D., Waltz T. Frede, H.G., and Breuer, L. 2012. Impact of elevation and weather patterns on the isotopic composition of precipitation in a tropical montane rainforest. Hydro.Earth Syst. Sci. Discuss., 9, 8425-8453,2012.

Yao Z.J., Lin J.,Huang H.Q., Song Z.F., Dong X.H., Liu X.(2009) Characteristics of isotope in precipitation, river water and lake water in the Manasarovar Basin of Qinghai: Tibet Plateau. *Environ Geol*. Doi:10.1007/s00254-008-1324-y.

Zhuang j.,(1997). Identification of the source of groundwater in coal mining districts by applying for environmental isotope techniques (in Chinese). *Coal Geol China* 9(2):48-49

.

APPENDICES

Appendix I: Description of sampling towns, sampling codes and type of samples

Surface water			Groundwater			Underground mine water		
Sampling Town	Sampling Code	Description of Sample	Sampling Town	Sampling Code	Description of Sample	Samling Town	Sampling Code	Description of Sample
Ankobra	ASP	Spring from the foot of a hill	Ankobra	ABH	Borehole	Bondaye	UD-3A	Main Sump (Sources: 1, 2 & 3)
Brumase	BSP	Spring from a rock	Brumase	BBH	Borehole	Bondaye	UD-3B	Overflow Pipe (Level 1 & 2)
Brumae	BSt2	Surface water from BSP	Himan	HBH1	Borehole	Bondaye	UD-9A	Central Sump (Sources: 8L & 9L)
Bondaye	BDSt	Spring from the foot of a hill	Himan	HBH2	Borehole	Bondaye	UD-9B	Level 9 drive to Central Sump
Bondaye	BDSt2	Spring from the foot of a hill	Himan	HW	Well	Bondaye	UD-9C	Central Sump (Sources: 4,5,6,7 & 8)
Prestea	PSW	Spring from a rock	Bondaye	BDW1	Well	Prestea	UD-6B	Spring water from tunnel 1
Ankobra	ARaW (US)	River Ankobra	Bondaye	BDW2	Well	Prestea	UD-6C	Spring water from tunnel 2
Ankobra	ARaW (MS)	River Ankobra	Bondaye	BDW3	Well	Prestea	UD-6E	Flow from Level 7 pipe
Ankobra	ARaW (DS)	River Ankobra	Bondaye	BDW4	Well	Prestea	UD-6F	Drainwater before Central Sump
Himan	HRMT (US)	River Assesre	Prestea	PW1	Well	Prestea	UD-6G	Central Sump
Himan	HRMM (MS)	River Assesre	Prestea	PW2	Well	Prestea	UD-6H	D/S Cross Cut 23
Ankobra	ARWE (DS)	River Assesre	Prestea	PW3	Well	Prestea	UD-17A	Settling Dam A (North Shaft Water)
Prestea	PUWF (US)	Pumped Underground water	Prestea	PW4	Well	Prestea	UD-17B	Settling Dam B (North Shaft Water)
Prestea	PUWM (MS)	Pumped Underground water	Prestea	PW5	Well	Prestea	UD-17C	Ankobra Shaft Water and 17L
Prestea	PUWE (DS)	Pumped Underground water	Prestea	PBH1	Borehole	Prestea	UD-17D	24L water to 17L Central Sump
Bondaye	BDU (MS)	Pumped Underground water	Prestea	PBH2	Borehole	Prestea	UD-17E	Central Sump (Sources:14,15,16 &17)

Appendix I: Description of **s**ampling towns, sampling codes and type of samples

Surface water			**Groundwater**			**Underground mine water**		
Sampling Town	Sampling Code	Description of Sample	Sampling Town	Sampling Code	Description of Sample	Sampling Town	Sampling Code	Description of Sample
Bondaye	BDUWF (MS)	Pumped Underground water	Prestea	PBH3	Borehole	Prestea	UD-17F	Drilling Discahrge line (Sources:10-24L)
			Prestea	PBH4	Borehole	Prestea	UD-24A	Central Sump
			Prestea	PBH5	Borehole	Prestea	UD-24B	North End No 2 Shaft Sump
			Prestea	PBH6	Borehole	Prestea	UD-24C	Ore Pass (Source: above 24L)
			Prestea	PBH7	Borehoe	Prestea	UD-24E	Bondaye water (Gutter water)

Appendix II: Scheme for sampling of water samples in GSBPL (NCM) underground mine

Prestea (Central Shaft)			Bondaye Shaft (Southern Part)		
Code/Level	Depth (m)	Number of samples	Code-Level	Depth (m)	Number of samples
UD-6	175.8	18	UDB-3	71.8	6
UD-17	597.3	18	UDB-9	323.8	9
UD-24	888.8	12			

Appendix III: Physico-chemical paramters for Surface water

Surface water

Sampling ID	Elevation (m)	pH	Temp (°C)	EC (µS/cm)	TDS (mg/L)	Sal ‰	Sampling ID	Elevation (m)	pH	Temp (°C)	EC (µS/cm)	TDS (mg/L)	Sal ‰
PSW	62.00	6.10	24.45	126.72	68.36	0.10	PUWF(US)	68.00	7.62	25.85	3770.00	2075.00	0.10
BDSt	86.00	6.54	25.25	19.89	23.45	0.10	PUWM(MS)	63.00	7.45	24.60	4460.00	2460.00	0.21
BDSt2	73.00	6.80	26.90	116.60	58.26	0.10	PUWE(DS)	35.00	7.54	24.50	2840.00	1570.00	0.13
ASP	60.00	6.77	24.90	190.00	100.00	0.02	BDU(US)	78.00	7.96	27.35	780.00	410.00	0.73
BSP	52.00	6.94	25.65	113.95	59.49	0.11	BDUWF(MS)	73.00	7.43	24.10	770.00	420.00	0.16
BST2	48.00	7.15	25.05	37.49	36.99	0.10	ARaWT(US)	34.00	6.95	24.60	140.00	80.00	0.10
ARWT(US)	35.00	6.45	24.45	158.72	84.36	0.13	ARaWM(MS)	33.00	6.99	25.00	680.00	380.00	0.10
HRWM(MS)	27.00	7.02	27.00	224.00	119.51	0.20	ARaWE(DS)	30.00	6.83	24.80	570.00	310.00	0.10
ARWE(DS)	29.00	7.17	25.65	297.75	158.26	0.16							
Range		**pH (6-8)**			**EC (20-4460)**		**Temp(24.1-27.4)**			**TDS (24.5- 2460.0)**			**Sal (0.02-0.73)**

Temp (Temperature) **EC** (Electrical Conductivity) **TDS** (Total Dissolved Solids) **Sal** (Salinity)

Appendix III: Physico-chemical paramters for Groundwater and Underground mine water (Continuation)

Groundwater							Underground mine water						
Sampling ID	Depth (m)	pH	Temp (^{o}C)	EC (µS/c)	TDS (mg/L)	Sal ‰	Sampling ID	Depth (m)	pH	Temp (^{o}C)	EC (µS/cm)	TDS (mg/L)	Sal ‰
PW1	49.00	6.43	24.80	5290.50	150.00	0.11	UD-3A	71.50	7.76	25.06	84500	465.00	0.10
PW2	54.00	5.83	27.00	424.05	224.55	0.46	UD-3B		7.84	25.35	720.00	400.00	0.05
PW3	58.00	3.63	26.00	863.35	454.30	0.85	UD-6B	175.80	5.37	25.70	995.05	450.00	0.10
PW4	59.00	5.71	26.00	404.35	212.15	0.38	UD-6C		5.42	27.75	1035.00	615.00	0.09
PW5	63.00	6.24	25.70	395.65	210.35	0.38	UD-6E		7.13	25.85	1050.00	580.00	0.10
HW	27.00	6.16	25.80	552.80	143.20	0.06	UD-6F		6.66	26.05	825.00	455.00	0.07
BDW1	93.00	5.48	26.05	173.50	91.59	0.19	UD-6G		6.63	25.95	840.00	460.00	0.06
BDW2	85.00	6.31	26.00	273.00	146.85	0.25	UD-6H		6.80	25.90	795.00	440.00	0.05
BDW3	80.00	5.97	27.35	373.80	196.95	0.20	UD-9A	323.30	7.94	25.85	865.00	475.00	0.06
BDW4	78.00	4.80	24.50	280.00	75.50	0.02	UD-9B		7.85	25.00	850.00	465.00	0.07
BBH	39.00	5.78	26.00	86.37	48.19	0.08	UD-9C		7.88	22.00	855.00	475.00	0.06
ABH	36.00	6.22	25.60	214.20	114.61	0.28	UD-17A	597.30	7.54	25.65	1695.00	935.00	0.06
HBH1	41.00	6.09	27.45	329.75	177.40	0.31	UD-17B		7.62	25.00	1775.00	975.00	0.04
HBH2	41.00	6.00	26.95	319.20	166.95	0.31	UD-17C		7.24	25.60	1305.00	645.00	0.07
PBHI	58.00	4.14	26.00	405.15	117.60	0.43	UD-17D		7.10	25.60	4140.00	2280.00	0.10
PBH2	59.00	6.44	25.95	378.05	199.05	0.41	UD-17E		7.82	25.40	2755.00	1515.00	0.70

Appendix III: Physico-chemical paramters for Groundwater and Underground mine water (Continuation)

Groundwater

Sampling ID	Depth (m)	pH	Temp (°C)	EC (µS/c)	TDS (mg/L)	Sal ‰
PBH3	54.00	6.03	27.05	453.25	199.50	0.37
PBH4	60.00	6.59	25.95	230.25	122.64	0.20
PBH5	48.00	6.00	26.00	191.80	103.41	0.19
PBH6	45.00	6.30	24.30	220.00	65.00	0.04
PBH7	69.00	5.07	24.08	320.00	90.00	0.05
Range		**3.6-6.6**	**24.3-27.5**	**86.4-863.3**	**66.4-454.3**	**0.04-0.19**

Underground mine water

Sampling ID	Depth (m)	pH	Temp (°C)	EC (µS/cm)	TDS (mg/L)	Sal ‰
UD-17F	597.30	7.46	23.10	1660.00	910.00	0.70
UD-24A	888.80	7.57	25.95	3065.00	1690.00	0.10
UD-24B		7.83	25.30	2900.00	1600.00	0.10
UD-24C		7.57	25.70	5650.00	3110.00	0.06
UD-24E		7.68	25.30	4615.00	2520.00	0.04
Range		**5.4-7.9**	**22-26.1**	**720-5650**	**400-3110**	**0.04-0.70**

Temp (Temperature) **EC** (Electrical Conductivity) **TDS** (Total Dissolved Solids) **Sal** (Salinity)

Appendix IV: Concentration of Major Anions

Surface water

Sampling ID	Elevation (m)	SO_4^{2-} (meq/L)	Cl^- (meq/L)	HCO_3^- (meq/L)	NO_3^- (meq/L)	PO_4^{3-} (meq/L)	Sampling ID	Elevation (m)	SO_4^{2-} (meq/L)	Cl^- (meq/L)	HCO_3^- (meq/L)	NO_3^- (meq/L)	PO_4^{3-} (meq/L)
PSW	62.00	4.56	1.12	1.52	0.04	0.18	PUWF(US)	68.00	42.78	1.47	7.48	0.02	2.27
BDSt	86.00	3.04	0.64	0.94	0.01	0.22	PUWM(MS)	63.00	49.30	3.28	9.02	0.01	3.06
BDSt2	73.00	3.25	1.32	0.94	0.08	<0.01	PUWE(DS)	35.00	11.85	1.99	6.98	0.02	1.30
ASP	60.00	3.00	0.65	1.38	<0.10	0.64	BDU(US)	78.00	7.48	0.80	4.66	0.01	0.41
BSP	52.00	3.06	0.95	3.90	0.06	0.04	BDUWF(MS)	73.00	4.67	2.49	4.14	0.01	0.90
BST2	48.00	4.75	0.72	1.06	0.03	0.41	ARaWT(US)	34.00	3.52	0.79	1.38	0.17	0.08
ARWT(US)	35.00	3.68	1.30	1.44	0.05	0.03	ARaWM(MS)	33.00	5.62	0.92	1.78	0.03	0.07
HRWM(MS)	27.00	3.34	1.14	1.54	0.04	0.01	ARaWE(DS)	30.00	3.03	0.92	1.74	0.01	<0.01
Range		**SO_4^{2-} (3.0-49.3)**		**Cl^- (0.6-3.3)**		**HCO_3^- (0.94 - 9.02)**		**NO_3^- (0.01-0.17)**			**PO_4^{3-} (0.01 – 3.06)**		

US (Upper Stream) **MS** (Mid Steam) **DS** (Down Stream)

Appendix IV: Concentration of Major Anions (Continuation)

Groundwater							Underground mine water						
Sampling ID	Depth (m)	SO_4^{2-} (meq/L)	Cl^- (meq/L)	HCO_3^- (meq/L)	NO_3^- (meq/L)	PO_4^{3-} (meq/L)	Sampling ID	Depth (m)	SO_4^{2-} (meq/L)	Cl^- (meq/L)	HCO_3^- (meq/L)	NO_3^- (meq/L)	PO_4^{3-} (meq/L)
PW1	49.00	3.25	1.39	1.58	0.54	0.14	UD-3A	71.50	9.17	6.90	4.46	0.16	1.00
PW2	54.00	5.69	2.06	0.32	0.28	<0.01	UD-3B		6.47	0.68	3.14	0.13	0.11
PW3	58.00	3.29	3.89	0.98	1.36	0.11	UD-6B	175.80	16.59	1.12	2.46	0.15	0.10
PW4	59.00	3.40	2.06	1.02	0.45	<0.01	UD-6C		8.68	1.27	3.30	0.16	1.04
PW5	63.00	3.24	1.76	1.92	029	0.10	UD-6E		12.41	1.47	3.42	0.35	0.34
HW	27.00	3.58	1.82	1.64	0.14	0.01	UD-6F		5.89	0.96	2.22	0.11	0.18
BDW1	93.00	3.06	0.98	0.90	0.20	0.06	UD-6G		9.01	0.86	2.30	0.13	0.25
BDW2	85.00	3.18	1.61	1.26	0.06	0.02	UD-6H		9.04	0.71	2.42	0.25	0.17
BDW3	80.00	3.24	1.39	0.74	0.41	2.00	UD-9A	323.30	6.48	0.79	4.52	0.23	1.11
BDW4	78.00	3.46	1.55	1.82	0.10	1.75	UD-9B		5.48	0.98	4.18	0.15	0.29
BBH	39.00	3.96	0.81	0.78	0.40	0.09	UD-9C		5.52	0.82	4.70	0.15	1.59
ABH	36.00	3.10	0.75	2.38	0.03	0.41	UD-17A	597.30	39.19	0.88	6.64	0.21	0.73
HBH1	41.00	3.32	1.39	1.20	0.10	1.63	UD-17B		13.68	0.81	5.66	0.08	0.77
HBH2	41.00	3.20	1.31	0.96	0.23	0.39	UD-17C		8.55	0.96	3.32	0.43	0.57
PBH1	58.00	2.85	2.21	0.30	0.39	0.30	UD-17D		49.06	1.49	8.02	0.14	3.23
PBH2	59.00	3.05	1.14	1.64	0.31	0.10	UD-17E		22.63	0.76	7.10	0.15	1.86
PBH3	54.00	3.19	1.39	1.22	0.49	0.11	UD-17F		17.94	1.91	5.82	0.08	0.77

Appendix IV: Concentration of Major Anion (Continuation)

Groundwater							Underground mine water						
Sampling ID	Depth (m)	SO_4^{2-} (meq/L)	Cl^- (meq/L)	HCO_3^- (meq/L)	NO_3^- (meq/L)	PO_4^{3-} (meq/L)	Sampling ID	Depth (m)	SO_4^{2-} (meq/L)	Cl^- (meq/L)	HCO_3^- (meq/L)	NO_3^- (meq/L)	PO_4^{3-} (meq/L)
PBH4	60.00	3.19	0.78	1.04	0.11	0.05	UD-24A	888.80	37.37	1.10	6.60	0.11	2.21
PBH5	48.00	2.15	0.72	1.16	0.04	0.36	UD-24B		28.82	0.78	4.74	0.22	1.34
PBH6	45.00	3.04	0.69	1.00	0.01	0.09	UD-24C		78.98	0.36	7.04	0.24	2.28
PBH7	69.00	3.04	1.10	0.28	0.06	1.14	UD-24E		60.10	0.16	5.48	0.09	1.68
Range		**(2.15-5.69)**	**(0.68-3.89)**	**(0.28-2.38)**	**(0.01-1.36)**	**(0.01-2.00)**	**Range**		**(5.48-78.98)**	**(0.16-6.90)**	**(2.22-8.02)**	**(0.08-0.43)**	**(0.10-3.23)**

UD (Prestea underground) **UDB** (Bondaye underground) **BH** (Borehole) **W** (Hand-dug well) **BD** (Bondaye) **P** (Prestea)

Appendix V: Concentration of Major Cations

Surface water

Sampling ID	Elevation (m)	Na^+ (meq/L)	K^+ (meq/L)	Ca^{2+} (meq/L)	Mg^{2+} (meq/L)	Sampling ID	Elevation (m)	Na^+ (meq/L)	K^+ (meq/L)	Ca^{2+} (meq/L)	Mg^{2+} (meq/L)
PSW	62.00	2.98	0.14	2.45	1.29	PUWF (US)	68.00	4.31	0.11	28.21	10.41
BDSt	86.00	0.12	0.02	1.81	1.55	PUWM (DS)	63.00	5.59	0.24	33.00	18.87
BDSt2	73.00	0.14	0.01	0.64	0.44	PUWE (DS)	35.00	3.28	0.15	19.80	7.41
ASP	60.00	0.31	0.04	2.66	1.25	BDU (US)	78.00	0.41	0.03	6.01	4.38
BSP	52.00	0.18	0.02	1.65	0.80	BDUWF (MS)	73.00	0.40	0.08	12.24	4.70
BSt2	48.00	0.16	0.02	0.64	0.70	ARaWT (US)	34.00	0.73	0.04	2.66	0.79
ARWT(US)	35.00	0.49	0.08	1.76	0.93	ARaWT (MS)	33.00	0.80	0.11	3.19	4.43
HRWM (MS)	27.00	0.25	0.10	1.48	0.91	ARaWT (DS)	30.00	0.40	0.07	2.13	1.53
ARWE (DS)	29.00	0.65	0.16	3.73	0.88						
Range		**Na^+ (0.12 – 5.59)**		**K^+ (0.01 – 0.24)**		**Ca^{2+} (0.64 – 33.00)**			**Mg^{2+} (0.44 – 18.87)**		

Appendix V: Concentration of Major Cations (Continuation)

Groundwater						Undergound mine water					
Sampling ID	Depth (m)	Na^+ (meq/L)	K^+ (meq/L)	Ca^{2+} (meq/L)	Mg^{2+} (meq/L)	Sampling ID	Depth (m)	Na^+ (meq/L)	K^+ (meq/L)	Ca^{2+} (meq/L)	Mg^{2+} (meq/L)
PW1	49.00	0.87	0.11	3.57	0.97	UD-3A	71.50	1.22	0.85	11.44	5.49
PW2	54.00	2.31	1.03	2.04	1.54	UD-3B		0.28	0.96	7.31	4.34
PW3	58.00	3.57	0.39	3.78	1.65	UD-6B	175.80	0.89	0.84	11.18	4.59
PW4	59.00	2.48	0.92	1.54	1.89	UD-6C		0.97	0.80	9.38	3.89
PW5	63.00	1.33	0.95	1.49	2.32	UD-6E		0.97	0.89	12.23	4.53
HW	27.00	0.97	0.18	5.39	0.76	UD-6F		0.49	0.84	5.91	3.61
BDW1	93.00	1.62	0.84	2.34	1.37	UD-6G		0.50	0.84	9.58	3.68
BDW2	85.00	1.88	1.06	2.29	1.46	UD-6H		0.39	0.83	7.12	3.89
BDW3	80.00	1.48	1.06	2.13	1.47	UD-9A	323.30	0.45	0.85	8.05	4.95
BDW4	78.00	0.73	0.88	4.32	1.57	UD-9B		0.28	0.83	6.98	4.32
BBH	39.00	1.04	0.83	2.51	1.28	UD-9C		0.44	0.83	7.44	4.58
ABH	36.00	0.61	0.82	4.31	1.77	UD-17A	597.30	0.88	0.85	27.94	6.90
HBH1	41.00	1.10	0.86	1.65	1.72	UD-17B		1.03	0.86	15.08	7.34
HBH2	41.00	1.11	0.84	1.01	1.69	UD-17C		1.05	0.86	9.23	4.57
PBH1	58.00	1.63	0.87	1.49	0.78	UD-17D		4.14	0.93	31.40	12.61
PBH2	59.00	1.27	0.82	1.74	1.21	UD-17E		1.47	0.88	24.88	11.61

Appendix V: Concentration of Major Cations (Continuation)

Groundwater						Undergound mine water					
Sampling ID	Depth (m)	Na^+ (meq/L)	K^+ (meq/L)	Ca^{2+} (meq/L)	Mg^{2+} (meq/L)	Sampling ID	Depth (m)	Na^+ (meq/L)	K^+ (meq/L)	Ca^{2+} (meq/L)	Mg^{2+} (meq/L)
PBH3	54.00	1.41	0.85	2.00	0.94	UD-17F		1.35	0.91	20.15	9.03
PBH4	60.00	0.75	0.83	1.12	1.54	UD-24A	888.80	4.01	0.90	25.28	10.49
PBH5	48.00	0.75	0.82	1.12	0.82	UD-24B		2.50	0.86	26.88	11.08
PBH6	45.00	0.74	0.83	3.26	0.76	UD-24C		3.40	0.90	43.00	14.50
PBH7	69.00	1.09	0.88	2.13	0.80	UD-24E		2.69	0.88	35.72	14.30
Range		**(0.61-3.57)**	**(0.11-1.06)**	**(1.01-5.39)**	**(0.76-2.32)**	**Range**		**(0.28-4.14)**	**(0.83-0.96)**	**(5.91-43.00)**	**(3.61-14.50)**

UD (Prestea Underground) **UDB** (Bondaye Underground) **BH** (Borehole) **W** (Hand-dug well) **BD** (Bondaye) **P** (Prestea)

Appendix VI: Concentration of Trace Element in Surface water

Surface water		FASS (mg/L)						HG-AAS (mg/L)
Sample ID	Elevation/m	Cd	Cu	Fe	Mn	Pb	Zn	As
PSW	62.00	<0.005	<0.005	0.06	0.02	<0.01	<0.001	0.01
BDSt	86.00	<0.005	<0.005	<0.005	<0.002	<0.01	<0.001	<0.001
BDSt2	73.00	<0.005	0.01	0.19	0.01	0.02	<0.001	0.02
ASP	60.00	<0.005	0.04	0.11	<0.002	<0.01	<0.001	0.01
BSP	52.00	<0.005	0.02	0.15	<0.002	<0.01	<0.001	0.01
BST2	48.00	<0.005	0.05	0.21	<0.002	<0.01	<0.001	0.01
ARWT(US)	35.00	<0.005	0.45	2.81	0.01	0.02	<0.001	0.04
HRWM(MS)	27.00	<0.005	0.18	1.62	<0.002	0.01	<0.001	0.04
ARWE (DS)	29.00	<0.005	0.27	2.42	<0.002	0.01	<0.001	0.03
PUWF(US)	68.00	0.01	1.15	0.04	0.26	0.22	<0.001	<0.001
PUWM(MS)	63.00	<0.005	<0.005	0.99	1.69	<0.01	<0.001	<0.001
PUWE(DS)	35.00	<0.005	1.24	0.95	<0.002	<0.01	<0.001	0.19

Appendix VI: Concentration of Trace Element in Surface water

Surface water		FASS (mg/L)						HG-AAS (mg/L)
Sample ID	Elevation/m	Cd	Cu	Fe	Mn	Pb	Zn	As
BDU(US)	78.00	<0.005	<0.005	1.22	0.02	<0.01	<0.001	0.18
BDUWF(MS)	73.00	<0.005	0.01	0.08	0.03	<0.01	<0.001	< 0.001
ARaWT(US)	34.00	<0.005	0.13	8.49	0.03	<0.01	<0.001	<0.001
ARaWM(MS)	33.00	<0.005	0.15	10.31	0.01	<0.01	<0.001	0.01
ARaWE(DS)	30.00	<0.005	0.15	11.55	0.01	<0.01	<0.001	0.02
Range		**(<0.005-0.01)**	**(<0.003-1.24)**	**(<0.01-11.55)**	**(<0.002-1.69)**	**(<0.01 – 0.22)**	**(<0.001-0.01)**	**(<0.001-0.19)**

Appendix VI: Concentration of Trace Elements in Groundwater samples

Groundwater		FASS (mg/L)						HG-AAS (mg/L)
Sample ID	Depth/m	Cd	Cu	Fe	Mn	Pb	Zn	As
PW1	49.00	<0.005	0.03	0.17	<0.002	<0.001	<0.001	0.02
PW2	54.00	<0.005	0.05	7.91	<0.002	<0.001	<0.001	0.02
PW3	58.00	0.89	0.07	0.19	0.32	0.01	<0.001	0.01
PW4	59.00	<0.005	0.46	1.52	0.01	<0.001	<0.001	0.02
PW5	63.00	<0.005	0.41	0.75	<0.002	<0.001	<0.001	<0.001
HW	27.00	<0.005	0.50	2.79	<0.002	<0.001	<0.001	0.02
BDW1	93.00	<0.005	0.03	0.11	<0.002	<0.001	<0.001	0.01
BDW2	85.00	<0.005	0.22	2.36	<0.002	<0.001	<0.001	<0.001
BDW3	80.00	<0.005	0.38	9.39	<0.002	<0.001	<0.001	0.03
BDW4	78.00	<0.005	0.07	0.04	<0.002	<0.001	0.01	0.02
BBH	39.00	<0.005	<0.005	0.01	<0.002	0.01	<0.001	0.02
ABH	36.00	<0.005	0.14	6.06	<0.002	0.02	<0.001	0.02
HBH1	41.00	<0.005	0.21	0.03	<0.002	<0.001	<0.001	0.01
HBH2	41.00	<0.005	0.19	0.01	0.02	<0.001	<0.001	<0.001
PBH1	58.00	<0.005	0.05	1.83	0.03	0.01	<0.001	0.01
PBH2	59.00	<0.005	0.05	<0.01	<0.002	<0.001	<0.001	0.02

Appendix VI: Concentration of Trace Element in Ground water

Groundwater		FASS (mg/L)						HG-AAS (mg/L)
Sample ID	Depth/m	Cd	Cu	Fe	Mn	Pb	Zn	As
PBH3	54.00	0.05	<0.005	0.09	0.09	<0.001	<0.001	0.01
PBH4	60.00	0.04	<0.005	0.04	0.14	<0.001	<0.001	<0.001
PBH5	48.00	<0.005	0.15	6.38	0.01	0.02	<0.001	0.02
PBH6	45.00	<0.005	0.15	2.86	<0.002	<0.001	<0.001	<0.001
PBH7	69.00	<0.005	0.01	<0.01	0.02	<0.001	<0.001	0.01
Range		**(<0.005-0.89)**	**(<0.03-0.50)**	**(<0.01-9.39)**	**(<0.02-0.32)**	**(<0.01-0.22)**	**(<<<0.001)**	**(<0.001-0.03)**

Appendix VI: Concentration of Trace Element in Underground mine water

Underground mine water		FASS (mg/L)						HG-AAS (mg/L)
Sample ID	Depth/m	Cd	Cu	Fe	Mn	Pb	Zn	As
UDB-3A	71.50	<0.005	0.01	<0.01	0.02	<0.01	<0.001	0.01
UDB-3B		0.050	0.21	7.69	0.02	<0.01	<0.001	<0.001
UD-6B	175.80	0.040	1.87	22.31	0.01	<0.01	<0.001	<0.001
UD-6C		0.004	1.88	45.53	<0.002	<0.01	<0.001	<0.001
UD-6E		0.030	1.12	8.13	0.01	<0.01	<0.001	<0.001
UD-6F		0.230	3.06	7.56	0.24	<0.01	<0.001	<0.001
UD-6G		0.140	2.45	7.99	0.11	<0.01	<0.001	<0.001
UD-6H		0.201	3.06	11.55	0.03	<0.01	<0.001	<0.001
UDB-9A	323.30	0.020	0.06	0.05	0.03	<0.01	<0.001	0.11
UDB-9B		<0.005	0.02	0.74	0.01	<0.01	<0.001	0.04
UDB-9C		0.001	0.04	0.06	0.01	<0.01	<0.001	0.27
UD-17A	597.3	0.010	1.16	0.04	0.01	<0.01	<0.001	0.07
UD-17B		0.040	1.14	2.20	0.01	<0.01	<0.001	0.07
UD-17C		0.040	0.39	1.47	0.02	<0.01	<0.001	0.04
UD-17D		0.040	3.52	0.03	0.02	<0.01	<0.001	0.51
UD-17E		0.030	0.57	0.03	0.01	<0.01	<0.001	0.34
UD-17F		0.010	0.12	1.73	<0.002	<0.01	<0.001	<0.001

Appendix VI: Concentration of Trace Element in Underground mine water (Continuation)

Underground mine water		FASS (mg/L)						HG-AAS (mg/L)
Sample ID	Depth/m	Cd	Cu	Fe	Mn	Pb	Zn	As
UD-24A	888.80	0.280	4.60	12.00	0.04	<0.01	<0.001	0.69
UD-24B		0.020	0.81	0.820	0.02	<0.01	<0.001	0.20
UD-24C		<0.005	0.02	0.020	<0.002	<0.01	<0.001	0.43
UD-24E		<0.005	0.03	0.030	0.01	<0.01	0.001	0.22
Range		**(<0.005 – 0.28)**	**(<0.03-4.60)**	**(0.02-43.53)**	**(<0.002-0.24)**	**(<<<0.01)**	**(<<<0.001)**	**(<0.001-0.69)**

Appendix VII: Ionic balance for Groundwater

Sampling	Cations (meq/L)					Anions (meq/L)				Ionic
ID	Na^+	K^+	Ca^{2+}	Mg^{2+}	$(Na^+ + K^+ + Ca^{2+} + Mg^{2+})$	SO_4^{2-}	Cl^-	HCO_3^-	$(SO_4^{2-} + Cl^- + HCO_3^-)$	Balance (%)
PW1	0.87	0.11	3.57	0.97	5.52	3.25	1.39	1.58	6.88	- 10.98
PW2	2.31	1.03	2.04	1.54	6.92	5.69	2.06	0.32	8.07	- 7.67
PW3	3.57	0.39	3.78	1.65	9.39	3.29	3.89	0.98	9.63	- 1.25
PW4	2.48	0.92	1.54	1.89	6.83	3.40	2.06	1.02	6.48	2.63
PW5	1.33	0.95	1.49	2.32	6.09	3.24	1.76	1.92	7.31	- 9.11
HW	0.97	0.18	5.39	0.76	7.30	3.58	1.82	1.64	7.19	0.75
BDW1	1.62	0.84	2.34	1.37	6.17	3.06	0.98	0.90	5.20	8.51
BDW2	1.88	1.06	2.29	1.46	6.69	3.18	1.61	1.26	6.13	4.36
BDW3	1.48	1.06	2.13	1.47	6.14	3.24	1.39	0.74	7.78	- 11.80
BDW4	0.73	0.88	4.32	1.57	7.50	3.46	1.55	1.82	8.68	- 7.31
BBH	1.04	0.83	2.51	1.28	5.66	3.96	0.81	0.72	5.62	0.37
ABH	0.61	0.82	4.31	1.77	7.51	3.10	0.75	2.38	6.67	5.95
HBH1	1.10	0.86	1.65	1.72	5.33	3.32	1.39	1.20	7.64	- 17.80
HBH2	1.11	0.84	1.01	1.69	4.65	3.20	1.31	0.96	6.05	- 13.40
PBH1	1.63	0.87	1.49	0.78	4.77	2.85	2.21	0.30	6.24	- 11.81
PBH2	1.27	0.82	1.74	1.21	5.04	3.05	1.14	1.64	6.40	- 10.66

Appendix VII: Ionic Balance for Groundwater (Continuation)

Sampling	Cations (meq/L)					Anions (meq/L)				Ionic
ID	Na^{+}	K^{+}	Ca^{2+}	Mg^{2+}	$(Na^{+}+ K^{+}+ Ca^{2+}+ Mg^{2+})$	SO_4^{2-}	Cl^{-}	HCO_3^{-}	$(SO_4^{2-} + Cl^{-} + HCO_3^{-})$	Balance (%)
PBH3	1.41	0.85	2.00	0.94	5.20	3.19	1.39	1.22	6.40	-10.34
PBH4	0.75	0.83	1.12	1.54	4.24	3.19	0.78	1.04	5.17	-9.87
PBH5	0.75	0.82	1.12	0.82	3.51	2.15	0.72	1.16	4.43	-11.63
PBH6	0.74	0.83	3.26	0.76	5.59	3.04	0.69	1.00	4.83	7.26
PBH7	1.09	0.88	2.13	0.80	4.90	3.04	1.10	0.28	5.62	- 6.87

Appendix VII: Ionic Balance for Underground mine water (Contiuation)

Sampling	Cation (meq/L)					Anions (meq/L)				Ionic
ID	Na^+	K^+	Ca^{2+}	Mg^{2+}	$(Na^+ + K^+ + Ca^{2+} + Mg^{2+})$	SO_4^{2-}	Cl^-	HCO_3^-	$(SO_4^{2-} + Cl^- + HCO_3^-)$	Balance (%)
UDB-3A	1.22	0.85	11.44	5.49	19.00	9.17	6.90	4.46	21.69	-6.62
UDB-3B	0.28	0.96	7.31	4.34	12.89	6.47	0.68	3.14	10.53	10.10
UD-6B	0.89	0.84	11.18	4.59	17.50	16.59	1.12	2.46	20.42	-7.71
UD-6C	0.97	0.83	9.38	3.89	15.07	8.68	1.27	3.30	4.45	2.08
UD-6E	0.97	0.89	12.23	4.53	18.62	1.41	1.47	3.42	17.99	1.73
UD-6F	0.49	0.84	5.91	3.61	10.85	5.89	0.96	2.22	9.36	7.39
UD-6G	0.50	0.84	9.58	3.68	14.60	9.01	0.86	2.30	12.55	7.57
UD-6H	0.39	0.83	7.12	3.89	12.23	9.04	0.71	2.42	12.59	-1.46
UDB-9A	0.45	0.85	8.05	4.95	14.30	6.48	0.79	4.52	13.13	4.26
UDB-9B	0.28	0.83	6.98	4.32	12.41	5.48	0.98	4.18	11.08	5.64
UDB-9C	0.44	0.83	7.44	4.58	13.29	5.52	0.82	4.70	12.78	1.98
UD-17A	0.88	0.85	27.94	6.90	36.57	39.19	0.88	6.64	44.65	-9.95
UD-17B	1.03	0.86	15.08	7.34	24.31	13.68	0.81	5.66	21.00	7.31
UD-17C	1.05	0.86	9.23	4.57	15.71	8.55	0.96	3.32	13.83	6.38
UD-17D	4.14	0.93	31.40	12.61	49.08	49.06	1.49	8.02	61.94	-11.58
UD-17E	1.47	0.88	24.88	11.61	38.84	22.63	0.76	7.10	32.50	8.88
UD-17F	1.35	0.91	20.15	9.03	31.44	17.94	1.91	5.82	26.50	8.49

Appendix VII: Ionic Balance for Underground mine water (Contiuation)

Sampling	Cation (meq/L)					Anions (meq/L)				Ionic
ID	Na^+	K^+	Ca^{2+}	Mg^{2+}	$(Na^+ + K^+ + Ca^{2+} + Mg^{2+})$	SO_4^{2-}	Cl^-	HCO_3^-	$(SO_4^{2-} + Cl^- + HCO_3^-)$	Balance (%)
UD-24A	4.01	0.90	25.28	10.49	40.68	37.37	1.10	6.60	47.39	-7.62
UD-24B	2.50	0.86	26.88	11.08	41.32	28.82	0.78	4.74	35.90	7.02
UD-24C	3.40	0.90	43.00	14.50	61.80	78.98	0.36	7.04	88.90	-17.98
UD-24E	2.69	0.88	35.72	14.30	53.59	60.10	0.16	5.48	67.50	-11.49

Appendix VIII: Pearson Correlation coefficient for physico-chemical parameters and Major ions at 95 % CI

	pH	*Temp/^{0}C*	*Cond/µS/m*	*TDS/mg/L*	*Na^+*	*K^+*	*Ca^{2+}*	*Mg^{2+}*	*SO_4^{2-}*	*Cl^-*	*HCO_3^-*	*NO_3^-*	*PO_4^{3-}*
pH	1												
Temp/^{0}C	-0.309	1											
Cond/µSm	**0.504**	-0.1418	1										
TDS/mg/L	0.496	-0.1499	**0.9988**	1									
Na^+	-0.076	0.1835	**0.6384**	**0.6359**	1								
K^+	0.203	0.1175	0.1420	0.1638	0.0703	1							
Ca^{2+}	**0.573**	-0.2165	**0.9600**	**0.9608**	**0.5231**	0.132	1						
Mg^{2+}	**0.649**	-0.2422	**0.9535**	**0.9562**	**0.5120**	0.228	**0.961**	1					
SO_4^{2-}	0.452	-0.0952	**0.9658**	**0.9665**	**0.6101**	0.162	**0.957**	**0.895**	1				
Cl^-	-0.218	0.1485	-0.2002	-0.2024	0.1751	-0.152	-0.189	-0.171	-0.2211	1			
HCO_3^-	**0.742**	-0.3641	**0.8162**	**0.8187**	0.3266	0.159	**0.885**	**0.914**	**0.7640**	-0.1141	1		
NO_3^-	-0.415	0.2216	-0.0780	-0.0863	0.3423	-0.398	-0.152	-0.177	-0.1276	0.3811	-0.212	1	
PO_4^{3-}	0.332	-0.1351	0.6948	**0.7061**	0.4853	0.252	**0.659**	**0.688**	**0.6456**	-0.0841	**0.657**	0.1859	1

Appendix IX: Stable Isotopes [δ^2H (‰) and $\delta^{18}O$ (‰)]

Underground water			Groundwater			Surface water		
Sample ID	δ^2H (‰)	$\delta^{18}O$ (‰)	Sample ID	δ^2H (‰)	$\delta^{18}O$ (‰)	Sample ID	δ^2H (‰)	$\delta^{18}O$ (‰)
UDB-3A	-4.73	-1.99	HW	-1.32	-1.31	ASP	-2.74	-1.12
UDB-3B	-4.67	-1.98	PW1	-6.48	-1.82	BSP	-4.93	-2.16
UD-6B	-4.44	-1.79	PW2	-4.29	-1.62	BSt2	-5.32	-1.83
UD-6C	-4.97	-1.77	PW3	+0.42	-1.59	BDSt	-5.12	-2.05
UD-6E	-6.57	-1.59	PW4	-6.05	-1.75	BDSt2	-3.83	-1.08
UD-6F	-6.43	-1.88	PW5	-6.12	-1.67	PSW	-4.71	-1.96
UD-6G	-7.63	-1.83	BDW1	-4.10	-2.28	ARaWT (US)	-0.93	-0.63
UD-6H	-6.20	-2.14	BDW2	+0.53	-1.63	ARaWM (MS)	+0.21	-0.49
UDB-9A	-8.54	-2.07	BDW3	-2.93	-1.68	ARaWE (DS)	-2.21	-0.50
UDB-9B	-5.65	-2.03	BDW4	-2.27	-0.87	HRWT (US)	+1.73	-0.24
UDB-9C	-5.98	-1.91	BBH	-5.70	-2.06	APWM (MS)	+3.02	+0.47
UD-17A	-4.96	-2.10	ABH	-6.43	-2.16	ARE (DS)	+2.85	-0.90
UD-17B	-3.26	-1.18	HBH1	-2.53	-1.43	PUMF (US)	-6.66	-1.78
UD-17C	-3.68	-2.00	HBH2	-1.68	-0.48	PUWM (MS)	-2.08	-1.15
UD-17D	-4.74	-2.17	PBH1	-2.71	-1.51	PUWE (DS)	-1.07	-1.01
UD-17E	-4.94	-2.22	PBH2	-4.44	-2.19	BDU (US)	-1.84	-0.79
UD-17F	-1.00	-0.95	PBH3	-5.00	-1.50	BDUW (MS)	-3.29	-0.98
UD-24A	-6.10	-2.17	PBH4	-8.88	-2.23			
UD-24B	-3.01	-1.83	PBH5	-5.62	-2.08			
UD-24C	-5.04	-2.03	PBH6	-2.41	-1.71			
UD-24E	-2.71	-1.63	PBH7	-2.99	-0.66			

Appendix X